



Pontificia Universidad
JAVERIANA
Colombia

DOCTORAL RESEARCH:

EFFECT OF CYCLIST'S POSTURE ON PERFORMANCE
AND INTERACTION WITH THE BICYCLE

Alejandra Paola Polanco Aguilar
alejandra.polanco@javeriana.edu.co

ADVISOR: Professor Dr. Daniel Suárez, Pontificia Universidad Javeriana
CO-ADVISOR: Associate Professor Alberto Doria, University of Padua

2020

THESIS DEFENSE COMMITTEE

Professor Dr. Frans Van der Helm, Delft University of Technology

Professor Dr. Darren Stefanyshyn, University of Calgary

Professor Dr. Juan Carlos Briceño, University of Los Andes

Professor Dr. Pedro Vizcaya Guarín, Pontificia Universidad Javeriana

Abstract

The aim of this thesis was to define a methodology for the posture selection of cyclists, based on quantitative indices representing the rider's performance and interaction with the bicycle.

A methodology based on an optimization problem was proposed. The methodology seeks to find a posture that minimizes race time. The race time is computed for each posture considering the cyclist's power delivery capacity and drag area in the specific posture. The solution is constrained by thresholds of exposure to vibrations and pressure, which are associated with the race time. For the computation of the race time, specific race conditions as the distance, road grade, wind speed, and environment are considered. Methods to characterize the drag area, power delivery capacity, pressure in contact areas, and vibrations transmitted were defined.

The methodology was employed for the posture selection and optimization of a group of cyclists riding on aerobars postures. Two postures were defined by the bicycle's fitting window at the upper and lower limits of the aerobars' height. The posture selection and optimization were performed for five bicycle-cyclist sets of varied characteristics. For the methodology's implementation, a short individual time-trial race and various road inclinations and wind speeds were considered.

The results showed that reducing the aerobars' height improved the drag area and deteriorated the power delivery capacity, pressure on the saddle, and vibrations on the saddle for all the tested cyclists. It was observed that the vibrations on the saddle imposed the strictest constraint for the cyclists, limiting the feasible exposure time and, in some cases, modifying the result obtained if the posture was selected considering only performance. Even though tendencies were observed in the variables characterized for the group of cyclists, it was found that the optimal posture selection depends on each cyclist and bicycle's characteristics and the race conditions. Regarding the characteristics of the cyclist and the bicycle, it was found that the drag area to power delivery capacity ratio and the saddle vibration of each rider in each posture govern the posture selection process. Regarding the race conditions, it was found that posture selection depends on the longitudinal wind speed, the road inclination, and the race distance. It was also found that intermediate aerobars' heights become optimal solutions only for race scenarios in which the constraints restrict the selection of posture. It was concluded that the selection of posture is a non-trivial process that should consider the trade-off between the possible improvements on aerodynamic drag and the losses in power delivery capacity and comfort on the saddle.

The methodology developed can be used as a tool for the selection and optimization of cyclists' posture considering objective measurements of performance and interaction variables. A methodology that simultaneously considered aerodynamics, power delivery capacity, pressure, and vibration was not previously available.

Contents

Nomenclature	1
CHAPTER 1. Introduction	7
1.1. RESEARCH OBJECTIVES.....	10
1.1.1. Objective 1	10
1.1.2. Objective 2	10
1.1.3. Objective 3	11
1.1.4. Objective 4	11
1.2. GENERAL METHODOLOGY	11
1.3. DOCUMENT STRUCTURE.....	13
CHAPTER 2. Description of cases of study: postures and bicycle-cyclist sets under study.....	15
2.1. ABSTRACT.....	16
2.2. BACKGROUND ON THE DEFINITION OF POSTURE IN CYCLING	16
2.2.1. Location and characteristics of the contact points with the bicycle.....	16
2.2.2. Inclination of body segments.....	17
2.2.3. Curvature of the trunk	17
2.2.4. Bicycle geometry.....	18
2.3. POSTURES CONSIDERED FOR THE METHODOLOGY IMPLEMENTATION	18
2.3.1. Aerobars posture	18
2.3.2. Height of aerobars.....	19
2.3.3. Postures characterized: Aerobars high (ABhigh) and Aerobars low (ABlow)	20
2.4. BICYCLE-CYCLIST SETS CONSIDERED FOR THE METHODOLOGY IMPLEMENTATION	20
CHAPTER 3. Performance: measurement of aerodynamic drag.....	25
3.1. ABSTRACT.....	26
3.2. INTRODUCTION	26
3.3. METHODS.....	27
3.3.1. Mathematical model.....	27
3.3.2. Experimental assessment.....	30
3.4. RESULTS AND DISCUSSION.....	33
3.4.1. Computation of the drag area.....	33
3.4.2. Effect of posture on the drag area	34
3.5. CONCLUSION.....	35
CHAPTER 4. Performance: measurement of power delivery capacity	37

4.1.	ABSTRACT.....	38
4.2.	INTRODUCTION.....	38
4.3.	METHODS.....	40
4.3.1.	Functional threshold power.....	40
4.3.2.	Critical power.....	42
4.3.3.	Bicycle-cyclist sets and postures measured.....	43
4.4.	RESULTS AND DISCUSSION.....	44
4.4.1.	Functional threshold power.....	44
4.4.2.	Critical power.....	45
4.4.3.	Effect of posture on power delivery capacity.....	47
4.4.4.	Implementation of critical power and functional threshold power protocols.....	47
4.5.	CONCLUSION.....	48
CHAPTER 5. Interaction: measurement of pressure in contact areas.....		49
5.1.	ABSTRACT.....	50
5.2.	INTRODUCTION.....	50
5.3.	METHODS.....	52
5.4.	RESULTS AND DISCUSSION.....	57
5.4.1.	Effect of posture on the longitudinal position of the center of pressure.....	57
5.4.2.	Effect of posture on the average pressure and maximum average pressure over time 60	
5.5.	CONCLUSION.....	66
CHAPTER 6. Interaction: measurement of vibrations transmitted to the cyclist.....		67
6.1.	ABSTRACT.....	68
6.2.	INTRODUCTION.....	68
6.3.	METHODS.....	70
6.4.	RESULTS AND DISCUSSION.....	72
6.4.1.	Computation of weighted power spectral densities.....	72
6.4.2.	Effect of posture on vibration total values.....	75
6.5.	CONCLUSION.....	79
CHAPTER 7. Effect of posture on cyclist's performance and interaction with the bicycle. Case of study: height of aerobars.....		81
7.1.	ABSTRACT.....	82

7.2.	INTRODUCTION	82
7.3.	METHODS.....	83
7.3.1.	Optimization problem	84
7.3.2.	Definition of the objective function: race time.....	85
7.3.3.	Definition of the constraints: thresholds for pressure and vibration	86
7.3.4.	Considerations for the optimization	87
7.3.5.	Bicycle-cyclist sets studied	88
7.4.	RESULTS AND DISCUSSION.....	90
7.4.1.	Scenario 1: selection of posture between two options	90
7.4.2.	Scenario 2: optimization of posture.....	97
7.5.	CONCLUSION.....	99
CHAPTER 8.	Concluding remarks.....	101
8.1.	EFFECT OF POSTURE IN PERFORMANCE	102
8.1.1.	Aerodynamic drag	102
8.1.2.	Power delivery capacity	102
8.1.3.	Aerodynamic drag and power delivery capacity trade-off	103
8.2.	EFFECT OF POSTURE IN INTERACTION	103
8.2.1.	Pressure in contact areas	103
8.2.2.	Vibration transmitted to the rider	104
8.3.	SELECTION OF POSTURE.....	104
8.4.	PRACTICAL IMPLICATIONS	106
8.5.	FUTURE RESEARCH.....	106
References.....		109
Appendices.....		121
Acknowledgments.....		153
Author's publications		154
Journal Articles.....		154
Conference Articles.....		154
Oral presentations		155
Curriculum Vitae		156

Nomenclature

**CHAPTER 3:
MEASUREMENT OF AERODYNAMIC DRAG**

SYMBOL	VARIABLE / PARAMETER	UNITS
A	Projected frontal area	[m ²]
a	Longitudinal acceleration of the bicycle	[m/s ²]
b	Vector with data of the linear identification problem	[-]
B_F	Bearing resistance	[N]
c_1	Parameter of equivalent bearing resistance	[N]
c_2	Parameter of equivalent bearing resistance	[N.s/m]
C_D	Drag coefficient	[-]
$C_D A$	Drag area	[m ²]
D	Aerodynamic drag	[N]
F_c	Tractive force on the rear wheel	[N]
f_r	Rolling resistance coefficient	[-]
$F_{Y,f}$	Normal interaction of the road with the front wheel	[N]
$F_{Y,r}$	Normal interaction of the road with the rear wheel	[N]
g	Gravitational acceleration	[m/s ²]
G_x	Weight component in the longitudinal direction	[N]
G_y	Weight component in the perpendicular direction	[N]
I	Rotational inertia	[kg.m ²]
m	Total translational mass	[kg]
\mathcal{M}	Matrix of the linear identification problem	[-]
M_{eq}	Equivalent mass	[kg]
N	Number of time intervals used for the identification	[-]
P	Power delivered by the cyclist	[W]
r	Effective wheel radius	[m]
R_f	Rolling resistance on the front wheel	[N]
R_r	Rolling resistance on the rear wheel	[N]
R_x	Total rolling resistance	[N]
v_b	Bicycle speed	[m/s]
$v_{w/b}$	Speed of the wind relative to the bicycle	[m/s]
x	Vector of unknowns of the linear identification problem	[-]
η	Power transmission efficiency	[-]
θ	Road inclination angle	[rad]
ρ	Air density	[kg/m ³]

**CHAPTER 4:
MEASUREMENT OF POWER DELIVERY CAPACITY**

SYMBOL	VARIABLE / PARAMETER	UNITS
AWC	Anaerobic work capacity	[J]
FTP	Functional threshold power	[W]
HR	Heart rate	[bpm]
LT	Lactate threshold	[mmol/min]
P	Power delivered by the cyclist	[W]
P_c	Critical power	[W]
t_{tot}	Time / Duration	[s]
VO ₂	Oxygen uptake	[ml/kg.min]
W'	Work above the critical power	[J]

**CHAPTER 5:
MEASUREMENT OF PRESSURE IN CONTACT AREAS**

SYMBOL	VARIABLE / PARAMETER	UNITS
A_r	Contact area matrix	[-]
COP	Center of pressure	[-]
$COP_{lat,time}$	Lateral position of the center of pressure (for each time step)	[cm]
\overline{COP}_{lon}	Global longitudinal position of the center of pressure (average of $COP_{lon,cycle}$ for total time)	[cm]
$COP_{lon,cycle}$	Longitudinal position of the center of pressure (average of $COP_{lon,time}$ for a pedaling cycle)	[cm]
$COP_{lon,time}$	Longitudinal position of the center of pressure for each time step	[cm]
FTP	Functional threshold power	[W]
p	Pressure of sensor	[kPa]
\bar{p}	Global average pressure (average of $p_{avg,cycle}$ for total time)	[kPa]
p_a	Acceptable pressure threshold	[kPa]
$p_{avg,cycle}$	Average pressure (average of $p_{avg,time}$ for a pedaling cycle)	[kPa]
$p_{avg,sensor}$	Average pressure on each sensor over time	[kPa]
$p_{avg,time}$	Average pressure of the contact area for each time step	[kPa]
p_{peak}	Max. average pressure over time: peak value of $p_{avg,sensor}$	[kPa]
P_{th}	Pressure threshold	[kPa]
t_e	Exposure duration	[h]
t_s	Time step	[s]
t_{tot}	Total registered time	[s]

**CHAPTER 6:
MEASUREMENT OF VIBRATION TRANSMISSION**

SYMBOL	VARIABLE / PARAMETER	UNITS
a_a	Acceptable acceleration threshold	[m/s ²]
$a_{a,seatpost}$	Acceptable acceleration threshold for the seatpost	[m/s ²]
$a_{a,stem}$	Acceptable acceleration threshold for the stem	[m/s ²]
A_{ref}	Reference acceptable acceleration exposure	[m/s ²]
a_v	Vibration total value	[m/s ²]
a_w	Weighted acceleration (rms)	[m/s ²]
a_{wlat}	Weighted rms acceleration on lateral axis	[m/s ²]
a_{wlon}	Weighted rms acceleration on longitudinal axis	[m/s ²]
a_{wver}	Weighted rms acceleration on vertical axis	[m/s ²]
a_{wx}	Weighted rms acceleration on x axis	[m/s ²]
a_{wy}	Weighted rms acceleration on y axis	[m/s ²]
a_{wz}	Weighted rms acceleration on z axis	[m/s ²]
a_{w1}	Weighted rms acceleration of exposure 1	[m/s ²]
a_{w2}	Weighted rms acceleration of exposure 2	[m/s ²]
PSD	Power spectral density	[(m/s ²) ² /Hz]
rms	Root mean square	[-]
t	Time	[s]
t_e	Exposure time	[h]
T_{ref}	Reference exposure duration	[h]
T_1	Exposure duration 1	[h]
T_2	Exposure duration 2	[h]
t_{tot}	Duration of measurement	[s]

CHAPTER 7:
EFFECT OF POSTURE ON CYCLIST'S PERFORMANCE AND INTERACTION WITH THE BICYCLE

SYMBOL	VARIABLE / PARAMETER	UNITS
a_{vAB}	Vibration total values measured close to the aerobars	[m/s ²]
a_{vS}	Vibration total values measured close to the saddle	[m/s ²]
c_1	Parameter of equivalent bearing resistance	[N]
c_2	Parameter of equivalent bearing resistance	[N.s/m]
$C_D A$	Drag area	[m ²]
f_r	Rolling resistance coefficient	[-]
g	Gravitational acceleration	[m/s ²]
g_k	Restrictions of the optimization problem	[-]
h	Height of the aerobars	[mm]
\mathcal{H}	Set of aerobars' heights	[-]
h_1	Lower limit of aerobars' height (posture: ABlow)	[mm]
h_2	Upper limit of aerobars' height (posture: ABhigh)	[mm]
m	Bicycle-cyclist set mass	[kg]
\bar{P}	Average power delivery capacity	[W]
\bar{p}_{AB}	Global average pressure on the aerobars (elbow pads)	[kPa]
p_{pAB}	Percentage of \bar{p}_{AB} respect to p_{thAB}	[%]
p_{pS}	Percentage of \bar{p}_S respect to p_{thS}	[%]
\bar{p}_S	Global average pressure on the saddle	[kPa]
p_{thAB}	Pressure threshold on the aerobars (elbow pads)	[kPa]
p_{thS}	Pressure threshold on the saddle	[kPa]
t_e	Exposure duration	[h]
t_r	Total race time	[s]
V_{pAB}	Percentage of a_{vAB} respect to V_{thAB}	[%]
V_{pS}	Percentage of a_{vS} respect to V_{thS}	[%]
V_{thAB}	Vibration thresholds on the aerobars	[m/s ²]
V_{thS}	Vibration thresholds on the saddle	[m/s ²]
v_b	Bicycle speed	[m/s]
v_w	Wind speed (positive: headwind)	[m/s]
X_r	Race distance	[m]
η	Power transmission efficiency	[-]
θ	Road grade	[rad]
ρ	Air density	[kg/m ³]

CHAPTER 1. Introduction

During cycling, the body adopts a posture different from the habitual (e.g., standing, seated, reclined), which is determined by the cyclist anthropometry and limited by the bicycle geometry. The posture of the rider is relevant because it can worsen or improve the riding experience. For this reason, the modifications of posture in cycling are usually driven by the improvement of performance and comfort [1].

The interest of cyclists of different levels, from recreational to professional, in performance is clear, as its improvement is a common general objective when practicing sports. In cycling, performance is affected by internal and external factors. Internal factors are inherent to the cyclist as the capacity to deliver power. External factors are related to the interaction with the environment, which are presented as resistive forces opposing the motion. Examples of resistive forces are the aerodynamic drag, rolling resistance, and gravity acceleration. The posture of cyclists can influence both their capacity to deliver power and their aerodynamic drag. Regarding the capacity to deliver power, it has been reported that humans' muscle fatigue and endurance vary according to the body tilt angle and the limbs' position relative to the heart [2]. Nevertheless, there is no general agreement about the effect of body posture variation in power delivery capacity. Some authors have reported improvement in power output by changing the posture [2]-[8], while others have reported that there is no relevant effect [9], [10]. Regarding aerodynamic drag, it is related to the bicycle-cyclist set's drag area. The drag area is the product of the drag coefficient and the projected frontal area. The drag coefficient considers factors like shape, position, and airflow and depends on the Reynolds number. The effective frontal area, and hence, the aerodynamic drag, depend on the cyclist's posture. The improvement of aerodynamic drag due to variations in posture has been reported by several authors [11]-[16]. It is worth highlighting that the selection of postures in cycling is a non-trivial process as it considers a trade-off between aerodynamic drag and power delivery capacity [6], [8].

From a survey performed in this study to 60 recreational-level (37%), amateur (60%), and professional cyclists (3%), it was found that, when modifying the posture in the bicycle, 63% prioritized comfort, 12% prioritized performance, and the remaining 25% aimed at a balance between performance and comfort. The survey results highlight that even though performance is one of the main goals in cycling, comfort is even more relevant. The reason associated with the relevance of comfort in cycling is that discomfort can lead to pain and overuse injuries, which can end up forcing the cyclist to stop practicing the activity temporarily. Discomfort is common in cycling because of the restrictions that the bicycle imposes on the rider. The main restrictions are that the rider's whole weight is loaded in three small contact areas (*i.e.*, buttocks-saddle, hand-handlebar, and feet-pedals), and the trunk is in flexion for the rider to remain in contact with the saddle and the handlebar. These conditions, combined with riding sessions that can be extended for hours, lead to scenarios of frequent discomfort and possible overuse injuries (*i.e.*, musculoskeletal disorders, compression neuropathies, joint pain, and numbness). According to Dettori [17] and Wilber [18], 85% of cyclists report having one or more overuse injuries, of which 35% required medical intervention.

Comfort is a highly subjective variable that depends on each person's mental and physical state, background, and expectations [19], [20]. For this reason, its assessment is difficult. As a subjective variable, it has been registered through visual scales in which the rider selects a level of discomfort [21]-[23]. Other variables as vibration transmission and pressure in contact areas have been used to objectively quantify comfort as a consequence of the interaction between the bicycle and the rider.

These two variables are relevant in cycling because of their potential negative effects on the rider depend on the time of exposure, which is considerable for cycling activities. In addition, these variables are influenced by the rider posture, among others, as its anthropometry, and the geometry and materials of the bicycle components. Regarding pressure, it has been reported that the body posture affects the pressure between contact areas [24], [25] as the location of the center of mass and load distribution vary. For example, pressure increases in the saddle and decreases in the handlebar as the cyclist adopts a vertical posture, increasing the probability of saddle sores [26]. Additionally, the pressure fields at each contact point are of interest. Some studies have addressed the pressure characteristics in saddle [22], [24], [25], [27]-[30]. To a lesser extent, pressure characteristics in the handlebar [31] and pedals have been analyzed [32]. Regarding vibration, it has been reported that hand position and wrist angle have a significant effect on the vibrations induced to the cyclist [33]. Even though there is not a wide amount of information available, posture is generally identified as one of the test conditions to control when studying the vibrational behavior of bicycle-cyclist sets.

The selection and modification of posture for cycling is a common activity. From the 60 cyclists that replied to the survey, 100% had performed at least one modification to the bicycle geometry consisting of the saddle's height. There are different methods to fix the bicycle's geometry (*i.e.*, perform a bicycle fitting). From the answers of the group of cyclists, it was found that the most frequent method to fit the bicycle was a commercial fitting in a specialized store (42%). Other approaches used were a trial and error method while riding (19%), searching on the internet for suggested measurements according to the body characteristics (14%), using the recommendations of a friend or acquaintance (13%), or by visual inspection on the store where the bicycle was bought. These methods used different tools and different information to perform bicycle modifications. In general terms, these approaches aim at improving performance using aerodynamically efficient postures (usually by reducing the frontal area) and reducing discomfort (usually by asking the rider for the perception of comfort). Currently, there are no reports in the literature about the selection of posture in cycling considering the aerodynamic drag, the power delivery capacity, the vibration transmission, and the pressure in contact areas simultaneously. Even though there are studies regarding the effect of posture on performance and interaction, further exploration is needed. The main reason is that the information available has been obtained with different methodologies and not for the same body postures. For this reason, the information cannot be directly compared. Additionally, for the power delivery capacity, there is no general agreement about the effect of posture. For the aerodynamic resistance, most of the experiments are performed in a wind tunnel, which requires resources that may not be widely available for research. For the pressure distribution, there is no available information regarding pressure in all contact points. Finally, for the vibration transmission to the cyclist, there is no information about the effect of posture variation beyond hand position and wrist angle.

This project's overall goal is to understand better the relationship between road cyclist's posture, performance, and interaction with the bicycle so appropriate postures can be suggested depending on the riding conditions (*i.e.*, rider and bicycle characteristics, road grade, and wind speed). For performance analysis, the capacity to deliver power and the aerodynamic drag are used to estimate the total race time, considering a possible trade-off between them. For cyclist-bicycle interaction, the pressure in contact areas and the vibration transmission to the rider are studied considering their dependence on exposure time.

1.1. RESEARCH OBJECTIVES

The research's general objective is to propose postures for bicycle-cyclist sets under specific riding conditions (i.e., characteristics of the cyclist, bicycle and road, and cyclist objectives) considering the relationship between posture, performance, and interaction with the bicycle.

A scheme of the specific objectives is presented in Figure 1.1. The four specific objectives defined for the research project and the associated hypotheses are described below.

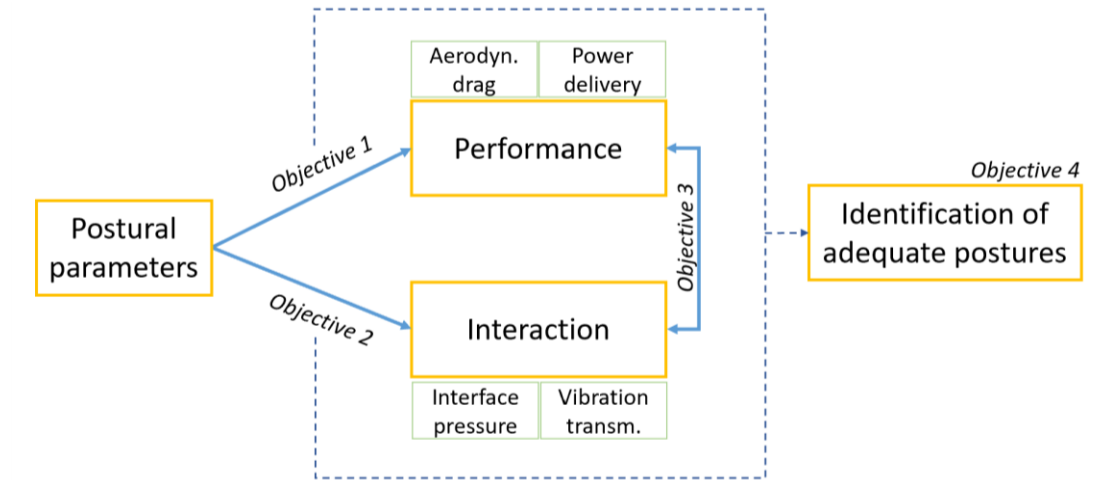


Figure 1.1. Methodology of the research.

1.1.1. Objective 1

Investigate the relationship between cyclists' body posture and performance regarding aerodynamic drag and power delivery capacity.

Objective 1 aims at revising the effect that variations of posture have on the performance of a cyclist. On the one hand, the posture influences the effective frontal area of the cyclist-bicycle set, which directly impacts the resistive force due to the surrounding air. On the other hand, the power delivery capacity is affected by posture due to the muscles' biomechanics and the respiratory function. Given that posture influences aerodynamic drag and power delivery capacity, optimal postures in cycling represent a compromise between power output and aerodynamics [16].

Experimental tests are performed to estimate the cyclist's capacity to deliver power and estimate the drag coefficient of the bicycle-cyclist set for the same postures.

It was hypothesized that power delivery capacity and aerodynamic drag vary with the posture. It was also hypothesized that the direction of improvement is the opposite for power delivery and aerodynamic drag (i.e., they are competitive).

1.1.2. Objective 2

Investigate the relationship between cyclists' body posture and interaction between cyclists and bicycles regarding pressure in contact areas and vibration transmission.

Objective 2 aims at studying the effect that variations of posture have on the interaction between the bicycle and the cyclist in terms of pressure in contact areas and vibration transmission. The pressure in contact points is affected by the posture due to an effect of load transfer (i.e., the pressure between contact points) and the segment that is effectively in contact with the bicycle (i.e., the pressure in each contact point). The vibration transmission is affected by the cyclist's posture as its mass is relevant compared with the bicycle's mass, affecting the system's dynamic behavior.

Experimental tests are performed to measure pressure distribution in contact points and to estimate the vibration transmitted to the rider.

It was hypothesized that pressure in contact points and vibration transmitted to the cyclist vary with the posture. A trade-off between the interaction indices and performance indices with conflicting directions of improvement was also hypothesized.

1.1.3. Objective 3

Define regressive models to describe posture-performance and posture-interaction relations.

Objective 3 aims at defining mathematical models that describe the variation of performance and interaction as a function of postural parameters. The models are constructed from the experimental data obtained during the development of objectives 1 and 2 for the same body postures.

It was hypothesized that mathematical models could be constructed to represent performance and interaction as a function of postural parameters.

1.1.4. Objective 4

Propose an optimization model to suggest adequate body postures depending on the riding conditions and cyclists' objectives.

Objective 4 aims at combining the information gathered on the relationship between road cyclist's posture, performance, and interaction with the bicycle. An optimization model is proposed to allow suggesting postures according to the cyclist requirements and constraints on performance and interaction with the bicycle.

It was hypothesized that for a specific cyclist-bicycle set, it is possible to determine postures considering performance and interaction indices simultaneously.

1.2. GENERAL METHODOLOGY

The methodology to achieve the general objective is presented in this section divided into four stages, as presented in Figure 1.2. The stages correspond to the processes to identify adequate postures for bicycle-cyclist sets. An adequate posture aims at improving bicycle speed while reducing the probability of overuse injuries due to high pressure or vibration transmission to the rider.

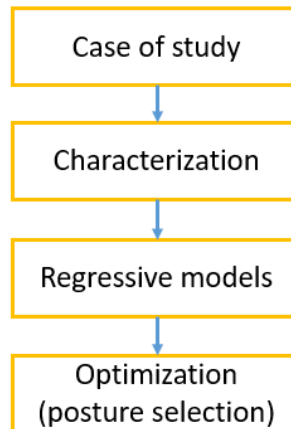


Figure 1.2. General scheme for posture identification.

The process begins with establishing the case of study, which is composed of the cyclist, bicycle, road, wind speed, and postural parameters to vary. Then, the aerodynamic drag, power delivery capacity, pressure in contact areas, and vibration transmission are characterized for the bicycle-cyclist set for the postures defined by the variation of the defined postural parameters. Afterward, the information of the measured postures is used to approximate the behavior of the aerodynamic drag, power delivery capacity, pressure in contact points, and vibration transmission of intermediate postures. Finally, an optimization model is used to select the posture that leads to the best race time meeting the limits related to interaction constraints. A detailed scheme of the process is presented in Figure 1.3.

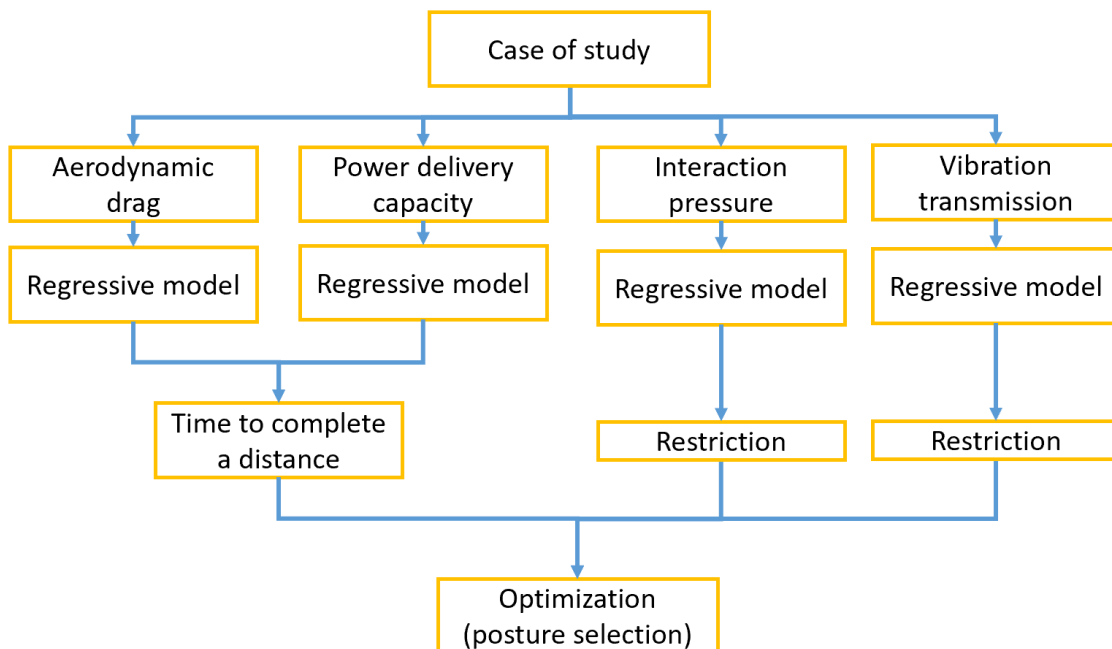


Figure 1.3. Detailed scheme for posture identification.

1.3. DOCUMENT STRUCTURE

This thesis document is organized following the blocks of the research methodology presented in Figure 1.3. Chapter 2 describes the case studies analyzed in this project detailing the postures and bicycle-cyclist sets' characteristics. Chapters 3 to 6 present the methodologies used to characterize the aerodynamic drag, power delivery capacity, pressure in contact areas, and vibration transmission, respectively. Each chapter includes a literature review of studies addressing the effect of posture in the variable addressed and presents the methodology and the results of its implementation to characterize the bicycle-cyclist sets included in the study. It is verified that each methodology is able to identify differences due to the variation of posture selected for the cases of study. In chapter 7, a methodology for selecting and optimizing postures based on the optimization of race time constrained by the interaction variables is presented. The methodology is implemented using the data registered in previous chapters for the bicycle-cyclist sets under study. Chapter 8 presents the general conclusions of the project. Finally, chapter 9 contains the references, and chapter 9, the appendices of the document.

CHAPTER 2. Description of cases of study: postures and bicycle-cyclist sets under study

2.1. ABSTRACT

The methodology proposed in this research to study the effect of posture on performance and interaction indices was implemented on a group of cyclists riding their own bicycles in two different postures. The characteristics of the bicycle-cyclist sets and the postures studied are fundamental for understanding the results obtained in this research's core chapters (*i.e.*, Chapters 3 to 7). This, because the performance and interaction variables have a strong dependence on the bicycles, cyclists, and postures assessed. For this reason, the characteristics of the riders, bicycles, and postures tested in the implementation of the methodology are described in this chapter. It is worth highlighting that this chapter is purely descriptive.

Five recreational-level cyclists (one woman and four men, mass: 73.8 ± 11.8 kg, height: 1.75 ± 0.06 m, age: 35.0 ± 6.7 years) voluntarily participated in the study. The riders participated in the study riding their own bicycles. Road bicycles of different qualities were included in the study. Bicycle-cyclist sets with varied characteristics were included to compare the results obtained for different cases.

The postural parameter selected for the implementation of the methodology was the height of the elbow pads while riding in aerobars. The postures tested were defined from each bicycle's fit window as the upper and lower limits of the aerobars' height. The difference between aerobars' height varied between 40 mm and 55 mm for each set.

2.2. BACKGROUND ON THE DEFINITION OF POSTURE IN CYCLING

The posture of a cyclist is defined by the bicycle's geometry and the body's positioning itself. Regarding the positioning of the body, the cyclist can modify the posture, independently from the bicycle's geometric configuration, by varying the location and characteristics of the contact points with the bicycle, the inclination of body segments, or the curvature of the trunk. Regarding the variation of posture due to the bicycle's geometry, it defines the general location of the contact points with the rider.

2.2.1. *Location and characteristics of the contact points with the bicycle*

The contact points are buttocks-saddle, hands-handlebar, and feet-pedals. For example, the buttocks can be repositioned in the saddle by moving forward or backward or tilting the pelvis. The hands can also be positioned in different handlebar spots for upright or aerodynamic postures or better maneuverability. The cyclist can also be positioned in aerobars. In this particular case, the elbows are also in contact with the bicycle, replacing the hands-handlebar contact point. Finally, the feet are rarely modified with respect to the pedals as the shoes are fixed to the pedals. The variations in this point are usually performed by modifying the bicycle. The only modification that can be performed at this point is the position and orientation of cleats. The variation in these parameters is exemplified in Figure 2.1.



Figure 2.1. Variation of posture due to the location of contact points.

2.2.2. Inclination of body segments

The angular position of the forearms, arms, and trunk modify the posture. For example, in upright postures, the forearm and arm tend to be aligned (i.e., approximately 180 °). The angle of the head/neck can also be varied, modifying the posture. For aerodynamic postures, cyclists seek to reduce the frontal area by, for example, lowering the head. The variation in these parameters is exemplified in Figure 2.2.

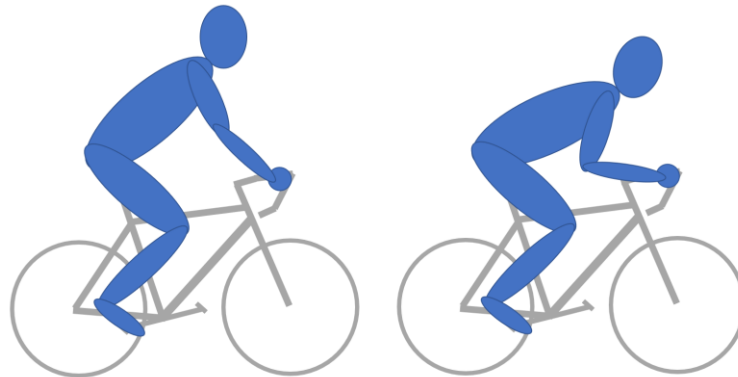


Figure 2.2. Variation of posture due to body segment orientation. Example: elbow angle. Left: straight arms, Right: bent arms.

2.2.3. Curvature of the trunk

The trunk curvature is modified by the pelvis and chest rotation, as exemplified in Figure 2.3.

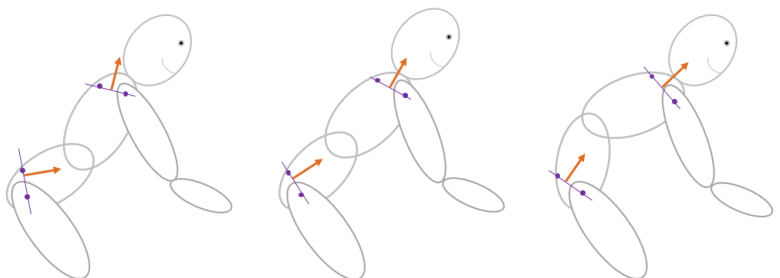


Figure 2.3. Variation of posture due to trunk curvature.

2.2.4. Bicycle geometry

The size of the frame constraints the range of the position of the contact points, and the configuration of the saddle, handlebar, and crank arm specify the location in the space. The saddle can be moved longitudinally (i.e., front, rear) by adjusting the saddle on the seat post and vertically by adjusting the seat post. The handlebar can be moved longitudinally and vertically with spacers on the handlebar post and longitudinally by changing the stem. Finally, the longitude of the cranks can be varied to modify the position of pedals. If the cyclist uses aerobars, the elbows' position can be modified depending on the aerobars vertically, longitudinally, and laterally. The main parameters for the geometric configuration of a bicycle are presented in Figure 2.4.



Figure 2.4. Variation of posture due to the location of contact points defined by the bicycle geometry.

2.3. POSTURES CONSIDERED FOR THE METHODOLOGY IMPLEMENTATION

For the implementation of the methodology proposed in this research to study the effect of posture on performance and interaction indices, one postural parameter was chosen to define the tested postures. It was defined that the implementation would be performed in aerobars postures differentiated by the height of the aerobars. This section describes the postures tested and the reasons for their selection.

2.3.1. Aerobars posture

The use of aerobars' postures is frequent in competitions in which the aerodynamic drag is relevant, and the danger of collision with other riders is relatively low. Examples of the events are most triathlon events and specific road cycling events (i.e., road time trials, individual and team pursuit, and short track time trials [34]). In events as mass-start races, the use of aerobars is not allowed because of the potential damage to other cyclists in case of an accident. The main advantage of using aerobars is the possibility of projecting the body forward; this means higher trunk flexion and knees anterior position [35], leading to lower drag areas. The main disadvantages are lower stability for steering and control [36].

The aerobars' postures are of particular interest in cycling because of their positive impact on aerodynamic drag reduction. In a first approach, an aerobars posture is designed to optimize aerodynamics by narrowing the arms, lowering the chin, and keeping the knees in [37].

Nevertheless, it has been reported that in aerobars posture, the power delivery capacity is negatively affected [6], [7], [38]-[42] and that the contact with the saddle area is concentrated in a smaller area leading to higher pressures in the anterior zone (i.e., compression of the genital area) [30], [37], [42]. Additionally, the advantages of riding in this posture regarding the time to complete a distance are significant only if the rider can sustain the posture during the race. For this reason, the trade-off between performance and other indices related to the interaction with the bicycle (e.g., pressure in contact points, vibration transmission, and comfort evaluation) is relevant for this scenario.

Several studies have analyzed the difference in performance when the posture is varied from an upright posture to an aerobars posture, and some studies have included in the analysis drops posture as an intermediate posture. The effect of changing from an upright posture to an aerobars posture has been studied on the capacity of power delivery [6], [7], [39], [41], the aerodynamic drag [40], and the pressure in the buttocks [30], generally concluding that in aerobars postures the power delivery capacity decreases, the frontal projected area decreases, and the potential for overuse injuries in the buttocks-saddle contact increases. Nevertheless, few studies have focused on the relevance of small modifications among the aerobars' postures. For example, different head/helmet and torso inclinations and positions of the elbows and saddle have been tested, concluding that these variables influence the aerodynamic drag while riding in aerobars postures [11], [13]. Similarly, from tests performed with different trunk angles, it was concluded that lower torso angles reduce the capacity to deliver power [38]. The effect of handlebar height and separation effect on aerodynamics was studied in [43], concluding that both affect the drag area. Appendix 2.1 presents further information about studies performed for aerobars postures. In addition, there is a gap in the guidelines to correctly define aerobars' postures concerning the guidelines for traditional postures. In the case of aerobars, it has been described for the arms that the upper arm should be approximately vertical with the elbows slightly ahead of the shoulders [37] forming an elbow angle close to 90° [44] and that the standard elbow spacing is 120 mm [13]. For the trunk and lower body, it has been suggested to maintain the hip flexion between 90° and 105° [44], slightly move the saddle forwards and upwards, and tilt it down when changing from a traditional posture to aerobars [45]. For this reason, some cyclists select their aerobars posture aiming for an aerodynamically aggressive posture and limiting it by their estimation of their capacity to sustain the posture (i.e., a trial and error approach).

2.3.2. Height of aerobars

The postural parameter selected is the height of the aerobars. This parameter was chosen because of three main reasons. First, the postures in aerobars are strongly defined by the bicycle geometry as the elbows are in contact with the bicycle, restricting the riders' movement; for this reason, aerobars postures are more repeatable than traditional postures. Second, the height of the aerobars can usually be varied in a relatively wide range using spacers. Third, the effect of the positioning of aerobars is of interest due to its low aerodynamic drag; nevertheless, aerobars' postures are difficult to sustain as they impose more strict restrictions on the rider, increasing discomfort.

The aerobars' height can be modified in three ways depending on the bicycle's fit window. First, the number of spacers on the stem can be varied. Second, the stem can be rotated or changed for

another stem with a different angle. Third, using spacers for the elbow pads. Figure 2.5 presents examples of handlebars with built-on aerobars and clip-on aerobars.

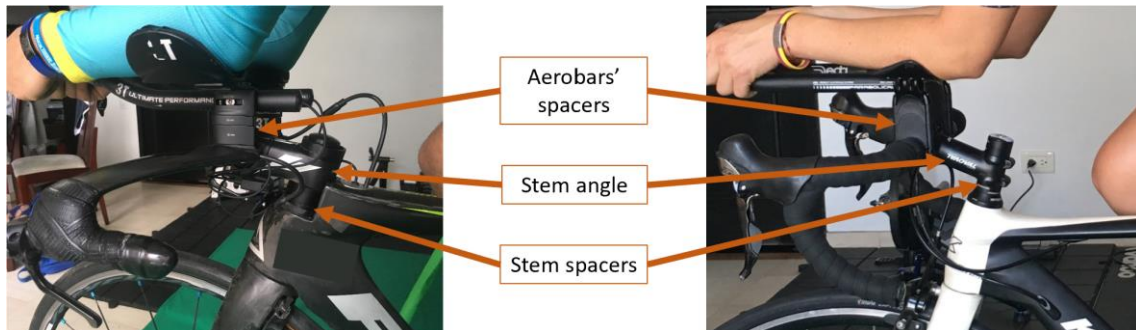


Figure 2.5. Examples of different types of handlebars with aerobars. Left: built-on aerobars. Right: clip-on aerobars.

2.3.3. Postures characterized: Aerobars high (ABhigh) and Aerobars low (ABlow)

For the implementation of the methodology, two postures were tested: with the aerobars in the highest and lowest configurable limits of the bicycle (*i.e.*, ABhigh and ABlow, respectively). The differences between the postures are defined only by the bicycle's geometry, varying mainly the trunk's angle. Besides the aerobars' height adjustment, the following considerations were made for each bicycle-cyclist set:

- Constant lateral and longitudinal position of pads with respect to the handlebar mount. The position of the elbow pads on the supporting structure was not modified.
- Constant lateral distance between pads and stem. The lateral position of the aerobars was measured and kept constant over the tests. It was verified that both aerobars were symmetric with respect to the sagittal plane.
- Constant angle with respect to the floor. A level was used to verify that the aerobars were installed at a 0 degrees angle (*i.e.*, parallel to the ground).
- Constant saddle height. The saddle height was not modified for the tests with the objective of using the condition in which the cyclist is used to ride.
- Constant longitudinal position of hands. The rider was instructed to keep the hands in a constant position.
- Constant trunk's curvature and buttocks' position on the saddle. The rider was asked to ride naturally and comfortably with constant postures.

2.4. BICYCLE-CYCLIST SETS CONSIDERED FOR THE METHODOLOGY IMPLEMENTATION

This study was performed in terms of bicycle-cyclist sets. It was decided that each rider should be characterized on their own bicycle to represent real riding conditions. With this choice, it was guaranteed that the variables measured would not be affected by the bicycle components. For example, the use of a different saddle could affect power delivery or pressure in contact areas. Another example is that the use of a different handlebar could affect handling with possible

implications on maneuverability and hence, security. In addition, with this choice, the postures tested for each rider are close to the postures usually used by them.

From the choice of including bicycle-cyclist sets, it is considered that each set is a particular case. For this reason, different variations of the aerobars' height are included in the study as this variable depends on the fit window of each bicycle. Also, given the wide variability of characteristics between bicycles and cyclists, it is expected for some variables as the drag area parameters to present a trend for the group of cyclists. In contrast, for variables as the pressure in contact areas, it is expected to find specific patterns for each set.

Five cyclists voluntarily participated with their bicycles in the implementation of the methodology proposed in this research. The riders signed an informed consent form (see Appendix 2.2). Different types of riders and bicycles were included in the study to explore the results obtained for riders and bicycles with specific characteristics. Also, the inclusion of a group of cyclists with varied characteristics allows exploring possible scenarios that can be found during the posture selection process. The group of cyclists was selected to include riders of both genders (four male and one female), with different ages (a male rider for each of the age categories Senior/Elite, Masters A, Masters B, and Masters C), and different anthropometrical characteristics (four classified as healthy weighted and one as overweighted). The common characteristics of the group of riders included in the study are that they were recreational level cyclists, had experience in road cycling, had participated in cycling or triathlon races, and had experience riding in time-trial postures with aerobars. In addition, the participants reported they had no injuries that could affect their cycling performance. Finally, considering that all the tests of the study were performed in a city located at an altitude of 2600 meters above sea level, only cyclists that were adapted to this altitude were included. This was verified to avoid possible altitude effects on cyclists' power output, such as those reported by Garvican-Lewis et al. [46]. To this end, it was checked that all the cyclists lived in the same city for at least five years. The riders performed the tests using standard cycling equipment (*i.e.*, cycling helmet, short-sleeve cycling jersey, padded cycling shorts, and clipless pedal shoes). Table 2.1 presents the main information of the riders that participated in the study.

	Variable	Units	Set				
			1	2	3	4	5
Rider	Height	[m]	1.67	1.72	1.76	1.78	1.83
	Mass	[kg]	59	72	92	73	73
	Age	[years]	38	26	42	39	30
	Gender	[-]	Female	Male	Male	Male	Male
	FTP from historical records	[W]	140	217	168	169	193

Table 2.1. Information on bicycle-cyclist sets' riders included in the study.

Regarding the bicycles, endurance, time trial, and aero road bicycles of different qualities were included. The time trial bicycles are designed to improve aerodynamic resistance; for this reason, the frame has a larger seat tube angle than road bicycles to allow the rider to adopt more aerodynamically-demanding postures. In these bicycles, the shifters and brake levers are located at the end of the aerobars. The triathlon bicycles usually have a smaller fit window than traditional road bicycles. The endurance bicycles are the traditional road bicycles designed to be faster than the bicycles of other cycling disciplines. The aero road bicycles are an intermediate type of bicycle between the endurance and the time trial bicycles with some features designed to be more

aerodynamically efficient than the endurance bicycles without the time trial bicycles' level of specialization. Table 2.2 presents the main information on the bicycles included in the study. Table 2.3 presents the settings of the bicycle for each cyclist.

	Variable	Units	Set				
			1	2	3	4	5
Bicycle	Type	[-]	Aero	Time trial	Aero	Endurance	Time trial
	Frame brand	[-]	Talon, Kestrel, USA	Transonic, Fuji, China	Talon, Kestrel, USA	Flamma, GW, Colombia	E117, Argon 18, Canada
	Frame size	[-]	52	48.4	55	49	51.5
	Frame material	[-]	Carbon fiber	Carbon fiber	Carbon fiber	Aluminum	Carbon fiber
	Tires	[-]	Zaffiro Pro slick, Vittoria, Italia (700 x 23c)	Ultrasport, Continental, Germany (700 x 23c)	Rubino Pro, Vittoria, Italia (700 x 23c)	Ultrasport, Continental, Germany (700 x 23c)	4000 S, Continental, Germany (700 x 23c)
	Saddle	[-]	Lady, Selle Italia, Italy	Adamo PS 1.1, ISM, USA	300, Oval concepts, USA	Galápagos, GW, Colombia	Stealth, PRO, The Netherlands
	Aerobars	[-]	Parabolica uno, Deda elementi, Italy	Revo, 3T, Italy	Parabolica uno, Deda elementi, Italy	Parabolica uno, Deda elementi, Italy	Trimax, Vision, USA
	Mass	[kg]	11.1	10.2	11.0	11.5	9.9

Table 2.2. Information on bicycle-cyclist sets' bicycles included in the study.

	Variable	Units	Set				
			1	2	3	4	5
Posture	Aerobars' height fit window	[mm]	55	55	55	55	40
	Aerobars' elbow pads lateral distance	[cm]	18	19	17	18	23
	Saddle height	[mm]	767	750	733	745	775

Table 2.3. Information on bicycle-cyclist sets' postures included in the study.

Figures 2.6 to 2.10 present photographs of the bicycle-cyclist sets in the two postures tested.





Figure 2.9. Bicycle-cyclist set 4.



Figure 2.10. Bicycle-cyclist set 5.

Figure 2.11 presents the difference in the upper body of the cyclists when riding in the tested postures. The figure shows the sagittal and coronal planes.



Figure 2.11. Lateral and frontal view of the cyclists' upper body in the tested postures.

CHAPTER 3. Performance: measurement of aerodynamic drag

Related publications:

[47] A. Polanco, S. Roa, D. Suarez, O. Lopez and L. Munoz, "Importance of wind speed and road grade for the estimation of drag area in cycling," *Sport. Biomech.*, 2020 [under review: minor changes].

[48] A. Polanco, J. Fuentes, S. Porras, D. Castiblanco, J. Uribe, D. Suarez and L. Munoz, "Methodology for the estimation of the aerodynamic drag parameters of cyclists," in *ASME 2019 International Design Engineering Technical Conference, IDETC 2019, Anaheim, USA, August 18-21, 2019*, pp. 1-8.

[49] S. Porras, A. Polanco, S. Roa, D. Suarez, O. Lopez and L. Munoz, "Experimental study of the aerodynamic drag on light vehicles," in *IV Congreso Internacional sobre Tecnologías Avanzadas de Diseño, Mecatrónica y Manufactura, AMDM 2018, Manizales, Colombia, 7-9 November, 2018*, pp. 516-518.

3.1. ABSTRACT

The aerodynamic drag force has a relevant effect on cycling performance since it is one of the major resistive forces acting on the bicycle. For this reason, the estimation of the drag area is of interest, and several efforts have been made to predict the aerodynamic parameters of bicycle-cyclist sets. The effect of posture on aerodynamic drag has been widely studied, and it is accepted that the posture of the cyclist is relevant to this parameter. Even small variations as modifications in the hands or the elbows' position while riding in aerobars can be performed to improve the cyclist's aerodynamics. The possibility of measuring the effect of small variations depends on the accuracy of the method used. Usually, small modifications in posture can be measured only when tested on wind tunnels. For this reason, this chapter implements a methodology for the measurement of aerodynamic drag in cycling with enough sensibility to measure differences due to the variation of the aerobars' height.

The methodology is based on outdoor road tests and includes data of the wind speed relative to the bicycle and the road grade to reduce the variability of the results due to these variables. The methodology was developed as a low-cost tool to estimate the drag area of cyclists. The methodology was implemented to identify the drag area values of different bicycle-cyclist sets in two postures with different aerobars' heights.

The drag area was estimated for all the bicycle-cyclist sets obtaining lower values for the posture with lower heights of the aerobars. An average difference of 10% (equivalent to 0.03 m^2) in the drag area between postures was obtained. Normalizing the drag area values by the aerobars' height displacement, a reduction of 2% in the drag area was computed for each centimeter of height modified. The drag area's average standard uncertainty was estimated as 5% of the drag area (equivalent to 0.013 m^2). The methodology's implementation permitted measuring differences in bicycle-cyclist sets' drag area due to the variation in aerobars' height.

3.2. INTRODUCTION

Aerodynamic resistance is directly related to the cyclists' performance because it increases the energy demand to move. In road cycling, at high speeds, the aerodynamic drag accounts for up to 90% of the total resistance opposing the bicycle movement [14], [50]. For this reason, it has been widely studied due to its relevance for performance improvement [11], [13], [50]-[54].

The aerodynamic drag can be represented through reduced-order models considering the longitudinal dynamics of the bicycle-cyclist set. In these models, the characteristics of the aerodynamic drag of the bodies are represented by the drag area ($C_D A$), which is the product of the drag coefficient (C_D) and the projected frontal area (A). The drag area has been estimated through tests performed in wind tunnels, computational simulations, and road tests (see Appendix 3.1). Each approach has specific characteristics, advantages, and disadvantages. The use of wind tunnels is characterized by its high reliability and sensitivity; thus, values obtained with this method are commonly used as a reference [50], [53]. Nevertheless, the costs associated with wind tunnels for cycling tests are high; additionally, these tests do not represent all the actual conditions of outdoor

cycling [50], [53]. For example, the testing conditions are usually "representative for the case where only the cyclist is moving and where the speed of the surrounding air is zero" [55]. The use of computational simulations has gained relevance as their results have shown good agreement with reference values; also, computational simulations provide detailed flow field information [16], [55]. This approach is under development as it has some limitations, mainly regarding the complexity of the bicycle and rider geometry [55], the complexity of the physics of the fluid in cases with massive separation, and the limitations of classical turbulence models under these conditions. The road tests are implemented with actual cycling conditions, which leads to results that reflect those conditions. Nevertheless, this type of tests' accuracy depends on several factors that vary according to the selected method. For example, the road inclination and the wind speed are limiting factors because the wind speed continuously varies, and the road grade depends on the testing route [51], [56], [57].

The effect of posture on aerodynamic drag has been widely studied, and it is accepted that the posture of the cyclist is relevant to this parameter. Even small variations in aerobars posture as the hands' longitudinal position in the aerobars, the lateral elbow distance [13], or the head orientation [11] can be performed to improve the aerodynamics of the cyclist. The possibility of measuring the effect of small variations depends on the accuracy of the method used. Usually, small modifications in posture can be measured only when tested on wind tunnels. For this reason, the objective of this chapter is to implement a methodology for the measurement of aerodynamic drag in cycling with enough sensibility to measure differences due to the variation of the aerobars' height.

This chapter presents an experimental outdoor methodology to identify the $C_D A$ of bicycle-cyclist sets. The methodology considers onboard anemometry and road grade measurements. The methodology is based on a mathematical model of the longitudinal dynamics of a bicycle-cyclist set that simultaneously estimates $C_D A$ and the rolling resistance coefficient (f_r). The methodology was successfully implemented to estimate the parameters for a group of cyclists riding in different postures differentiated by the height of the aerobars.

3.3. METHODS

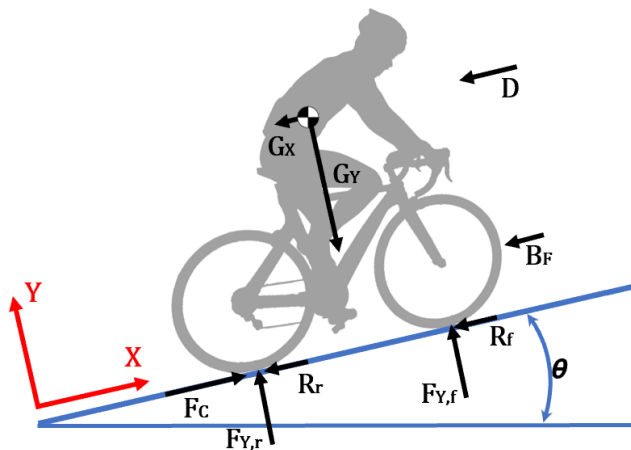
The experimental method used to identify the $C_D A$ is based on a mathematical model of the longitudinal dynamics of the bicycle-cyclist set. This section presents the mathematical model, the experimental protocol, and the sets included in the study.

3.3.1. *Mathematical model*

When a bicycle is ridden straight forward, its motion can be described using a reduced-order model for its longitudinal equation of motion. The model represents all the forces acting on the set formed by the bicycle and its rider. Each reduced-order representation of a force is typically constructed using equivalence principles, aiming to represent the main influences of the riding conditions on each term.

Figure 3.1 shows a two-dimensional representation of the free body diagram of a bicycle-cyclist set on the sagittal plane. A reference frame oriented in the direction of the motion is used for the

representation of the forces. Three resistive forces are considered: first, the aerodynamic drag (D); second, the total rolling resistance (R_x), obtained by adding the rolling resistance forces acting on the rear and front wheels (R_r and R_f , respectively); third, the bearing resistance (B_F). The weight is represented in the rotated frame through G_x and G_y , which are its components in the longitudinal and perpendicular directions with respect to the road, respectively. The forces $F_{Y,f}$ and $F_{Y,r}$, represent the normal interaction of the road with the front and rear wheels, respectively. In the diagram, the action of the rider is represented by the tractive force on the rear wheel (F_c).



- B_F : bearing resistance
- D : aerodynamic drag
- F_c : tractive force
- $F_{Y,f}$: normal interaction with front wheel
- $F_{Y,r}$: normal interaction with rear wheel
- G_x : weight component in x direction
- G_y : weight component in y direction
- R_r : rolling resistance force on front wheel
- R_f : rolling resistance force on rear wheel
- θ : inclination angle

Figure 3.1. Bicycle-cyclist set free body diagram.

The reduced-order expression for the aerodynamic drag force is shown in Eq. (3.1), where D is represented as a function of air density (ρ), drag coefficient (C_D), projected frontal area (A), and speed of the wind relative to the bicycle ($v_{w/b}$) [58]. Often, the product $C_D A$ is known as drag area.

$$D = \frac{1}{2} \rho C_D A v_{w/b}^2 \quad (3.1)$$

The rolling resistance is modeled considering the product of the rolling resistance coefficient with the normal load on a given tire. For this model, it is assumed that the same rolling coefficient (f_r) represents both tires. It is also assumed that the road has a steady grade. Under those assumptions, Eq. (3.2) presents the total rolling resistance:

$$R_x = R_r + R_f = mg \cos(\theta) f_r \quad (3.2)$$

where g is the gravitational acceleration. The equivalent bearing resistance (B_F) is obtained representing the dissipation originated by the bearings of the bicycle. It is modeled as a linear function of the bicycle speed (v_b), with two parameters, c_1 and c_2 [59] as shown in Eq. (3.3).

$$B_F = c_1 + c_2 v_b \quad (3.3)$$

The longitudinal component of weight (G_x) is shown in Eq. (3.4). It is obtained considering that the road grade is represented by an inclination angle (θ), which is measured with respect to a horizontal reference.

$$G_x = mg\sin(\theta) \quad (3.4)$$

The traction force (F_C) can be expressed in terms of the power delivered through the rear wheel to the road and the bicycle speed. Since the power that the cyclist delivers to the pedals (P) can be measured, it is useful to compute F_C in terms of P , v_b , and the power transmission efficiency of the bicycle (η), as shown in Eq. (3.5).

$$F_C = \frac{\eta P}{v_b} \quad (3.5)$$

Finally, when the wheels' slip is negligible, the bicycle's longitudinal motion can be represented using a single degree of freedom. In that case, the equivalent mass (M_{eq}) is used to represent all the inertial terms of the bicycle. M_{eq} can be obtained by adding the total translational mass (m) and the translational equivalent of the rotational inertia of each wheel. This translational equivalent depends on the rotational inertia (I) and the effective radius (r) of each wheel. Eq. (3.6) presents an expression for the equivalent mass.

$$M_{eq} = \left(m + 2 \frac{I}{r^2} \right) \quad (3.6)$$

The longitudinal equation of motion can be constructed, considering the longitudinal external forces that act on the bicycle, the equivalent mass, and the longitudinal acceleration of the bicycle (a). The condensed expression for the equation of motion is presented in Eq. (3.7).

$$M_{eq}a = F_C - D - R_x - G_x - B_F \quad (3.7)$$

The expanded version of the equation of motion can be obtained by replacing the terms in Eq. (3.7). For a case in which the scope is the identification of $C_D A$ and f_r , the terms can be rearranged, as shown in Eq. (3.8).

$$\frac{1}{2} \rho C_D A v_{w/b}^2 + mg\cos(\theta)f_r = \frac{\eta P}{v_b} - M_{eq}a - mg\sin(\theta) - c_1 - c_2 v_b \quad (3.8)$$

It is worth noticing that Eq. (3.8) is an instantaneous expression. When a set of constant-speed experiments are performed, it is useful to integrate the equation of motion over each time interval, leading to an averaged version of the equation. The averaged version of the equation seeks to represent the motion in a way in which the effect of random perturbations during the test can be reduced. Equation 3.9 shows the averaged version of the expression corresponding with a given time interval. The overline notation is used for the averages, emphasizing the terms that are integrated along time.

$$\frac{1}{2} \rho C_D A \overline{v_{w/b}^2} + mg \overline{\cos(\theta)} f_r = \eta \left(\frac{\overline{P}}{\overline{v_b}} \right) - M_{eq} \overline{a} - mg \overline{\sin(\theta)} - c_1 - c_2 \overline{v_b} \quad (3.9)$$

In this case, the identification of the unknowns corresponds to the solution of a linear identification problem of the form $\mathcal{M}x = b$. The unknown vector x is composed of the two parameters to identify, as shown in Eq. (3.10).

$$x = \begin{bmatrix} C_D A \\ f_r \end{bmatrix} \quad (3.10)$$

The linear identification problem requires to take into account at least two different intervals. The matrix \mathcal{M} of the linear identification problem is a $N \times 2$ matrix, where N is the number of different intervals used for the identification. The two components of matrix \mathcal{M} for a given row j (with $1 \leq j \leq N$) are presented in Eq. (3.11) and Eq. (3.12).

$$\mathcal{M}_{j,1} = \frac{1}{2} \rho_j (\overline{v_{w/b}^2})_j \quad (3.11)$$

$$\mathcal{M}_{j,2} = mg(\overline{\cos(\theta)})_j \quad (3.12)$$

The last term in the formulation of the linear identification problem is the vector b , which has N rows. Equation (3.13) presents the term that corresponds to a given row j .

$$b_j = \eta \left(\frac{\overline{P}}{v_b} \right)_j - M_{eq} \bar{a}_j - mg(\overline{\sin(\theta)})_j - c_1 - c_2 (\overline{v_b})_j \quad (3.13)$$

When $N > 2$, the linear identification problem is redundant. This condition is useful to deal with the uncertainty associated with the experimental measurement. The matrix form of the linear least-squares method can be used for the solution of this redundant linear identification problem. The identified resistive parameters are obtained, as shown in Eq. (3.14).

$$\begin{bmatrix} C_D A \\ f_r \end{bmatrix} = (\mathcal{M}^T \mathcal{M})^{-1} \mathcal{M}^T b \quad (3.14)$$

3.3.2. Experimental assessment

An experimental methodology used to identify $C_D A$ and f_r of different bicycle-cyclist sets is based on outdoor road tests considering onboard anemometry and road grade measurement. The objective of the methodology is to measure enough data to be able to identify $C_D A$ and f_r from the model presented in Eq. (3.9). For this, the cyclists perform several one-way rides along a test route at different constant speeds (*i.e.*, trials or intervals in the mathematical model). The road grade is previously characterized, and the wind speed relative to the bicycle is measured during the tests. The power delivered by the cyclist, the bicycle speed, and the ambient conditions are also registered on the route and averaged for each trial. Inertial and geometrical parameters of the bicycle-cyclist set are also measured or estimated. The protocol is summarized in Appendix 3.2.

Five recreational cyclists voluntarily participated in the tests after signing an informed consent form (mass: 73.8 ± 11.8 kg, height: 1.75 ± 0.06 m, age: 35 ± 7 years). The riders used their own bicycles and

standard cycling clothes. The tests were performed in two aerobars postures with different heights. For road bicycles, clip-on aerobars were used. Depending on each bicycle's characteristics, the height was varied using spacers on the headtube stem or the aerobars support. Table 3.1 presents a summary of the information of each bicycle-cyclist set (further detail can be found in Tables 2.1, 2.2, and 2.3 in chapter 2). The tests were performed in an asphalt, straight route, located at an altitude of 2600 meters above sea level, with a length of 450 m, and exclusive dedication to bicycles. Each cyclist performed 10 trials on each posture. The trials were performed at constant speeds between 18 km/h and 27 km/h. The tires of all the bicycles were inflated at 8 bar.

	Variables	Units	Set				
			1	2	3	4	5
Rider	Mass	[kg]	59	72	92	73	73
	Height	[m]	1.67	1.72	1.76	1.78	1.83
	Gender	[-]	Female	Male	Male	Male	Male
Bicycle	Type	[-]	Aero	Time trial	Aero	Endurance	Time trial
	Mass	[kg]	11.1	10.2	11	11.5	9.9
	Aerobars' height difference	[mm]	55	55	55	55	40

Table 3.1. Bicycle-cyclist sets tested for the estimation of drag area in cycling.

The bicycle speed was measured with a speed sensor (Speed sensor 2, GARMIN, USA) located on the rear wheel hub coupled to a GPS cycle-computer (Forerunner 910XT, GARMIN, USA). The wind speed relative to the bicycle was measured with the onboard anemometer based on a pitot tube and developed specifically for this application, shown in Figure 3.2. The development of the anemometer is presented in detail in [48]. The test section's altimetry was measured with a topographical-grade Global Navigation Satellite System (GR-5, Topcon, Japan). The power delivered by the rider was measured with a power meter located in the pedals (Vector, GARMIN, USA). The average acceleration of each trial was numerically computed using the bicycle speed and the total interval duration. Figure 3.3 presents the setup used for the tests.



Figure 3.2. Anemometer developed for the estimation of drag area in cycling.



Figure 3.3. Setup for the implementation of the protocol to measure aerodynamic drag.

The air density was computed according to the model presented by [60]. For this, the temperature, relative humidity, and atmospheric pressure were registered with a weather station (Weather meter 4500, Kestrel, USA). The mass of the bicycle-cyclist set, including the mass of the instrumentation and riding equipment, was measured. The power transmission efficiency of the bicycle was taken from the literature [61]. The equivalent mass was computed from the wheels' inertia and effective radius. Table 3.2 summarizes the information of parameters defined for the implementation of the methodology.

Parameter	Units	Value
Transmission efficiency	[%]	97
Wheels' inertia	[kg.m ²]	0.05
Wheels' effective radius	[m]	0.33

Table 3.2. Parameters used for estimation of drag area

A road methodology with onboard wind speed measurement was chosen because there is not enough availability of wind tunnels in South America with the size necessary to measure the aerodynamic parameters of full-size bicycle-cyclist sets. Additionally, an onboard anemometer was used because the importance of including data of the wind speed relative to the bicycle was studied in [47], concluding that its omission negatively affects the drag area's estimation.

In this study, the results were obtained assuming that the rolling resistance coefficient was constant for each bicycle-cyclist set. Additionally, it was assumed that there was no strong crosswind during the tests.

The speeds used for the different trials were defined considering that, as found in [47], a larger number of trials leads to lower errors on the estimation of the parameters. Nevertheless, the time required to perform the tests also increases as the number of trials increases.

3.4. RESULTS AND DISCUSSION

3.4.1. Computation of the drag area

Table 3.3 summarizes the information of the parameters registered and computed for the measured bicycle-cyclist sets. Table 3.4 presents the results of the drag area and rolling resistance coefficient obtained for the different bicycle-cyclist sets. For the testing road segment, the average road grade was -0.13%, the minimum was -0.68%, and the maximum was 0.39%. It can be observed that the tailwind and headwind presented variations up to 11.9 m/s and 12.9 m/s, respectively. The tailwind and headwind values emphasize the relevance of including the wind speed in the estimation of the drag parameters.

Variable	Units	Posture	Set				
			1	2	3	4	5
Temperature	[°]	ABhigh	21.5	17.8	18.9	22.3	29.6
		ABlow	20.8	19.3	26.1	22.9	22.1
Relative humidity	[%]	ABhigh	56.2	55.9	59.2	58.7	42.6
		ABlow	51.9	44.0	47.8	50.2	52.2
Atmospheric pressure	[kPa]	ABhigh	75.4	75.1	75.2	75.2	75.2
		ABlow	75.4	75.1	75.2	75.2	74.9
Air density	[kg/m ³]	ABhigh	0.88	0.89	0.87	0.89	0.86
		ABlow	0.88	0.89	0.89	0.87	0.88
Total mass	[kg]	ABhigh	71.4	87.4	104.3	85.6	83.9
		ABlow	70.0	84.9	104.6	85.6	84.2
Equivalent mass	[kg]	ABhigh	72.3	88.3	105.5	105.2	84.8
		ABlow	79.9	85.8	105.2	105.5	85.1
Maximum tailwind	[m/s]	ABhigh	7.5	0.1	10.4	4.6	8.2
		ABlow	6.5	7.0	11.9	7.4	11.5
Maximum headwind	[m/s]	ABhigh	5.4	7.8	10.8	10.2	12.9
		ABlow	11.4	12.7	8.9	6.0	8.5

Table 3.3. Parameters measured and computed for the estimation of drag area and rolling resistance coefficient.

Variable	Units	Posture	Set				
			1	2	3	4	5
Drag area ($C_D A$)	[m ²]	ABhigh	0.28	0.26	0.27	0.33	0.29
		ABlow	0.25	0.23	0.23	0.31	0.26
Rolling resistance coefficient (f_r)	[-]	[-]	0.005	0.005	0.007	0.007	0.004

Table 3.4. Drag area and rolling resistance coefficient of cyclists in aerobars postures.

The Monte Carlo method was used to estimate the standard uncertainty of the $C_D A$ considering the recommendations presented in [62]. The propagation of uncertainty was performed for the model with the data acquired during the tests using 10^6 Monte Carlo trials. The distributions of the uncertainties of the variables used to estimate $C_D A$ were defined from the resolution and

specifications of the instruments, and values reported in the literature. The associated standard uncertainties for each $C_D A$ estimation is presented in Table 3.5. The average uncertainty estimated was 0.013 m^2 .

Variable	Units	Posture	Set				
			1	2	3	4	5
Drag area uncertainty	[m ²]	ABhigh	0.013	0.015	0.013	0.013	0.016
		ABlow	0.012	0.008	0.016	0.012	0.013

Table 3.4. Drag area and rolling resistance coefficient of cyclists in aerobars postures.

3.4.2. Effect of posture on the drag area

Regarding the results of the identification of the drag area, it can be observed that for all the sets, the values decreased when changing from ABhigh to ABlow. An average reduction between postures of 10% (equivalent to 0.03 m^2) was found. To perform a comparison with values reported in the literature, it is worth highlighting that a strict comparison of the values reported in different studies is difficult because the experimental conditions are varied (*e.g.*, experience and type of cyclists, type of bicycle, clothing, and accessories used). Nevertheless, when comparing the results obtained with data available in the literature (see Appendix 3.1), a good level of agreement was found on the values and the percentage difference when changing the posture. Furthermore, it was found that the $C_D A$ values vary among the sets, but the general trend is constant. The $C_D A$ decreases when the posture is varied from ABhigh to ABlow. Regarding the results of the identification of the rolling resistance coefficient, it can be observed in Appendix 3.1 that the values obtained in this study are in the range of the values reported in other studies.

Figure 3.4 presents a comparison of the $C_D A$ between postures for the tested sets. As expected, the same tendency is observed for all the sets with a reduction of $C_D A$ between 0.02 m^2 and 0.04 m^2 . When normalizing the drag area to the aerobars' height difference of each bicycle, an average variation of 0.01 m^2 in $C_D A$ was obtained for each centimeter of aerobars height decreased. It can be observed that the $C_D A$ of set 4 is notably higher than the one of the other sets; this can be attributed to the characteristics of the rider and the bicycle. On the one hand, the rider is tall; on the other hand, the bicycle is a standard road bicycle. Actually, the bicycle of set 5 is the most basic bicycle of the group tested, meaning that its aerodynamic performance is the lowest of the group. Both characteristics increase the $C_D A$.

Figure 3.5 presents the average and standard deviations of the $C_D A$ estimations. Using the $C_D A$ estimation obtained as the average value and the standard deviation estimated through the Monte Carlo method, a two-way balanced analysis of variance (ANOVA) was used to verify the differences between the estimations of $C_D A$ in the tested postures for the different measured sets. Using a significance level of 5%, it was obtained that the posture and the set affect the $C_D A$ value. The Tukey's honestly significant difference criterion was used for a multiple pairwise comparison of the sets' means. It was obtained that the $C_D A$ of all the sets except sets 2 and 3 is significantly different (p -values < 0.015). A one-way balanced ANOVA was performed for each set to verify the differences in the estimation of $C_D A$ between postures. It was obtained that for all the sets, the difference between the $C_D A$ estimated for ABhigh and ABlow was statistically significant (p -values < 0.0045).

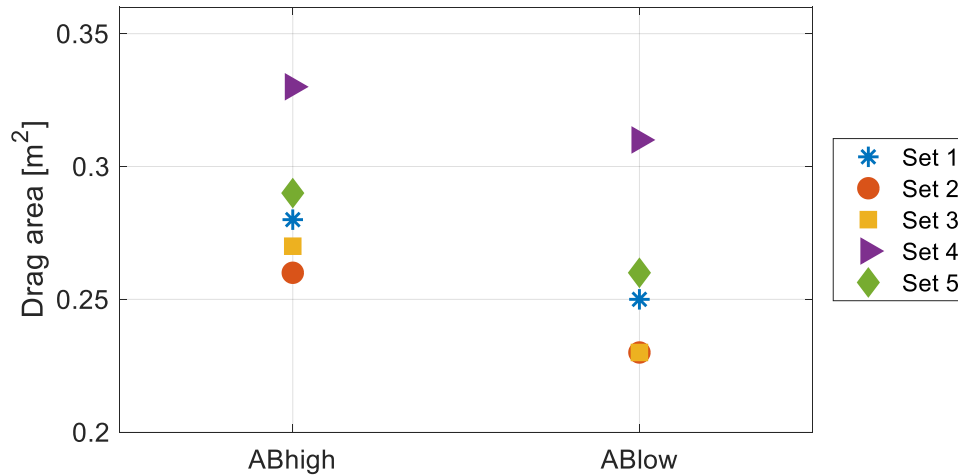


Figure 3.4. Comparison of drag areas obtained for the tested bicycle-cyclist sets.

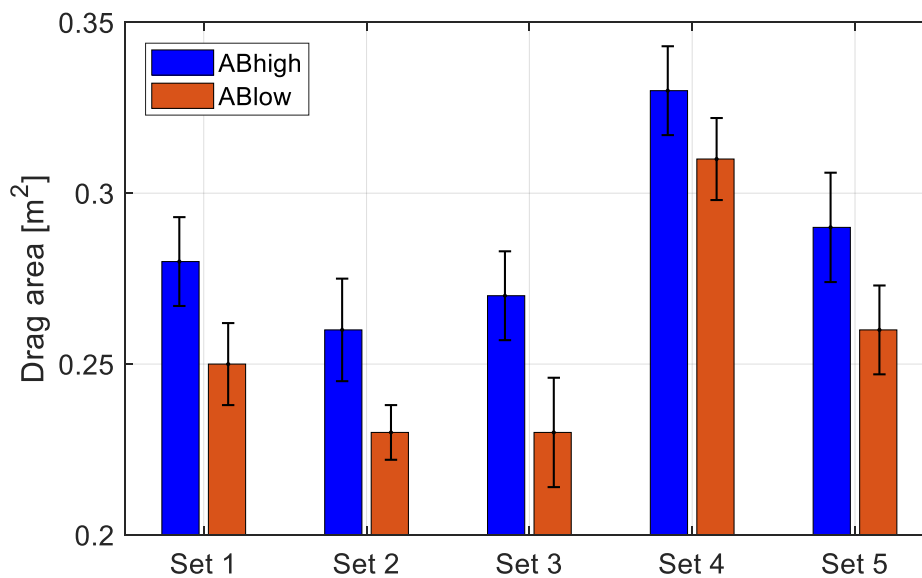


Figure 3.5. Average and standard deviations estimated for the drag area of the tested bicycle-cyclist sets.

3.5. CONCLUSION

An outdoor methodology for the estimation of the drag area of bicycle-cyclist sets was successfully implemented. The methodology is based on road tests and considers the measurement of wind speed relative to the bicycle and data from the road grade for the calculations.

For the bicycle-cyclist sets studied through the implementation of the methodology, it was possible to measure the difference in drag area occasioned by the modification of the posture. It was obtained that as the height of the aerobars reduces, the drag area decreases. The average and uncertainties estimated indicate that the methodology has enough sensibility to measure differences between the postures even for relatively small changes as the height of aerobars.

CHAPTER 4. Performance: measurement of power delivery capacity

Related publications:

[63] A. Polanco, C. Tarazona, D. Suárez and L. Muñoz, "Effect of the use of a noncircular chainring on the power delivered by recreational cyclists," in *ASME 2018 International Design Engineering Technical Conference, IDETC 2018, Quebec City, Canada, August 26-29, 2018*, pp. 1-6.

[64] O. Acevedo, L. Muñoz, A. Polanco and D. Suárez, "Influence of the chainring geometry on the critical power of recreational cyclists," in *ASME 2020 International Design Engineering Technical Conference, IDETC 2020, Virtual Conference, August 17-19, 2020*

4.1. ABSTRACT

The monitoring and improvement of performance are relevant in sports, and cycling is not an exception. Different indices are used to represent the athlete's cardiovascular and metabolic fitness. Considering that in cycling the speed depends, among others, on the power delivered to the pedals, the fitness of cyclists is also represented by the power delivery capacity of the cyclist associated with a given exercise duration. The critical power and functional threshold power are often used to represent the cyclists' power delivery capacity. This chapter's main focus is to study the feasibility of implementing protocols for the measurement of critical power and functional threshold power to identify differences in power delivery capacity due to variations in the aerobars' height.

Two protocols to measure power delivery capacity in terms of critical power (P_c) and functional threshold power (FTP) indices were implemented. The protocols were implemented to compare the results when riding with different aerobars' postures. Five recreational-level cyclists participated in the tests with their road bicycles. The functional threshold power tests were performed with all the cyclists, while the critical power tests were performed with one cyclist.

It was found that as the aerobars' height is lowered, the power delivery capacity decreases. From the functional threshold power protocol results, an average reduction of 10%, equivalent to 17 W, was obtained. A reduction of 5%, equivalent to 12 W, was observed from the critical power protocol results. On average, each centimeter lowered in the aerobars' height led to a reduction of 1.9% in the power output. The use of critical power and functional threshold power as indices of cyclists' power delivery capacity permits identifying the influence of the aerobars' height on cyclists' performance.

4.2. INTRODUCTION

Besides health, performance is one of the main objectives of athletes. For this reason, the improvement of performance is of interest to cyclists of different levels, from recreational to professional. The most direct indicator of performance is related to the speed that the cyclist is able to sustain, represented as the time required to complete a distance or the distance covered in a given time. If these values improve, then the performance improves. The speed depends on internal and external factors. The internal factors are inherent to the cyclist as the capacity to deliver power, while the external factors are related to the interaction with the environment, which are presented as resistive forces opposing the motion. Among the mentioned factors, this chapter focuses on the capacity to deliver power; this capacity varies according to physiological characteristics, training level, nutrition, race strategies, posture, and time of the day, among others. The capacity to deliver power is important because it contains information about the cyclist's health and sportive capacity, but also, because it can be used to define training strategies based on intensity threshold (*i.e.*, exercise domains).

Cyclists' capacity has been studied through different indices that represent cardiovascular and metabolic fitness. One of the most important indices is the exercise intensity associated with the lactate threshold (LT) that has been used in studies as [6], [65], [66]; this represents a level of

intensity that can be sustained without abruptly increasing the level of lactate in the blood. The level of lactate in the blood is a result of the amount of lactate produced and the body's capacity to remove it. The accumulation of lactate leads to muscle fatigue. Another important index, and one of the most frequently used in studies as [2], [5], [7], [67]-[70], is the maximal oxygen uptake (VO_2max), which represents the amount of oxygen that the body can process and use during exercise. Also, the heart rate (HR) has been used in studies as [7], [69], [71] as an indicator of performance as it represents the response of the body to a given exercise intensity. It has been used to represent performance, but it is a result of the stress of the cardiovascular system and not a direct determinant of it. Cyclists' power delivery capacity has also been represented with the power vs. time curve; this is a hyperbolic function that represents that higher intensities can be sustained for shorter times, and vice versa. Indices as the critical power (P_c) and the work above the critical power (W') have been used to represent this relation in studies as [63], [65], [67], [69], [71]-[75]. The P_c is theoretically, a power output that can be delivered indefinitely, and in practical terms, it demarcates the threshold between heavy and severe exercise domains. More recently, the functional threshold power (FTP) has gained importance among recreational and professional cyclists due to its relatively simple implementation, and it has been used in studies as [66], [68], [70]. The FTP is an indicator of one point in the power vs. time curve, usually at 20-minutes or 1-hour. Appendix 4.1 presents information about studies in cycling that represent performance through these indices.

Several types of tests to quantify the different performance indices related to power delivery have been developed and implemented throughout the years. The tests vary from simple tests measuring the time that an athlete needs to complete a course to elaborated tests performed in a laboratory using equipment to measure physiological parameters as respiratory volume exchange or lactate level in blood. According to [76], [77], the tests to obtain performance indices related to power delivery in cycling are classified into six categories as constant work, constant duration, constant power, incremental for peak power, incremental for anaerobic threshold, and critical power. The constant work tests consist of completing a fixed distance or a fixed amount of work as quickly as possible. These tests are sometimes referred to as time trials. The constant duration tests consist of traveling the longest possible distance or performing as much work as possible in a fixed time. This type of test is used to register the FTP. The constant power tests consist of maintaining a constant power output until exhaustion. Exhaustion is usually defined when the cyclist cannot pedal at the defined cadence. The incremental for peak power tests consist of pedaling with increasing intensity until reaching maximum effort. The maximum power output delivered is the peak power. This type of test is used to measure the VO_2max , which is the oxygen uptake at the maximum power output. The incremental for anaerobic threshold tests consist of a series of trials at constant power output. The trials are performed with increasing intensity. This type of test is used to measure the LT (or anaerobic threshold). The critical power tests consist of a series of constant power or constant duration tests at different intensities to register the associated time to exhaustion and identify the power vs. time curve. This type of test is used to compute P_c and W' . Appendix 4.1 presents information about studies that make use of the different types of tests described to study power delivery capacity in cycling.

The instrumentation and equipment used for implementing these tests vary depending on the type of test and the precision required. In general terms, a bicycle ergometer or a bicycle with power measurement is required for all the tests. This equipment permits measuring variables as the power delivered and time elapsed, which are the base for the measurement of P_c or FTP. For other variables, more specialized resources are needed. For example, for identifying the LT, invasive procedures to obtain blood samples and special equipment for analyzing lactate in the samples are required. Another example is the spirometer needed for measuring gas exchange and respiratory gases for the measurement of VO_{2max} . Appendix 4.1 presents information about the equipment used in different studies related to power delivery in cycling.

The effect of posture on power delivery capacity has been studied mainly in terms of the power delivered by the cyclist at VO_{2max} [2], [5]-[7], LT [6], and P_c [71]. In all these studies, it is concluded that body posture during cycling affects the power delivery capacity. In general terms, it is acknowledged that upright postures allow cyclists to deliver higher power levels. Nevertheless, few studies have addressed the effect of posture on P_c as [71] and none on FTP. Additionally, the effect of the change of aerobars' height on the power delivery capacity has not been studied. For these reasons, the objective of this chapter is to implement a methodology for the measurement of power delivery capacity in cycling with enough sensibility to measure differences due to the variation of the aerobars' height.

This chapter presents the implementation of one protocol to measure P_c and one protocol to measure FTP. These indices of performance were chosen because they include a direct value of power output that can be sustained on a given condition; under this consideration, these values of power delivered can be used in a model of the longitudinal dynamics of the bicycle-cyclist set to compute a race time for a given route. The protocols were implemented to measure cyclists' power delivery capacity in postures with different aerobars' height.

4.3. METHODS

This section describes the protocols used for measuring power delivery capacity in terms of P_c and FTP. The bicycle-cyclist sets studied are also described.

4.3.1. *Functional threshold power*

The Functional Threshold Power is the maximum constant power that a cyclist can sustain for one hour. It is obtained in a test of 1 hour of self-paced pedaling or as 95% of the power sustained on a 20-minutes self-paced test [66], [68]. This index has gained relevance along with the development of indoor trainers with power measurement and power meters; due to this equipment's availability, performing FTP tests and training with power has become more frequent. For this reason, this performance index has been used for the scheduling of training plans by different commercial cycling platforms (*e.g.*, TrainingPeaks, Zwift, TheSufferFest).

The FTP is usually measured indoors to control the testing conditions. Considering that keeping a constant power output during one hour in a trainer is difficult due to the concentration required

and the monotony of the test, modified protocols as the 20-minutes FTP with and without 5-minutes conditioning efforts are performed more frequently.

A modified protocol to measure functional threshold power was implemented in this study. The test consisted of a 10-minutes warm-up followed by a 5-minutes test, a recovery period, a 20-minutes test, another recovery period, a 1-minute test, and finally, a cool-down. This test was designed by a commercial cycling platform (TheSufferFest) and was chosen for this study because it collects information on the cyclist capacity to deliver power in different time ranges. Figure 4.1 presents the intensity curve suggested for the test. For each posture, the protocol was implemented once with a recovery period between trials of at least one week. The protocol is summarized in Appendix 4.2.

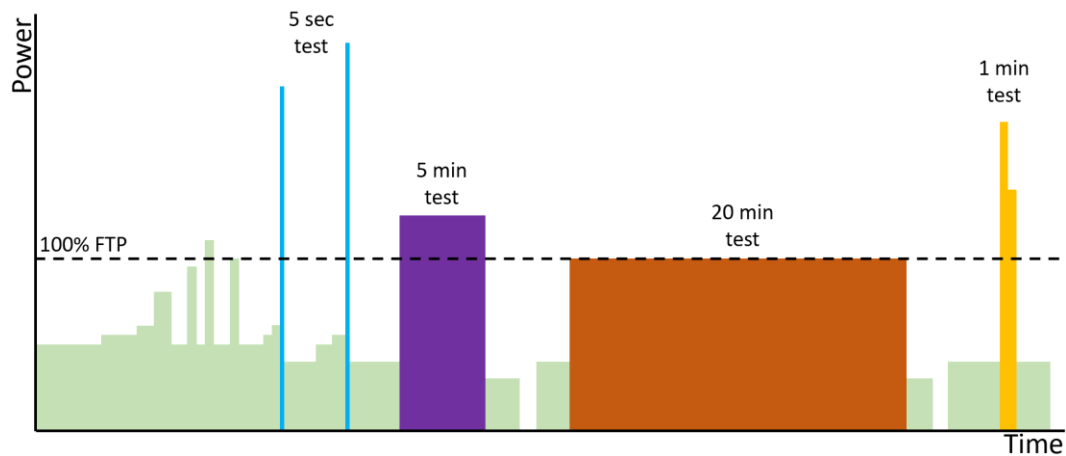


Figure 4.1. Intensity curve for the modified functional threshold power test.

The tests were performed indoors using a smart trainer with power measurement (Kickr, Wahoo, USA), cadence sensor (Cadence 2, GARMIN, USA), a heart rate sensor (Rhythm+, Scosche, USA), and a monitor to display the data to the cyclist. The cyclist controlled the resistance by changing the gears. The cyclist was able to hydrate ad libitum. Figure 4.2 presents the setup used for the tests.

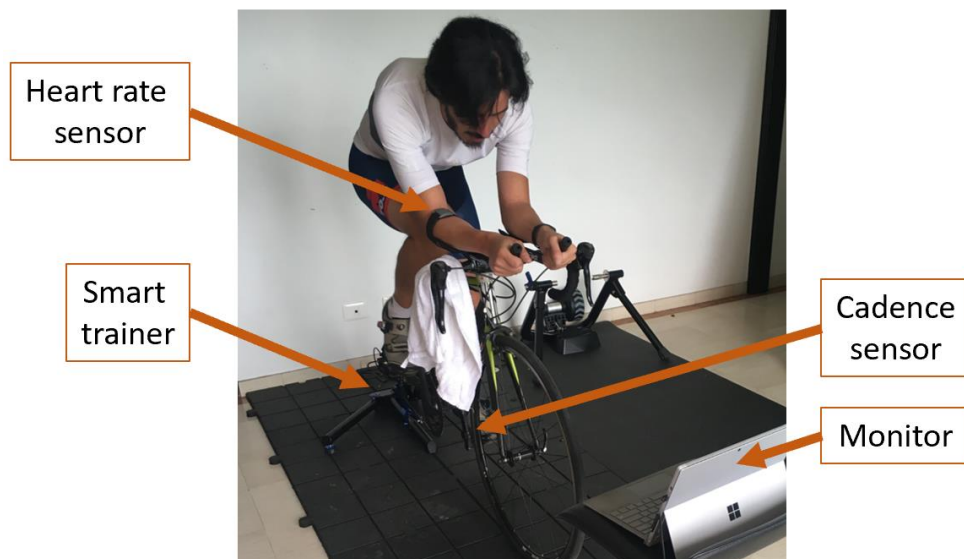


Figure 4.2. Setup for the implementation of the protocol to measure power delivery capacity.

4.3.2. Critical power

The critical power is theoretically the highest sustainable power [69], [78]. Nevertheless, it has been concluded that P_c cannot be delivered indefinitely [79]-[82]. For this reason, the practical definition of P_c is that it demarcates the threshold between heavy and severe exercise domains. The critical power has been used for predicting future performance [69], [72]. The Work above the critical power was previously named anaerobic work capacity (AWC) because the model originally considered a relation between aerobic and anaerobic work. The anaerobic work capacity was related to work performed in Wingate tests, high-intensity exercise, and oxygen deficit and was understood as a measure of anaerobic capacity related to the high-intensity performance ability [83]. The anaerobic work capacity was mathematically understood as a finite reserve of energy storage available previous to exercise [80]. In recent works, W' has been still defined as an anaerobic energy source even though there is no consensus on its role [72]. The relation between P_c and W' has been understood as W' being expended when the exercise is performed above P_c and replenished only when the exercise is terminated, or the work rate is performed below P_c [84].

The hyperbolic model that relates power and time is presented in Eq. (4.1). In this model, the time (t_{tot}) in seconds is the duration of the test at a given power output (P) in watts, P_c is the asymptote of power in watts, and W' in Joules is the degree of curvature of the hyperbole. The model is graphically represented in Figure 4.3.

$$t_{tot} = \frac{W'}{P - P_c} \quad (4.1)$$

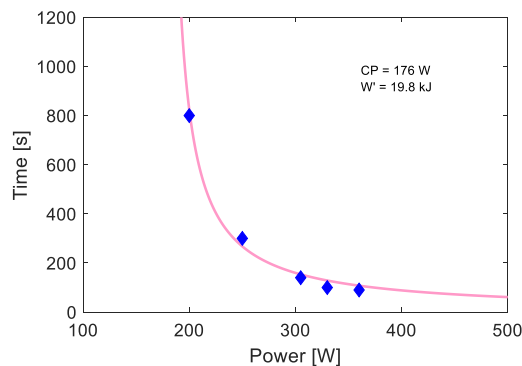


Figure 4.3. Graphical representation of the power vs. time hyperbolic model. Image based on data from [75].

The identification of the two parameters of the power vs. time model requires performing at least two constant power or constant duration tests at different intensities. Nevertheless, the identification is usually performed with four or more trials to improve the model's accuracy. The time and average output power of each test are registered for each trial and used to estimate P_c and W' . There are different expressions of the hyperbolic model presented in Eq. (4.1). The estimation of the parameters varies depending on the model used. For example, if the nonlinear power vs. time model of Eq. (4.1) is used, P_c is calculated as the asymptote, and the degree of curvature of the hyperbole is W' . If the expression presented in Eq. (4.2) (named power vs. 1/time model) is used, P_c is calculated as the y-intercept and W' as the slope.

$$P = \frac{W'}{t_{tot}} + P_c \quad (4.2)$$

The power vs. 1/time model is highlighted here because it has been used with some methodological simplifications. On one side, the parameters' estimation usually requires inter-trial recovery times of at least 24 hours. Nevertheless, it has been reported that the use of the power vs. 1/time model with recovery periods of 3 hours or less is feasible [72]. On the other side, given that this is a linear model in terms of 1-time, the use of data from only two trials has been reported with successful results [73].

The protocol to measure critical power implemented consists of performing three bicycle trials for each posture. In each trial, the cyclist pedals until exhaustion at fixed power and cadence. The power output of each trial is different, and the cyclist pedals until exhaustion. Exhaustion is considered as the moment in which the cadence drops more than 10 rpm for more than 10 s, or the cyclist decides to stop pedaling. A recovery period of 30 minutes between trials is used, meaning that all the trials are performed on a session day. Following the suggestions of [72], the trials are performed with increasing difficulty (*i.e.*, from lower to higher power outputs). The protocol is implemented indoors using a trainer, the cyclist's bicycle, a power meter, a chronometer, a cadence sensor, and a heart rate sensor. During the trials, only the cadence is displayed to the cyclist. During the tests, the cyclist can hydrate *ad libitum*. A warm-up and cool-down are performed before and after each trial. The protocol is summarized in Appendix 4.2.

For the implementation of the protocol, each trial's power outputs were defined from an estimate of the FTP of each rider using historical records. The power outputs were defined to avoid tests with durations of less than 1 minute or more than 20 minutes; this, because out of this time range, the mathematical model tends to overestimate or underestimate P_c and W' . The power outputs were defined as 105%, 115%, and 125% of the FTP. The power output was controlled by the trainer, varying the resistance according to the cadence. A recovery period of at least 48 hours between session days was used. The order of the body postures was randomized throughout session days to avoid a fatigue effect. The warm-up consisted of pedaling at 50% of the estimated FTP for 5 minutes and performing 10-seconds sprints at the end of minutes 2, 3, and 4. The cool-down consisted of unloaded pedaling for 3 minutes. A smart trainer with power measurement (Kickr, Wahoo, USA), cadence sensor (Cadence 2, GARMIN, USA), a heart rate sensor (Rhythm+, Scosche, USA), and a monitor to display the data to the cyclist were used for the tests.

4.3.3. *Bicycle-cyclist sets and postures measured*

Five recreational cyclists voluntarily participated in the tests after signing an informed consent form (mass: 73.8±11.8 kg, height: 1.75±0.06 m, age: 35±7 years). The riders used their own bicycles and standard cycling clothes. The tests were performed in two aerobars postures with different heights. For road bicycles, clip-on aerobars were used. Depending on each bicycle's characteristics, the height was varied using spacers on the headtube stem or the aerobars support. Table 4.1 presents a summary of the information of each bicycle-cyclist set (further detail can be found in Tables 2.1, 2.2, and 2.3 in chapter 2).

	Variable	Units	Set				
			1	2	3	4	5
Rider	Mass	[kg]	59	72	92	73	73
	Height	[m]	1.67	1.72	1.76	1.78	1.83
	Age	[years]	38	26	42	39	30
	Gender	[-]	Female	Male	Male	Male	Male
	FTP from historical records	[W]	170	230	220	180	237
Bicycle	Type	[-]	Aero	Time trial	Aero	Endurance	Time trial
	Aerobars' height difference	[mm]	55	55	55	55	40

Table 4.1. Bicycle-cyclist sets included in power delivery capacity tests.

4.4. RESULTS AND DISCUSSION

This section presents the results of the implementation of the protocols to measure critical power and functional threshold power.

4.4.1. Functional threshold power

The average power delivered for different time ranges during the FTP modified protocol is summarized in Table 4.2. Other variables registered during the tests are reported in Table 4.3. It can be observed that for all the cyclists in all the time ranges, the average power delivered decreased when changing from ABhigh to ABlow, with one exception for cyclist 4 in the 1-minute test. For the FTP (*i.e.*, 20-minutes test), an average reduction of 10% (equivalent to 17 W) was obtained for all the cyclists when changing from ABhigh to ABlow posture. It can also be observed that, for each cyclist, the cadence and maximum HR were similar between tests. The cadence differences were between 1 rpm and 5 rpm, and the differences in HR were between 0 bpm and 6 bpm. The tests were performed at similar times of day for each cyclist, with similar ambient conditions. The recovery time between session days was at least one week for all the cyclists (9.2 ± 3.0 days).

Variable	Units	Posture	Cyclist				
			1	2	3	4	5
20 min Power (FTP)	[W]	ABhigh	161	228	180	179	233
		ABlow	140	217	168	169	193
5 min Power	[W]	ABhigh	175	286	218	214	264
		ABlow	162	273	206	206	238
1 min Power	[W]	ABhigh	224	455	363	293	395
		ABlow	181	424	349	304	363
5 sec Power	[W]	ABhigh	445	658	1015	589	707
		ABlow	431	639	960	535	701

Table 4.2. Average power delivered for different time ranges during Functional threshold power tests.

Variable	Units	Posture	Cyclist				
			1	2	3	4	5
Avg. Cadence	[rpm]	ABhigh	77	69	79	76	86
		ABlow	82	70	82	73	83
Max. Heart rate	[bpm]	ABhigh	162	180	166	167	184
		ABlow	168	179	166	172	178
Avg. Heart rate	[bpm]	ABhigh	125	139	138	126	142
		ABlow	139	139	137	133	138
Temperature	[°C]	ABhigh	20.8	19.85	19.8	20	19.2
		ABlow	20	18.6	18.8	21.6	19.3
Relative humidity	[%]	ABhigh	45	60	60	60	59
		ABlow	49	57	60	41	59
Time of day	[hh:mm]	ABhigh	16:45	16:10	9:40	12:30	8:00
		ABlow	17:30	17:20	9:10	9:40	7:00

Table 4.3. Additional variables registered during the Functional threshold power tests.

Figure 4.4 compares the FTP normalized to the riders' mass. The general tendency of a power delivery capacity reduction due to the reduction of the aerobars' height is observed. The power delivery capacity was decreased between 0.1 W/kg and 0.4 W/kg. When comparing the cyclists' normalized power with charts available in the literature [85], the cyclists who participated in this study were classified as moderate, fair, and untrained. It should be kept in mind that the values reported in the literature were measured in upright postures; for this reason, the classifications of the cyclists of this study could improve when measuring values in upright postures rather than in aerobars postures.

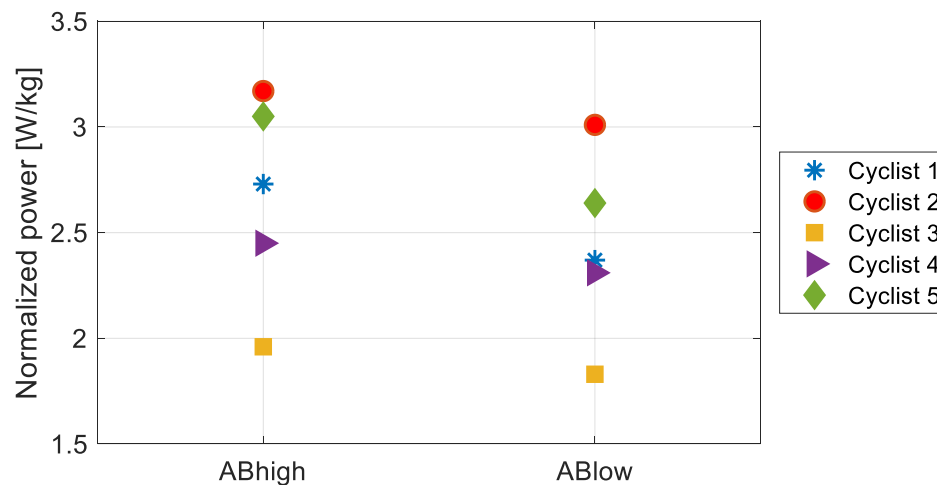


Figure 4.4. Functional threshold power (FTP) normalized with the riders' mass.

4.4.2. Critical power

The critical power protocol was implemented with fewer riders than the initially programmed (*i.e.*, one out of five cyclists) because some riders retired from the tests. Some disadvantages of the

critical power tests were identified from the reasons listed by the cyclists to retire, as analyzed in section 4.4. The mean power delivered and the times registered for the different trials of the rider whose P_c was measured are presented in Table 4.4. The results of P_c and W' obtained for the postures tested are presented in Table 4.5. It can be observed that the average power registered in the trials for the same intensity was constant. It can also be observed that the higher difference in duration between trials of the same intensity was registered for the low-intensity tests, while for the high-intensity trials, the durations were similar. An average reduction of 5% (equivalent to 12 W) on the P_c was obtained when changing from ABhigh to ABlow. Other variables registered during the tests are reported in Table 4.6. The tests were performed at similar times of day, with similar ambient conditions, and a recovery period between session days of 10 days.

				Cyclist
Trial intensity	Posture	Variable	Units	5
Low	ABhigh	Avg. power	[W]	248
		Duration	[s]	360
	ABlow	Avg. power	[W]	248
		Duration	[s]	254
Medium	ABhigh	Avg. power	[W]	272
		Duration	[s]	131
	ABlow	Avg. power	[W]	272
		Duration	[s]	142
High	ABhigh	Avg. power	[W]	296
		Duration	[s]	100
	ABlow	Avg. power	[W]	296
		Duration	[s]	100

Table 4.4. Power and time data registered during critical power tests.

			Cyclist
Variable	Units	Posture	5
P_c	[W]	ABhigh	229
		ABlow	216
W'	[J]	ABhigh	6393
		ABlow	7910

Table 4.5. Results of Critical power (P_c) and Work above the critical power (W').

			Cyclist
Variable	Units	Posture	5
Temperature	[°C]	ABhigh	20.3
		ABlow	19.9
Relative humidity	[%]	ABhigh	41
		ABlow	52
Time of day	[hh:mm]	ABhigh	9:20
		ABlow	8:50

Table 4.6. Additional variables registered during the critical power tests.

4.4.3. *Effect of posture on power delivery capacity*

It has been reported that humans' muscle fatigue and endurance vary according to the body tilt angle and the limbs' position relative to the heart [2]. Nevertheless, there is no general agreement about the effect of body posture variation in power delivery capacity. Some authors have reported improvement in power output by changing the posture [2]-[8], while others have reported that there is no relevant effect [9], [10].

The results of the FTP and P_c show that for the cyclists tested, the body posture influenced the capacity to deliver power (see Table 4.2 and Table 4.5). The differences obtained for FTP when changing from ABhigh to ABlow were between 5% and 16% (*i.e.*, between 10 W and 30 W) for the different cyclists. The difference obtained for P_c when changing the posture was 5% (corresponding to 12 W). It is worth highlighting that it has been reported that the validity of the estimation of W' with the protocol implemented for the estimation of critical power (*i.e.*, with short recovery periods) needs further research [72]. For this reason, W' was not analyzed in this work.

The results obtained agree with studies in the literature reporting an effect of posture in power delivery capacity. It should be considered that the effect observed depends strongly on the postures tested and the characteristics of the riders. For this reason, it is possible that the differences between the studies supporting and contradicting the influence of posture on power delivery capacity are due to the experiment characteristics. For the postures and the bicycle-cyclist sets included in this study, it was found that the power delivery capacity measured in terms of critical power and functional threshold power vary with posture in terms of aerobars' height. The registered variation was expected given that the posture variation can lead to modifications in the muscles' biomechanics or the respiratory dynamics. On the one hand, depending on the posture, the operating region of the force-length relationship in leg muscles can vary, affecting power delivery. On the other hand, the lung mechanics and, hence, the respiratory functions can be affected by trunk inclination, which is modified by the aerobars' height.

4.4.4. *Implementation of critical power and functional threshold power protocols*

The protocols used in this study to measure P_c and FTP were chosen due to their relatively simple implementation. It was intended to use protocols that did not require invasive procedures or specific medical knowledge and could be performed with relatively common equipment. The results of this study indicate that it is possible to implement the protocols described for the measurement of the effect of posture in power delivery capacity.

During the implementation of the tests, some drawbacks of the P_c protocols were identified. In interviews with the riders, they reported not feeling motivated with the trials at constant power delivery rates. Two main reasons were listed. First, the test conditions are different from normal riding conditions as there is not available information during the tests (only the cadence is displayed to the riders). Second, pedaling until exhaustion is stressful. In addition, it should be taken into account that the traditional protocol for testing P_c requires performing an incremental for peak power test to determine the intensities of the constant power tests relative to the VO_{2max} power. For example, the use of power outputs defined at 80%, 100%, and 105% of power at VO_{2max} has

been reported [72]. For this reason, two approaches can be used for the implementation of the P_c protocol. First, measure the power at VO_2max , which would increase the complexity of the protocol. Second, estimate the test intensities using other sources as performance data from historical records or an FTP test, which can lead to the necessity of repeating several trials due to imprecision in the intensities' definition. Additionally, the traditional protocol requires performing the trials on different days, which severely increases the experimental costs (from one day to at least three days for each testing condition).

Even though the FTP protocol has a drawback because there is not yet a general agreement on the relation of FTP with traditional indices of cardiovascular and metabolic fitness as the LT and VO_2max , the volunteer riders reported a preference for this type of test than for the P_c protocol. In addition, obtaining the FTP for one condition (*e.g.*, a posture) requires approximately 1 hour, while obtaining the P_c for the same condition requires at least 2 hours in one testing session if simplified protocols are used, or in three or more testing sessions if traditional protocols are used. Besides the experimental cost associated, requiring longer testing times, especially over different sessions, can extend the implementation of the protocols for weeks, which can lead to a bias in the measurement of performance due to training or detraining of the cyclists and can be unfeasible due to alterations in the training schedule of the measured cyclists. For these reasons, the FTP tests have called researchers' attention to test the power delivery capacity of non-professional cyclists and continues under study. Regarding the validity of FTP tests, it has been reported that the FTP can provide an approximation of P_c [68], peak power on an incremental test, and relative VO_2max [70].

As a recommendation for the implementation of power delivery tests using smart trainers, from preliminary tests performed before this study, it was also noticed that the capacity of the trainer to adjust the resistance and keep a constant power is essential; otherwise, the tests cannot be performed at constant power outputs, and a pacing effect can modify the results.

4.5. CONCLUSION

Two protocols for the measurement of power delivery capacity were implemented in a group of cyclists. Functional threshold power and critical power indices were measured with the protocols as representations of the power output that the cyclists can sustain for relatively long periods (*i.e.*, higher than 20 minutes). The protocols permitted measuring the power output difference when changing the posture, indicating that the protocols have enough sensibility to measure differences in power delivery capacity due to the aerobars' height variation. For the bicycle-cyclist sets studied, it was obtained that when the height of the aerobars is reduced, the power delivery capacity for different time ranges decreases.

It was found that the implementation of the functional threshold power protocol used in this study presents some advantages with respect to the critical power protocol used. The main reason is that both protocols were able to quantify differences in the power output when changing the aerobars height, but the riders preferred constant-duration tests (as time trial tests used in the functional threshold power protocol) over constant-power tests (as critical power tests).

CHAPTER 5. Interaction: measurement of pressure in contact areas

5.1. ABSTRACT

High values of pressure applied to the tissue and the stimulus duration have been related to discomfort and overuse injuries. For more extended periods of exposure, the acceptable pressure is lower. Considering that long hours of training and competition are frequent in cycling, the analysis of the pressure on the tissues in contact with the bicycle is relevant. The pressure is affected by the rider and bicycle characteristics, and several variables as cadence, posture, power output, and gender, among others. For this reason, there is not a general agreement in the study of the characteristics of pressure in the saddle contact. This chapter presents a methodology for measuring and analyzing the pressure field in contact areas between the rider and the bicycle.

A methodology for registering the pressure field in the buttocks-saddle and elbow-aerobars' pads interfaces was used. The methodology is based on indoor tests performed while pedaling at a constant cadence on a smart trainer. A flexible pressure sensing mat was used to acquire the pressure field in the contact areas. The methodology was implemented to measure the pressure fields of five bicycle-cyclist sets. The tests were performed while riding in two different aerobars postures differentiated by the height of the aerobars. The indices used to study the results were average pressure, peak pressure, and longitudinal position of the center of pressure.

It was found that when the riders changed from Aerobars high to Aerobars low, the center of pressure in the saddle moved to the front between 0.6 cm and 1.6 cm. Also, the average pressure increased between 0.8 kPa and 9.6 kPa. Regarding the longitudinal position of the center of pressure of the elbow pads, the average pressure of the elbow pads, and the peak pressure in both contact areas, the variation due to the change of posture depends on the bicycle-cyclist set.

It is concluded that the methodology can be used to identify differences in the longitudinal position of the center of pressure, the average, and peak pressure when changing the height of the aerobars' pads. The results highlight the necessity of analyzing the effect of posture on the pressure in contact areas for each bicycle-rider set (i.e., bicycle-cyclist set).

5.2. INTRODUCTION

In cycling, the rider's weight is supported in the small areas of contact with the bicycle (*i.e.*, buttocks-saddle, hands-handlebar, and feet-pedals); for this reason, the pressures in contact areas are relatively high. The study of pressure in contact points is relevant because it has been related to discomfort, and more importantly, with overuse injuries [24], [29], [31], [32], [86]-[88]. Examples of common overuse injuries related to the contact with the saddle are sores/chafing/ulceration, perineal/ischial tuberosity pain and numbness, and impotence [17], [45]. Regarding the contact with the handlebar, the most common overuse injuries are ulnar neuropathy or cyclist's palsy [17], [31], [45]. The prevalence of lower leg, including feet injuries, is less reported than other overuse injuries [17]. The injuries caused by the interaction with the saddle are more frequent than the ones generated by the interaction with the handlebar and pedals because more than 40% of body weight is supported in the saddle [45], [89]. For this reason, several studies have been performed to analyze the pressure field in the saddle-buttocks contact point as [24], [25], [28], [29], [86], [87], [90], [91],

and some studies have been performed in the handlebar-hands interface as [31] and the pedals-feet contact point as [32].

It is worth highlighting that the magnitude of pressure by itself is not an indicator of potential tissue damage; what is important is the pressure-time relation because it has been reported that the adverse effects of pressure are related to both its magnitude and duration [92]-[94]. As explained in [95], “low pressures delivered to muscle tissue over a long exposure period may cause injury, but high pressures delivered for a very short time may not affect tissue viability.” For this reason, different studies refer to the pressure-time injury threshold, pointing out acceptable and unacceptable pressures for a given exposure time. An inverse relation between the exposure time and the safe levels of pressure has been identified. Acceptable and unacceptable levels of pressure-times of exposure have been identified for pressure sores [96] and even cell death [95], [97] in different living beings (*e.g.*, humans, dogs, rats). Given the long hours associated with cycling training activities and cycling competition events, attention has been drawn to the pressure in contact points during this activity.

Different indices have been used to analyze the pressure fields of the contact points while cycling. The indices that are more frequently used are the mean pressure and peak pressure presented either as absolute values [24], [25], [28], [29], [31], [86], [87] or normalized by the body mass [90]; these indices have sometimes been presented in terms of force instead of pressure [25], [28], [32]. The location and displacement of the center of pressure (COP) have also been used [25], [87]. Most of the studies found in the literature have been performed while pedaling, and the indices have been obtained for an observation window of several pedal cycles (at least three pedaling cycles). Additionally, most studies have been performed in a laboratory using an ergometer or cycle simulator/trainer to control test conditions as cadence and power delivery, which are commonly defined as constants. The pressure, force, and COP location are registered with pressure sensing mats constructed with a matrix of sensors (piezoresistive or capacitive) located in flexible fabrics. Appendix 5.1 presents further information on studies about pressure in contact points found in the literature.

Different solutions have been proposed to modify the pressure characteristics in contact points. For example, it has been reported that the variation of the saddle tilt angle modifies the pressure distribution between the anterior and posterior regions of the pelvis (*i.e.*, pubic arch and ischium, respectively) [91]. Most of the solutions are focused on the design of the bicycle components. For the buttocks, modifications to the saddle as relief channels [89], complete saddle nose removal [86], partial nose cutout [87], among others, have been used, aiming at effectively distributing weight and reducing pressure on the perineum to decrease the risk of discomfort or injury [28], [86]. For the hands, different types of paddings have been included in the gloves to reduce the average peak pressure on sensitive zones of the hands [31].

The effect of body posture on the pressure in contact areas has called the attention of some researchers. It has been reported that in postures with the trunk bent forward (*e.g.*, drops), the pressure in the seat decreases with respect to postures with larger trunk angles (*e.g.*, tops) [24], [25], [29]. As reported by Bressel and Cronin [24], the effect is possibly due to a shift of the weight

from the saddle to the handlebar or the pedals. Even though there is an agreement on the general effect of posture, there is a disagreement about the effect of the rider's gender. In one study, the findings indicate that the effect of posture is only relevant for male riders [24], while in another study [29], it was reported that the effect is relevant only for male riders using a saddle with a hole in the perineal zone; finally, another study [25] concluded that the effect is relevant also for women. No studies have been performed about the effect of changing the aerobars' height on the pressure in contact areas. It is observed that the study of pressure in saddle remains a matter of debate. For these reasons, this chapter's objective is to implement a methodology for measuring pressure in contact areas between the bicycle and the rider with enough sensibility to measure differences due to the aerobars' height variation.

This chapter presents a protocol to measure and analyze the pressure in the buttocks-saddle and elbow-aerobars' pads interfaces. The protocol was implemented with a group of cyclists riding in different aerobars postures. The analysis was performed mainly based on the position of the center of pressure and the average and peak pressures in the contact areas.

5.3. METHODS

A methodology based on indoor tests to measure the pressure field in the buttocks-saddle and elbow-aerobars' pads contact areas was used to evaluate the effect of posture in the interface pressure. For this, the power output was controlled with a cycle simulator, the cadence was displayed to the rider with a cadence sensor, and the field pressure was measured with a flexible pressure sensing mat.

For this implementation, the tests consisted of pedaling on a cycle simulator with a defined posture at a fixed cadence selected by the rider and a constant power output equal to the FTP of the rider. The power output was defined as constant because it has been reported that this variable affects the pressure field in the saddle contact area. The power output was defined in terms of the FTP to be representative of the power delivered by the cyclist while training or competing. The protocol is summarized in Appendix 5.2.

A smart trainer (Kickr, Wahoo, USA) and a Garmin cadence sensor (Cadence sensor 2, GARMIN, USA) were used for the tests. A pressure mat (Bike saddle, Novel, Germany) with 512 capacitive sensors of 1 cm², located on a 320 x 160 mm² area, was used. Figure 5.1 presents the setup used for measuring the pressure on the saddle-buttocks contact area.



Figure 5.1. Setup for the measurement of pressure in contact areas.

At the beginning of the tests, the flexible mat was aligned and fixed to the saddle and the aerobars' elbow pads with tape. Once the mat was fixed, the cyclist pedaled for 10 minutes to warm up, delivering a power level equal to 50% of its FTP. At the end of the warm-up, the cyclist dismounted the bicycle, and the mat was zeroed while unloaded. Then, the area of the mat corresponding to the saddle or the elbow pads was registered by pressing the corresponding area with a static force, obtaining a pressure field during the postprocessing as exemplified for a saddle in Figure 5.2 (left). The area of the pressure sensing mat that corresponded to the saddle was identified as exemplified in Figure 5.2 (right). For the elbow pads, the areas corresponding to the sensor mat were approximated as rectangles.

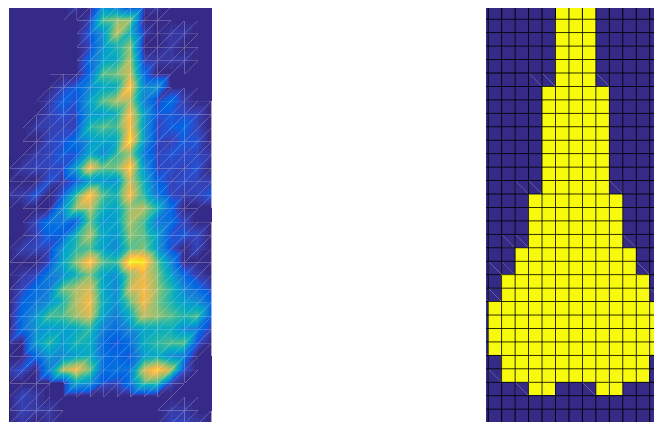


Figure 5.2. Example of the identification of the saddle area in the sensing mat. Left: initial sensed area. Right: saddle area.

Two coordinate systems were defined for the saddle and elbow pads on the pressure sensing mat. The coordinate systems were defined in the longitudinal and lateral orthogonal directions, as presented in Figure 5.3. The origin of the saddle's coordinate system was located in the tip of the nose, and in the elbow pads, it was located in the rear section of the aerobars. For both cases, the origin was laterally located in the geometric center of the components' areas.

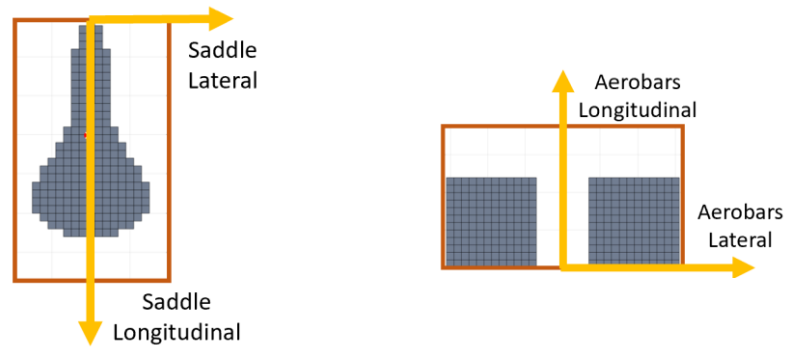


Figure 5.3. Definition of the coordinate system. Left: saddle. Right: Aerobars' pads.

After the data for defining the components' areas in the sensing mat was acquired, the cyclist began pedaling at a constant cadence and power output. Once the pedaling was stable, the pressure fields were registered on each posture for a total registered time (t_{tot}) of 1 minute. A sampling frequency of 30 Hz was used. During the postprocessing, the areas of contact between the saddle-buttocks and the pads-elbows interfaces were identified for each time step (t_s). A matrix named Ar was used to represent the sensors inside the contact area. The matrix was defined as presented in Eq. (5.1) by comparing the pressure of each sensor (p) with a pressure threshold (P_{th}). A P_{th} value of 0.4 kPa was used as implemented in [24] for noise reduction. The variables i and j represent the rows and columns of the sensing mat sensors.

$$\forall 1 \leq i \leq 16, \forall 1 \leq j \leq 32, \quad Ar_{i,j,t_s} = \begin{cases} 1, & p_{i,j,t_s} \geq P_{th} \\ 0, & p_{i,j,t_s} < P_{th} \end{cases} \quad (5.1)$$

Figure 5.4 presents an example of contact areas identified for a bicycle-cyclist set in the saddle-buttocks and elbow-pads interfaces. The example figure presents in dark color all the sensors in the components' areas that registered pressures over P_{th} in at least one time step.

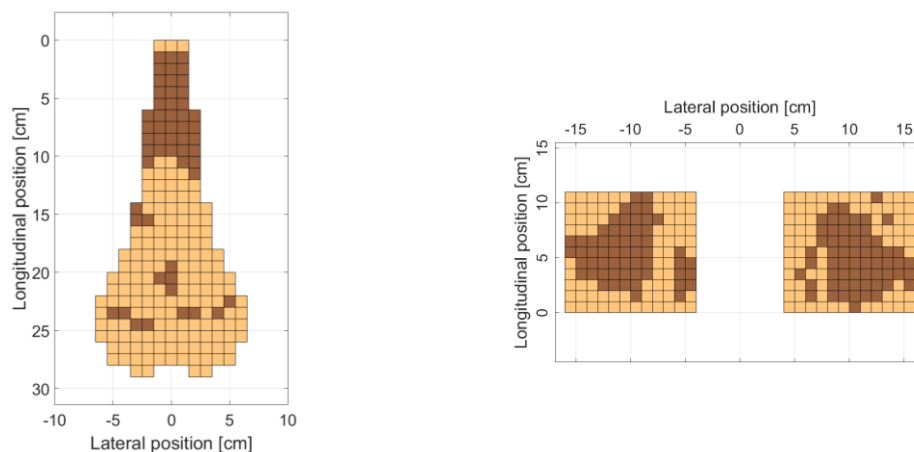


Figure 5.4. Example of the contact in the interface. Light color: area of the component. Dark color: area of contact. Left: Buttocks-saddle. Right: Elbows-pads.

The pressure data was divided into pedaling cycles using the lateral motion of the Center of pressure computed for each time step ($COP_{lat,time}$). The general equation for calculating the center of pressure in the x direction of a xy plane is presented in Eq. (5.2).

$$COP_x = \frac{\int \int p(x,y) * x \, dx \, dy}{\int \int p(x,y) \, dx \, dy} \quad (5.2)$$

Given that in this study, the data is discrete, and the calculation is performed for each time step, the discrete expression for the computation of $COP_{lat,time}$ presented in Eq. (5.3) can be used.

$$\forall 0 \leq t_s \leq t_{tot}, \quad COP_{lat,time} \cong \frac{\sum_{i=1}^{16} \sum_{j=1}^{32} p_{i,j,t_s} * i * Ar_{i,j,t_s}}{\sum_{i=1}^{16} \sum_{j=1}^{32} p_{i,j,t_s} * Ar_{i,j,t_s}} \quad (5.3)$$

The $COP_{lat,time}$ was used to identify the cycles because due to the oscillating motion of the hip while pedaling, the cycles can be identified as exemplified in Figure 5.5 (top). Using a discrete Fourier transform, the pedaling cadence can be obtained in the frequency domain as the peak with the highest magnitude, as exemplified in Figure 5.5 (bottom).

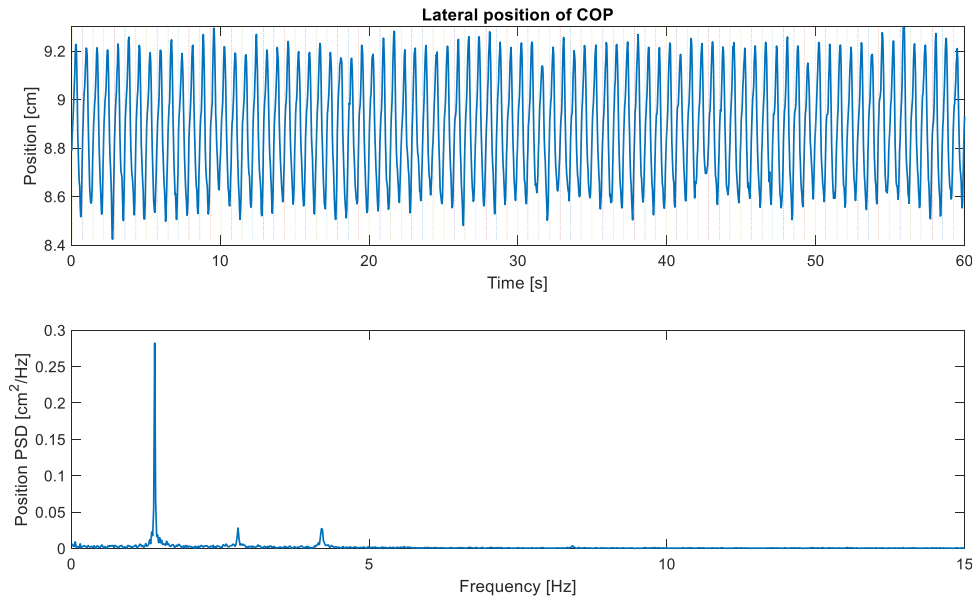


Figure 5.5. Example of data of lateral COP used to identify pedaling cycles and cadence. Top: time domain. Bottom: frequency domain.

For each pedaling cycle, the longitudinal position of the COP ($COP_{lon,cycle}$) and the average pressure ($p_{avg,cycle}$) were computed. These indices are computed as the average over time of the longitudinal position of the COP ($COP_{lon,time}$) and the average pressure in the contact areas ($p_{avg,time}$) computed for each time step of each cycle, respectively. Equation (5.4) presents the expression for the computation of $COP_{lon,time}$, and Eq. (5.5) presents the expression for $p_{avg,time}$.

$$\forall 0 \leq t_s \leq t_{tot}, \quad COP_{lon,time} = \frac{\sum_{i=1}^{16} \sum_{j=1}^{32} p_{i,j,t_s} * j * Ar_{i,j,t_s}}{\sum_{i=1}^{16} \sum_{j=1}^{32} p_{i,j,t_s} * Ar_{i,j,t_s}} \quad (5.4)$$

$$\forall 0 \leq t_s \leq t_{tot}, \quad p_{avg,time} = \frac{\sum_{i=1}^{16} \sum_{j=1}^{32} p_{i,j,t_s} * Ar_{i,j,t_s}}{\sum_{i=1}^{16} \sum_{j=1}^{32} Ar_{i,j,t_s}} \quad (5.5)$$

An additional index was computed to observe the zone of the saddle or aerobars' pads in which higher pressures were registered. For each sensor in the contact area, the pressure was averaged over the total registered time ($p_{avg,sensor}$) as in Eq. (5.6). Then, the maximum of these pressures was identified as p_{peak} .

$$\forall 1 \leq i \leq 16, \quad \forall 1 \leq j \leq 32, \quad p_{avg,sensor} = \frac{\sum_{t_s=0}^{t_{tot}} p_{i,j,t_s} * Ar_{i,j,t_s}}{\sum_{t_s=0}^{t_{tot}} 1} \quad (5.6)$$

It is worth highlighting that the indices are obtained, considering that the cadence and power output are constant and hence do not influence the results. It should be noticed that the results obtained with indoor measurements do not reflect the effects of vibrations transmitted to the cyclist, which can influence the pressure in contact areas.

Five recreational cyclists voluntarily participated in the tests after signing an informed consent form (mass: 73.8±11.8 kg, height: 1.75±0.06 m, age: 35±7 years). The riders used their own bicycles and standard cycling clothes. The tests were performed in two aerobars postures with different heights. For road bicycles, clip-on aerobars were used. Depending on each bicycle's characteristics, the height was varied using spacers on the headtube stem or the aerobars support. Table 5.1 presents a summary of the information of each bicycle-cyclist set (further detail can be found in Tables 2.1, 2.2, and 2.3 in chapter 2).

	Variable	Units	Set				
			1	2	3	4	5
Rider	Mass	[kg]	59	72	92	73	73
	Height	[m]	1.67	1.72	1.76	1.78	1.83
	Age	[years]	38	26	42	39	30
	Gender	[-]	Female	Male	Male	Male	Male
	FTP	[W]	140	217	168	169	193
Bicycle	Type	[-]	Aero	Time trial	Aero	Endurance	Time trial
	Aerobars' height difference	[mm]	55	55	55	55	40
	Saddle	[-]	Lady, Selle Italia, Italy	Adamo PS 1.1, ISM, USA	300, Oval concepts, USA	Galápagos, GW, Colombia	Stealth, PRO, The Netherlands
	Aerobars	[-]	Parabolica uno, Deda elementi, Italy	Revo, 3T, Italy	Parabolica uno, Deda elementi, Italy	Parabolica uno, Deda elementi, Italy	Trimax, Vision, USA

Table 5.1. Bicycle-cyclist sets included on the pressure in contact areas tests.

5.4. RESULTS AND DISCUSSION

The results of the study are summarized in Tables 5.2 and 5.3. From the indices computed for each cycle ($COP_{lon,cycle}$ and $p_{avg,cycle}$), the averages were computed (named \overline{COP}_{lon} and \bar{p}) and are presented in Table 5.2 for the saddle-buttocks contact area and in Table 5.3 for the elbow-pads contact area summarizing the information from all the pedaling cycles. The tables also present the maximum average pressures over time (p_{peak}) obtained for each case. It should be remembered that for the saddle, higher values of \overline{COP}_{lon} mean moving backward, while for the elbow pads, they mean moving forward.

Variable	Units	Posture	Set				
			1	2	3	4	5
\overline{COP}_{lon}	[cm]	ABhigh	15.2	3.8	5.8	11.7	7.5
		ABlow	13.9	2.7	4.2	10.1	6.9
\bar{p}	[kPa]	ABhigh	13.9	39.0	52.2	15.8	26.1
		ABlow	14.7	48.6	58.5	20.9	28.1
p_{peak}	[kPa]	ABhigh	26.6	148.3	125.8	34.2	74.7
		ABlow	35.9	146.3	110.3	71.4	79.6

Table 5.2. Indices obtained for the buttocks-saddle contact during the pressure tests (average).

Variable	Units	Posture	Set				
			1	2	3	4	5
\overline{COP}_{lon}	[cm]	ABhigh	4.5	6.2	4.4	3.2	2.6
		ABlow	4.5	5.1	4.8	4.0	2.6
\bar{p}	[kPa]	ABhigh	19.5	29.8	28.9	25.1	31.8
		ABlow	22.0	25.9	31.5	23.4	35.8
p_{peak}	[kPa]	ABhigh	82.6	76.4	109.0	74.2	116.7
		ABlow	86.4	71.8	86.8	68.6	126.0

Table 5.3. Indices obtained for the elbows-pads contact during the pressure tests (average).

5.4.1. Effect of posture on the longitudinal position of the center of pressure

The COP position for each posture is presented in Figure 5.6 for the measurement in the saddle and aerobars' pads. The results for the \overline{COP}_{lon} magnitudes are compared between riders and postures, including the standard deviation in Figure 5.7 for the saddle and Figure 5.8 for the pads (see Figure 5.3 for a reference of the coordinate systems). A one-way ANOVA was performed using a significance level of 5% to verify the differences in the \overline{COP}_{lon} between postures. For the saddle, it was obtained that for all sets, except set 5, the differences are statistically significant. For the aerobars' pads, it was obtained that for all sets, except set 2, the differences are statistically significant.

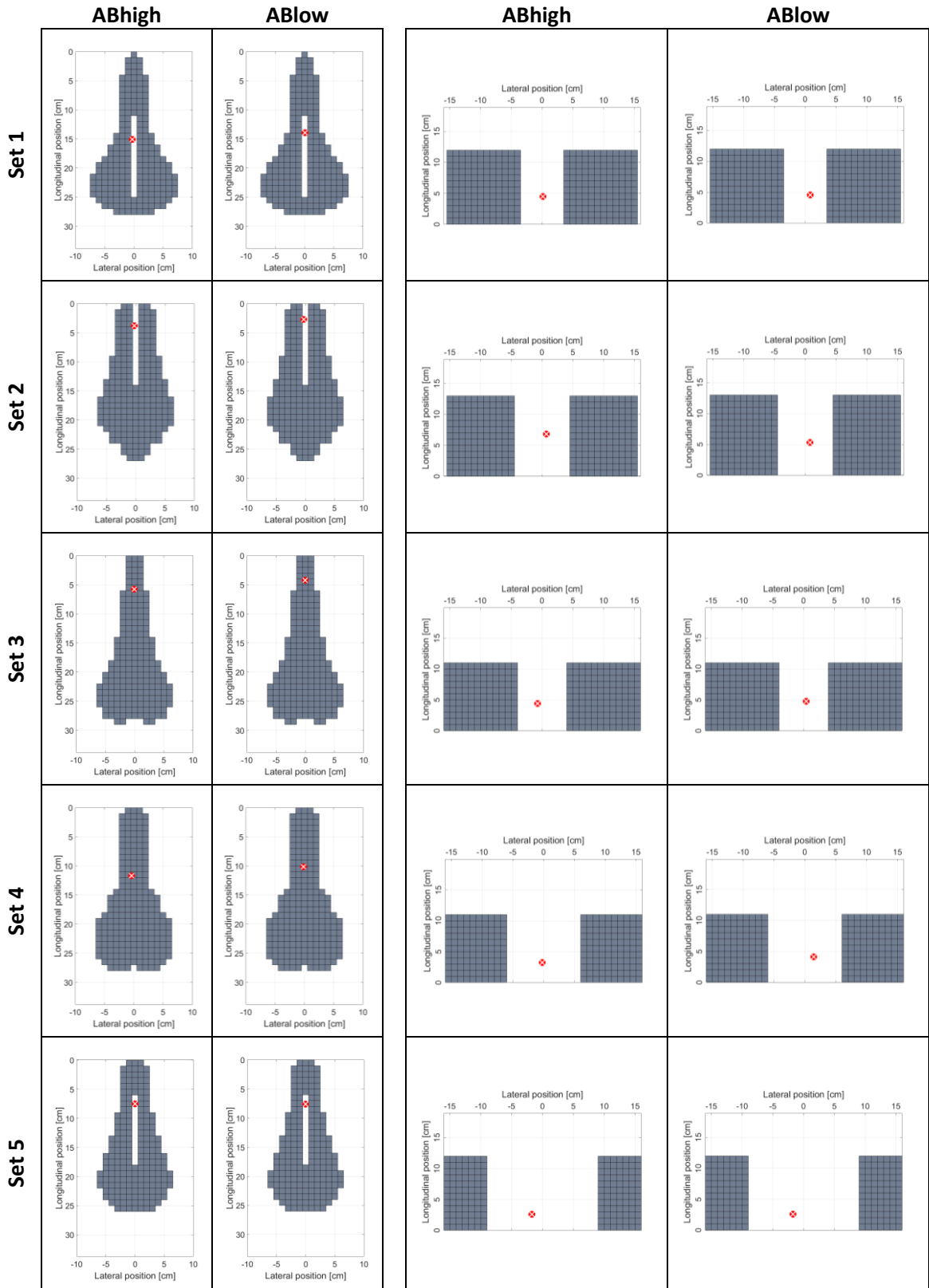


Figure 5.6. Position of the center of pressure in the saddle and aerobars' pads for the different cyclists and postures.

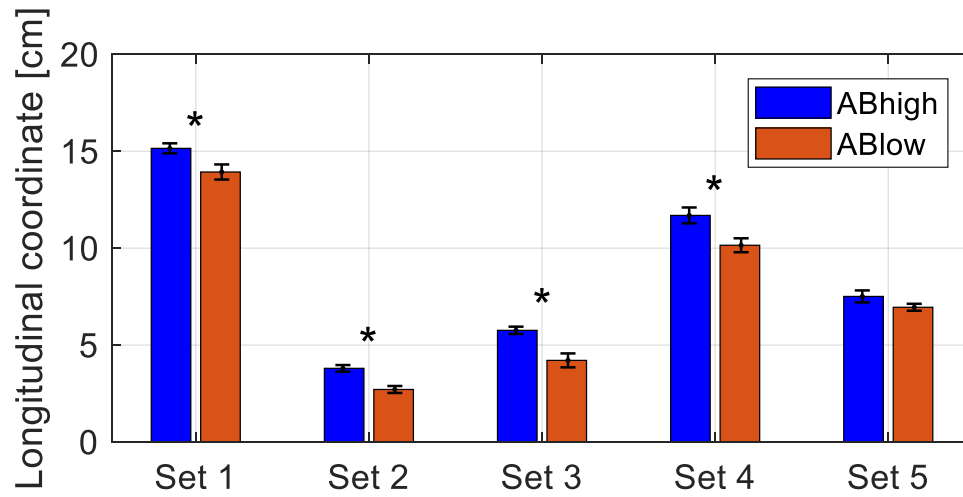


Figure 5.7. Longitudinal position of the center of pressure in Saddle.

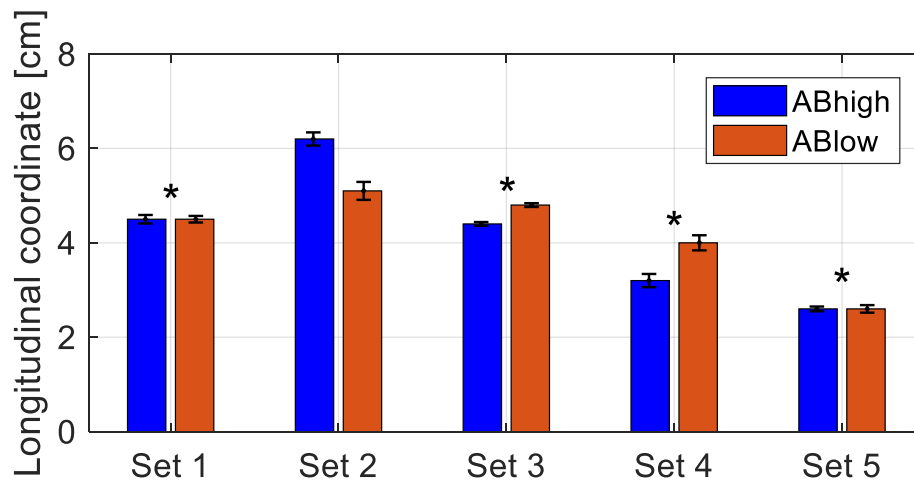


Figure 5.8. Longitudinal position of the center of pressure in Aerobars' pads.

From the data registered in the saddle (see Figure 5.7), it can be observed that, when the riders changed from Aerobars high to Aerobars low, the COP in the saddle moved to the front. This, because the body is bent forward, and as the body moves to the front, the hip is rotated or repositioned in the saddle. The \overline{COP}_{lon} presented a different variation for each cyclist between 0.6 cm and 1.5 cm. The average variation of the longitudinal COP position between postures was 1.2 cm (corresponding to a variation of 22%). From the data registered in the aerobars' pads, there is not a global trend on the \overline{COP}_{lon} results. For some cyclists, the COP moved forward (cyclists 1, 3, and 4), while for others, it moved backward (Cyclists 2 and 5). Even though there is a statistically significant difference for the \overline{COP}_{lon} on the pads of most riders, in practical terms, the variation registered for cyclists 1 and 5 is less than 1 millimeter, which is negligible. The maximum variation in the COP, in this case, was 0.7 cm.

5.4.2. Effect of posture on the average pressure and maximum average pressure over time

The results of \bar{p} are presented in Figure 5.9 for the saddle and in Figure 5.10 for the aerobars' pads. The tendency in the results is also presented in Figures 5.11 ad 5.12. The magnitude and standard deviation results are presented. According to one-way ANOVA results, the differences in the average pressure between postures are statistically significant (p -values < 0.004) in the saddle and elbow pads for all the sets.

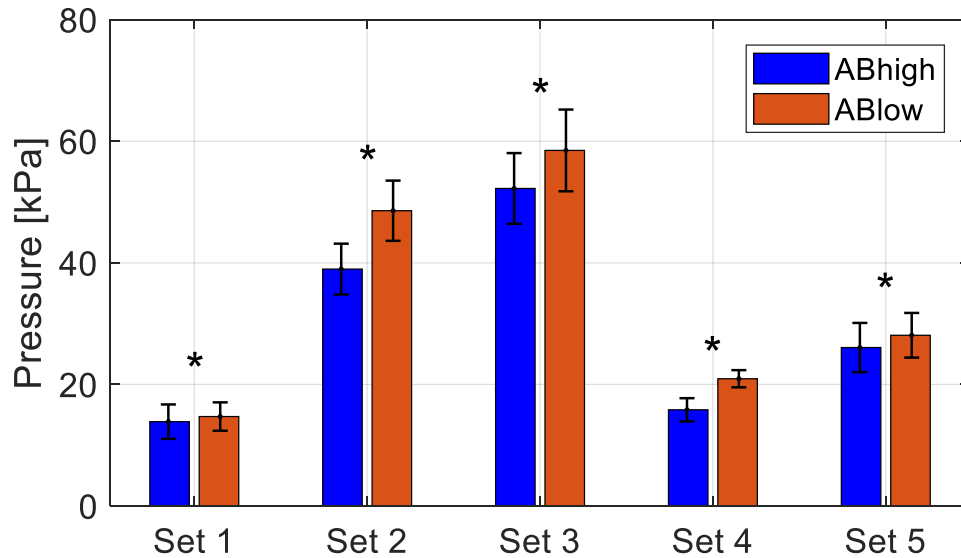


Figure 5.9. Average pressure in the saddle.

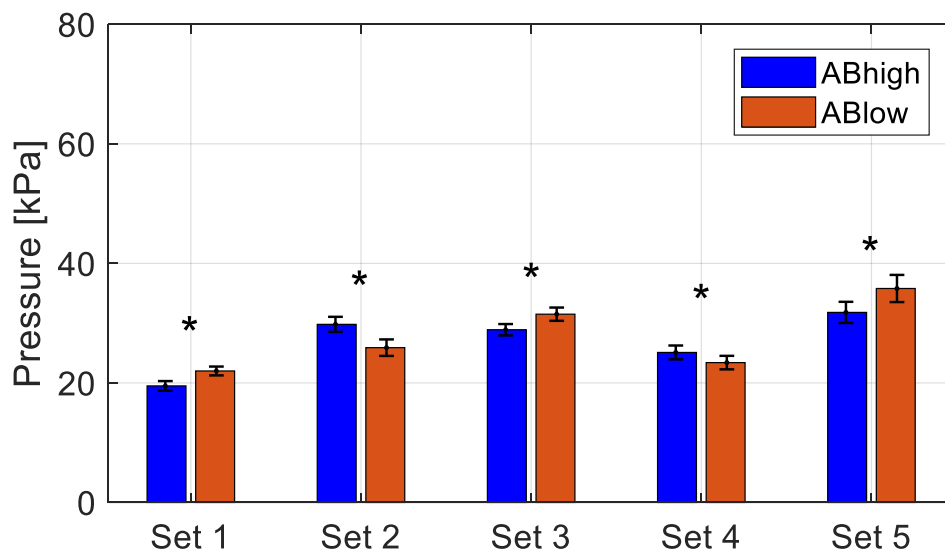


Figure 5.10. Average pressure in the Aerobars' pads.

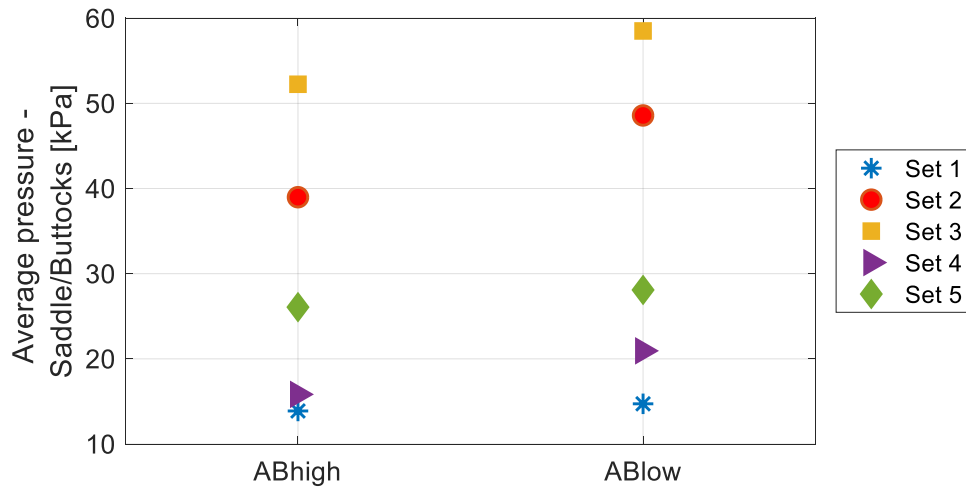


Figure 5.11. Tendency between postures of average pressure in the saddle.

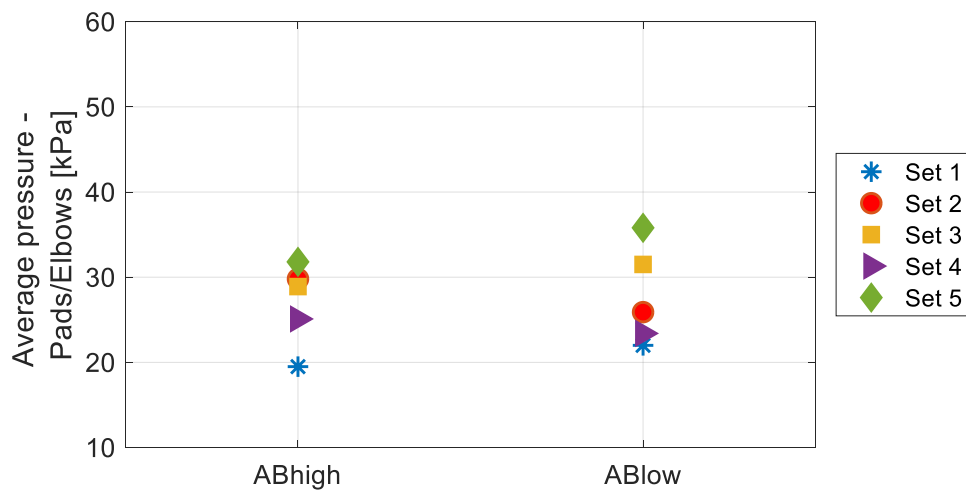


Figure 5.12. Tendency between postures of average pressure in the elbow pads.

The results of the p_{peak} are presented in Figure 5.13 for the saddle and in Figure 5.14 for the elbow pads. The details of the position of the peak pressures registered for each cyclist are presented in Figure 5.15 for the saddle and elbow pads.

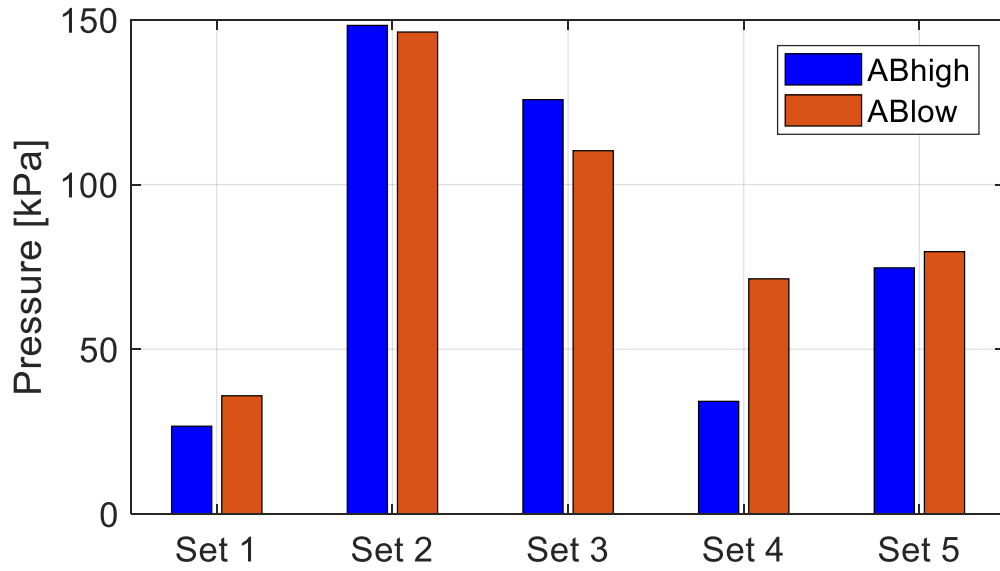


Figure 5.13. Peak pressure in the saddle.

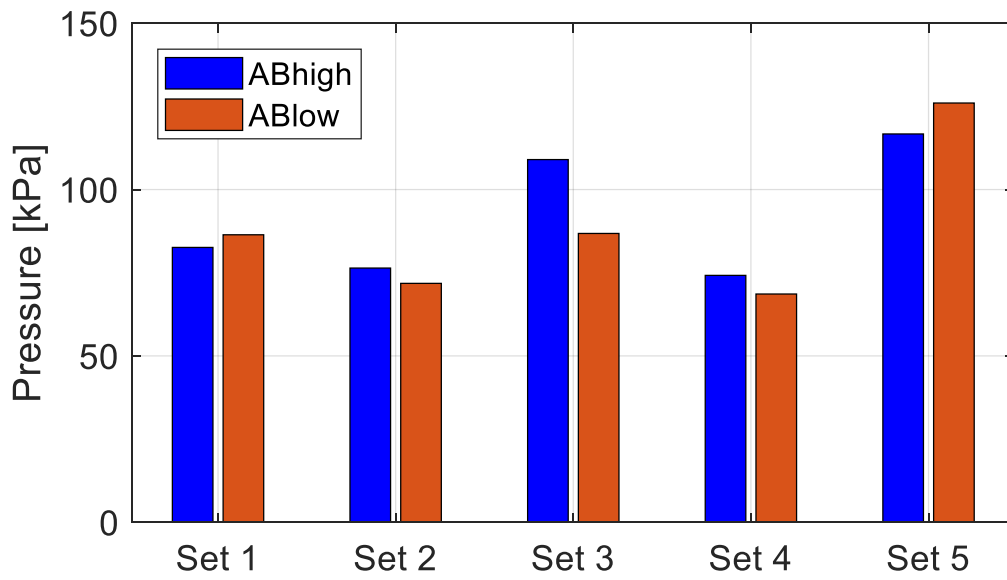


Figure 5.14. Peak pressure in the Aerobars' pads.

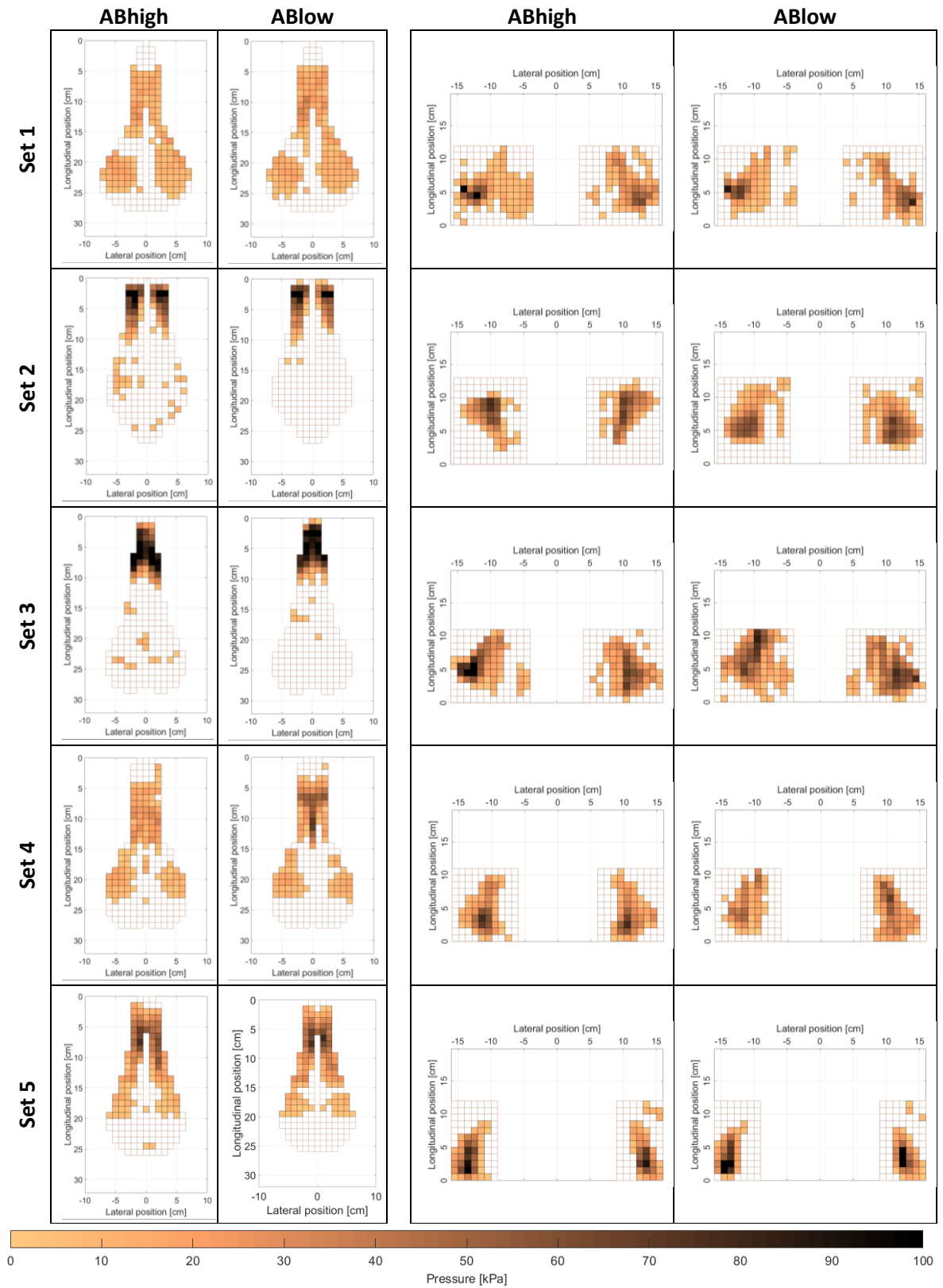


Figure 5.15. Peak pressure in the saddle for the different cyclists and postures.

It was expected that the average pressure and peak pressure would increase in the pads and decrease in the saddle when changing from ABhigh to ABlow due to an effect of load transfer from the saddle to the handlebar. Nevertheless, this behavior was not observed as a general trend. On the one hand, for all the cyclists the \bar{p} of the saddle increased when reducing the aerobars' height; this could be attributed to a reduction in the area of contact with the saddle when changing to ABlow, which combined with the support of the same weight leads to an increase in the pressure. On the other hand, the \bar{p} on the pads and the p_{peak} on the saddle and pads increased for some riders and decreased for the others. Different behaviors of the pressure fields were registered for each bicycle-cyclist set because they depend on the bicycle and the rider's characteristics. Each saddle has a particular geometry, each rider has particular anthropometry, and each rider has a particular way of seating in the saddle. See, for example, the difference in the positioning preference of the riders in Figure 5.16. Regarding the saddle, the rider on the left has a preference for seating in the saddle's anterior part, while the rider on the right uses a bigger zone of the saddle to seat. Regarding the aerobars' pads, the rider on the right supports the elbows, while the rider on the left supports the forearms. These differences between riders can also be observed in Figure 5.15, in which the patterns of the contact areas between the riders and the bicycle are evident. About these differences between riders, it has been reported that even for a group of cyclists using the same saddle, the pressure distribution pattern is different for each rider [89].



Figure 5.16. Examples of seating preferences of different cyclists.

The values of \bar{p} registered in the saddle lie in the 13.9 kPa to 58.5 kPa range for the saddle and 19.5 kPa to 35.8 kPa for the aerobars. The values of p_{peak} registered lie in the 26.6 kPa to 148.3 kPa range for the saddle and 68.6 kPa to 126.0 kPa for the aerobars' pads. The registered values are in agreement with values reported in the literature for the analysis of pressure in the buttocks-saddle contact (see Appendix 5.1 [24], [28], [86]). The relatively large variation of the values reported in the literature can be attributed to the difference of the testing conditions over the studies considering that the characteristics of the riders, the saddles, the power outputs, and the postures are varied. Also, the computation of the indices can be performed in several ways; for example, the sensors of the matrix included in the calculations (*e.g.*, all the sensors, the sensors of the saddle area, or the sensors of the contact area) can modify the results. There are not available reference values of pressure in the elbow-pads contact areas. It is worth highlighting that for some riders, the average and peak pressure values in the elbow-pads contact areas was higher than in the buttocks-

saddle contact remarking the importance of considering the pressures applied to the rider's body in other locations rather than the saddle, especially when riding in aerodynamic postures (*i.e.*, with the body bent forward).

The importance of analyzing the average pressure and peak pressure while cycling lies in the potential adverse effect of pressure on the tissues in contact with the bicycle. There are no specific thresholds defining loads that can be harmful to the human body while cycling. According to [93], this is due to the high dependence of the tissue tolerance to load on the tissue condition (*e.g.*, location, age, hydration), making it challenging to establish pressure thresholds. Nevertheless, the following thresholds have been used for the evaluation of cushions [94]: 30mmHg (4kPa) as it represents capillary pressure at heart level, 60mmHg (8kPa) is a threshold frequently used for pressure ischemia, and 120/90mmHg (16/12kPa) represents systolic/diastolic pressures. Also, a peak pressure threshold of 8.8kPa was reported for the analysis of comfort in automobiles [98]. It is worth highlighting that all the thresholds previously mentioned are exceeded by the pressures registered in this study for cycling. Considering the pressure-time relation, curves as the ones presented in Figure 5.17, reported on a study about pressure sores in seated humans, have been used [96]; in these plots, the curve presents a time-dependent threshold of pressure for the apparition of sores (reconstructed from data obtained in [99]). Both pressure-time threshold curves correspond to the expression shown in Eq. (5.7), where p_a is the acceptable pressure threshold in kPa for a given exposure time t_e in hours. The ranges of the average pressure values obtained in this study in the saddle and elbow pads were included in the subplots of Figure 5.17. It can be observed that with the average pressures registered, the acceptable time thresholds to avoid sores varies between 1 and 3 hours. The mentioned time range can be considered normal, and even short, training and competing times for sportive cycling practice. This means that the pressure values registered while cycling are high considering the time that cyclists ride the bicycle; for this reason, discomfort, pain, and overuse injuries on the buttocks and hands are frequently reported by cyclists. The reason why the cyclists can endure long periods of time riding with the high pressures registered for the saddle contact is that the oscillating motion of the legs and hip creates an oscillation in the pressure field. The reference values of pressure thresholds have been identified for constant load, and as stated by [24], the oscillations allow blood to flow on arteries and tissues in contact in this region. Nevertheless, the previous analysis highlights the importance of reducing the pressure in the contact areas when possible.

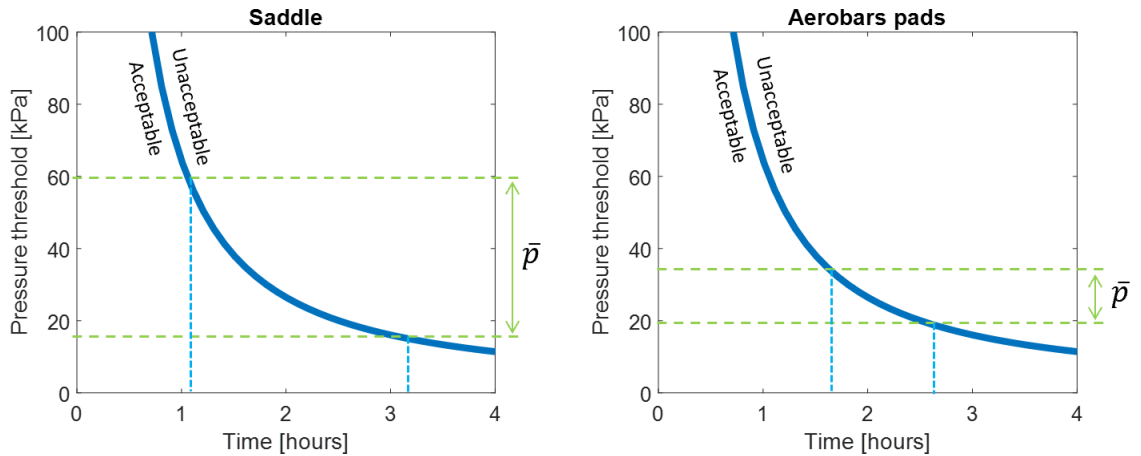


Figure 5.17. Pressure-time threshold for the apparition of saddle sores in humans. Recreated with the model reported in [96] fitted to the data of [99].

$$p_a = [471.9 * (t_e^{-4/3}) + 11.5] * 0.13 \quad (5.7)$$

5.5. CONCLUSION

A methodology for the measurement of pressure in buttocks-saddle and elbow-aerobars' contact areas was successfully implemented. The methodology was able to identify differences in the longitudinal position of the center of pressure, the average, and peak pressures when changing the height of the aerobars' pads.

For the bicycle-cyclist sets studied through the implementation of the methodology, it was obtained that when reducing the height of the aerobars, the position of the center of pressure in the saddle moves forward, and the average pressure in the saddle increases. Regarding the position of the center of pressure in the aerobars' pads, the average pressure in the pads, and the peak pressures in both contact areas, the effect of posture varied among the cyclists. For some cyclists, the change of posture led to higher magnitudes, leading to lower magnitudes for others. The results indicate that reducing the height of the aerobars leads to higher probabilities of discomfort, pain, or overuse injuries in the saddle, while the effect on the elbows is different for each cyclist.

The values for the pressure field's indices in the buttocks-saddle interface obtained by implementing the proposed methodology are in agreement with other values in the literature. The magnitudes of pressure registered for the cyclists are high when compared to pressure-time thresholds for the prevention of saddle sores considering that cycling activities usually require long riding periods; for this reason, minimizing the pressure in the contact areas while cycling is important.

CHAPTER 6. Interaction: measurement of vibrations transmitted to the cyclist

Related publications:

[100] A. Doria, E. Marconi, L. Munoz, A. Polanco and D. Suarez, “An experimental-numerical method for the prediction of on-road comfort of city bicycles,” *Vehicle Syst. Dyn.*, pp. 1-24, 2020.

[101] A. Polanco, E. Marconi, L. Munoz, D. Suarez and A. Doria, “Effect of rider posture on bicycle comfort,” in *ASME 2019 International Design Engineering Technical Conference, IDETC 2019, Anaheim, USA, August 18-21, 2019*, pp. 1-8.

[23] A. Polanco, D. Suárez and L. Muñoz, “Effect of body posture on comfort during cycling,” in *ASME 2017 International Design Engineering Technical Conference, IDETC 2017, Cleveland, USA, 6-9 August, 2017*, pp. 1-9.

6.1. ABSTRACT

In cycling, the irregularities of the road are transmitted through the bicycle to the rider through the contact points. Besides the magnitudes of the vibrations, the exposure time is important for analyzing the effect of vibrations transmitted to the human body; in cycling, it is common to spend long hours on the bicycle for training and competition. For this reason, the study of vibrations in this context is relevant because high levels of exposure to vibrations can lead to discomfort and even injuries. It is generally recognized that the rider's posture has a relevant effect on vibration transmission measurement. For this reason, it is usually stated that the posture is kept constant during the tests. Nevertheless, only a few studies have quantified the effect of body posture in vibration transmission. The effect of the variation of postures such as the aerobars' position on the vibration transmission to the rider has not been studied.

An outdoor road methodology was used to quantify the vibration transmitted to the cyclist. The methodology was implemented to measure the vibrations in the stem and steering tube of five bicycle-cyclist sets. The measurements were performed in two aerobars postures with different heights. The tests were performed at a constant speed on a smooth asphalt road. The vibrations were quantified using the rms of the tridimensional accelerations in the steering tube and the seatpost. The human sensitivity to vibrations was considered for the analysis according to the International Standards ISO 2631 and ISO 5349.

For the seatpost, it was obtained that only the vibrations in the vertical direction are relevant when considering human sensitivity. For the steering tube, it was obtained that the vibrations in the vertical and longitudinal directions are relevant. The accelerations registered in the steering tube were, on average, 61% higher than the ones registered in the seatpost for the bicycle-cyclist sets measured. When changing the aerobars' height, the effect on the vibrations was different for each cyclist; in some cases, significant effects were registered. For the cases of significant effect, lowering the aerobars' height led to higher accelerations in the seatpost (7% on average) and lower accelerations in the steering tube (15% on average). The implementation of the methodology permitted measuring differences in the vibrations in the steering tube and seatpost of road bicycles due to the variation in aerobars' height.

6.2. INTRODUCTION

Cyclists are exposed to vibration due to the irregularity of the road. The study of vibration is of relevance as it affects the activity development of people ranging from discomfort [102] to health risks [103]. For the study of vibration in cycling, the bicycle and cyclist have to be studied as a set given that the mass of the cyclist is relevant when compared with the mass of the bicycle influencing its overall behavior [104], [105]. The vibration perceived by the cyclist depends on the geometry, mass, inertia, and structural characteristics of the bicycle components and the characteristics, posture, and expectations of the cyclist [106]-[108].

Vibration transmission is usually studied by measuring vibrations in the points of interest, mainly in terms of accelerations. For this, accelerometers are located as close as possible to the points of interest. The accelerations measured are related to the human body sensitivity through

International Standards. The ISO 2631 [108] is used to analyze whole-body vibration, while the ISO 5349 standard [109] is used for the arm-hand system. These standards present different acceleration indices that can be used to evaluate vibration transmission. The basic evaluation method uses the root mean square (rms) of the accelerations weighted with a curve for considering the human sensitivity to vibrations. The rms of the weighted acceleration (a_w) is defined as in Eq. (6.1) [108], where t_{tot} is the duration of the measurement in seconds, and t is the time.

$$a_w = \sqrt{\frac{1}{t_{tot}} \int_0^{t_{tot}} a_w^2(t) dt} \quad (6.1)$$

The accelerations are weighed in frequency because “the manner in which vibration affects health, comfort, perception, and motion sickness is dependent on the vibration frequency content” [108]. Different curves are used depending on the case under analysis (*i.e.*, whole body or hand transmitted vibration) and the direction of vibration.

For the evaluation of comfort and perception, it is recommended to perform the assessment combining the vibrations registered in three orthogonal coordinates to obtain the vibration total value (a_v) as in Eq. (6.2) [108], where a_{wx} , a_{wy} , and a_{wz} are the weighted rms accelerations on the x , y , and z axes, respectively. Higher values of a_v are related with worse scenarios of comfort and perception. For whole-body vibrations, the frequency of interest is in the range of 0.5 Hz to 80 Hz, while for hand-arm transmitted vibrations, it is in the 8 Hz to 1000 Hz range.

$$a_v = \sqrt{a_{wx}^2 + a_{wy}^2 + a_{wz}^2} \quad (6.2)$$

It is worth noting that the posture adopted while cycling is different from the seated posture considered by the ISO 2631 [108]. The international standard considers a posture of normal sitting with an upright trunk, while in cycling, the body is bent forward. For this reason, the seated posture of the ISO 2631 is assumed as an approximation of the actual studied posture.

The measurement of vibrations in cycling can be performed through laboratory or road tests. The laboratory tests require a source of excitation for the bicycle; for this reason, the use of mechanical devices as hydraulic shakers under the wheels [33], [110], [111], and treadmills with bumps [102] has been reported for continuous excitation. Also, the use of impulsive methods to excite the system has been reported [100], [112], [113] (see Appendix 6.1 for the description of a method developed during the Internship at Padova University). For the case in which the bicycle is not translating, there is a difficulty associated with keeping the bicycle vertical. In this case, setups including the use of elastic cables wrapped on different components of the bicycle and fixed to a structure [33], [102], [110], [111], [113] have been reported as the most common solution. For the outdoor road tests, the excitation source is the road irregularity. The main difficulty in this approach is how the bicycle is propelled. In some studies, the rider is pedaling to move the bicycle [114]-[118]; nevertheless, some studies have adopted other techniques to isolate the vibrations without measuring the vibrations due to pedaling. For example, using a coast down approach [119], towing the bicycle, or pushing the rider in the back from another vehicle [104], [120], or performing the tests in a road with a negative slope or descending stairs [111], [121]. The instrumentation used for registering the

vibrations is similar for indoor and outdoor tests. Uniaxial and triaxial accelerometers are used for registering accelerations, while strain gauges and are used for force measurement in different bicycle components. Appendix 6.2 presents information about studies in which this instrumentation has been used.

Studies about the level of exposure of cyclists to vibrations [114], [117] and the development of instrumentation for the analysis of vibration in cycling [118] have reported their results in terms of the vibration total value a_v , including the weighting for human sensitivity. Other results about the effect of experimental setup variables, the relative contribution of bicycle components, or the quality of different road surfaces have been presented through simplified indices as the rms of the acceleration including only the vertical direction, instead of the three axes [33], [110], [111], [119]. Some other studies have presented the results as acceleration rms without weighting the acceleration signals or without mentioning the international standards [104], [115], [116], [121]. Finally, indices not contemplated in the international standards have been used to analyze vibration in cycling. For example, the power absorbed in the interphase, considering force and speed simultaneously, has been used [102], [110], [111], [118], [120].

It is acknowledged that posture has a significant effect on the vibrations transmitted to the rider while cycling. For this reason, in different studies, it is described that the posture is controlled by asking the rider to maintain a natural constant position [102], [104], [110], [120]. Nevertheless, few studies have quantified the effect of posture in vibration transmission. For example, in [33], it was concluded that the change in the position of the hands on the handlebar and even relatively small changes such as the wrist angles have a significant effect on vibration transmission. The effect of the variation of postures as the aerobars' position on the vibration transmission to the rider has not been studied. For this reason, the objective of this chapter is to implement a methodology for the measurement of vibration transmitted to the cyclist with enough sensibility to measure differences due to the variation of the aerobars' height.

This chapter presents a protocol to measure and analyze the vibration transmitted to the cyclist through the buttocks-saddle and elbow-aerobars' pads interfaces. The protocol was implemented with a group of cyclists riding in different aerobars postures. The vibration transmission was quantified through the vibration total value in the seatpost and headtube.

6.3. METHODS

A methodology based on road tests to measure vibration transmitted to the rider through the seatpost and the head tube was used. Three-dimensional accelerations were measured while the rider pedaled on a testing route at a constant speed. The vibrations were registered with wireless triaxial accelerometers with a sampling frequency of 5000 Hz (SlamStick LOG-0002-025G-PC, MIDE, USA). Tests were performed locating the accelerometers on the seatpost and steering tube. Clamp supports were used to place the accelerometers as presented in Fig 6.1. A GPS (Forerunner 910, GARMIN, USA) and a speed sensor (Speed sensor 2, GARMIN, USA) were used to register and display the speed to the rider in real-time. The riders traveled three times at a constant speed of 25 km/h on a straight route with smooth asphalt and a length of 400 m.

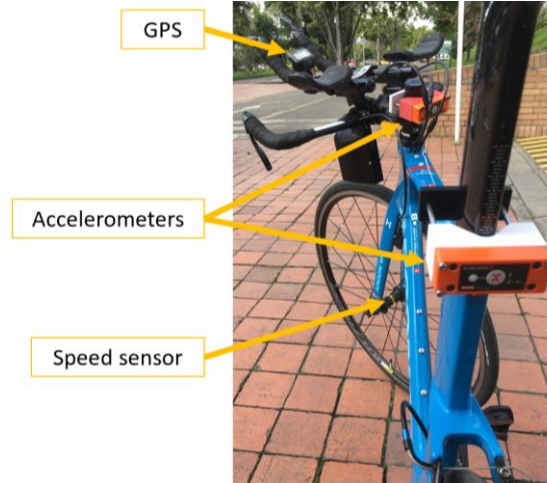


Figure 6.1. Setup for the measurement of vibration transmission.

The acceleration signals acquired were segmented using the GPS signal. Due to the position of the accelerometers on the bicycle, the axes were slightly rotated with respect to the vertical and longitudinal axes of the bicycle. For this reason, the signals were rotated considering the bicycle geometry as presented in Figure 6.2 to obtain the accelerations in the vertical, longitudinal, and lateral axes (a_{wver} , a_{wlon} , and a_{wlat} , respectively). The ISO 2631 [108] describes that the direction of the measurement of vibrations should be defined by the main axes of the body. This indicates that the z-axis would be aligned with the trunk of the cyclist. Nevertheless, in this study, the z-axis is defined in the vertical direction to have a constant orientation reference for the different postures and riders measured.

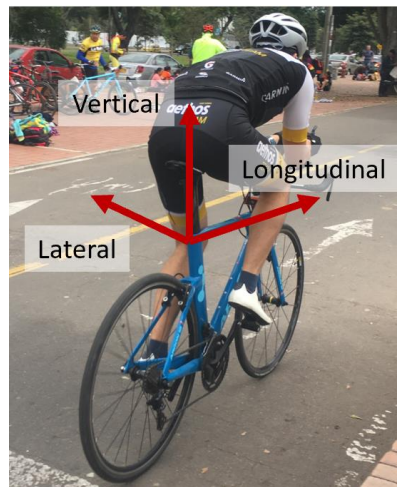


Figure 6.2. Acceleration orientations analyzed in the study.

The rotated signals were transformed from the time domain to the frequency domain. The signals were weighted to consider human sensitivity to vibrations, considering the orientation and location, according to the ISO 2631 and ISO 5349 [108], [109]. The rms of the weighted accelerations were computed, and the vibration total value (a_v) was computed for the seatpost and the steering tube as in Eq. (6.2).

It is worth highlighting that the accelerometers' position is not in the contact between the rider and the bicycle as the instrumentation could cause discomfort and reduce the maneuverability. Nevertheless, the position selected on the bicycle eases repeatability on the location of the accelerometers, which is useful for comparing different conditions as the riders' posture. Appendix 6.3 presents a summary of the protocol for the measurement of vibration transmitted to the rider.

Five recreational cyclists voluntarily participated in the tests after signing an informed consent form (mass: 73.8 ± 11.8 kg, height: 1.75 ± 0.06 m, age: 35 ± 7 years). The riders used their own bicycles and standard cycling clothes. The tests were performed in two aerobars postures with different heights. For road bicycles, clip-on aerobars were used. Depending on each bicycle's characteristics, the height was varied using spacers on the steering tube or the aerobars support. Table 6.1 presents a summary of the information of each bicycle-cyclist set (further detail can be found in Tables 2.1, 2.2, and 2.3 in chapter 2).

	Variable	Units	Set				
			1	2	3	4	5
Rider	Mass	[kg]	59	72	92	73	73
	Height	[m]	1.67	1.72	1.76	1.78	1.83
	Age	[years]	38	26	42	39	30
	Gender	[-]	Female	Male	Male	Male	Male
	FTP	[W]	140	217	168	169	193
Bicycle	Type	[-]	Aero	Time trial	Aero	Endurance	Time trial
	Aerobars' height difference	[mm]	55	55	55	55	40

Table 6.1. Bicycle-cyclist sets included in the vibration transmission tests.

6.4. RESULTS AND DISCUSSION

The vibration total values (a_v) were computed from vibration signals obtained considering the human sensitivity according to ISO2631 [108] for the seatpost and ISO5349 [109] for the steering tube.

6.4.1. Computation of weighted power spectral densities

Figure 6.3 presents an example of the weighting filters' effect on the vibrations measured for set 1 in ABhigh posture. The vibrations are presented as the average of the power spectral densities (PSDs) of the accelerations registered for the different trials. The signals obtained for the vertical, longitudinal, and lateral axes are displayed. Regarding the accelerations in the three orthogonal directions, it can be observed from the unweighted (*i.e.*, original) signals that the magnitude of the accelerations in the lateral direction is negligible, while the magnitudes of the vibrations in the vertical and longitudinal directions are similar. This was expected because the bicycle dynamics for the case tested (*i.e.*, constant speed, flat, and smooth road) are dominant in the sagittal plane. The differences in the magnitudes of accelerations in different directions are in agreement with previous results [118]. Regarding the effect of the human sensitivity weighting, it is worth highlighting that

for the whole-body vibration (in this case transmitted through the seatpost), there is a weighting curve for the vertical direction and another for the lateral and longitudinal directions. For the hand-transmitted vibration, the same weighting curve is used in all directions. According to the use of the weighting curves, it can be observed for the seatpost that the vibrations in the longitudinal and lateral directions are severely attenuated. In the vertical direction of the seatpost and all the directions of the steering tube, the signals are completely attenuated for frequencies higher than 50 Hz. The weighting curves highlight a high sensitivity to hand-transmitted vibrations in the range from 3 Hz to 51 Hz (with a peak around 12 Hz), considering that the magnitudes of vertical accelerations out of such range are weighted with an attenuation of -10dB. Similarly, for a seated person, there is high sensitivity in the 0.4 Hz to 40Hz range (with a peak around 6 Hz), and the magnitudes out of this range are also weighted with an attenuation of -10dB. The same behavior was observed for the vibrations of the other riders (see Appendix 6.4 to Appendix 6.7).

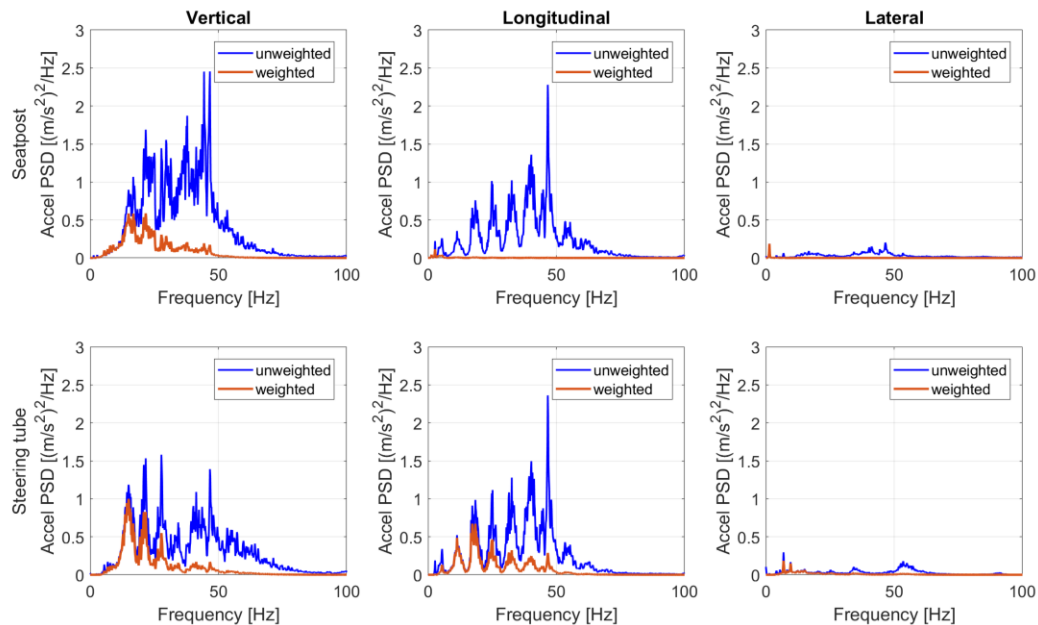


Figure 6.3. Effect of human sensitivity on the average acceleration power spectral densities. Example for Cyclist 1 riding in ABhigh posture.

The averages of the acceleration PSDs of the riders are presented in Figure 6.4 for the seatpost and in Figure 6.5 for the steering tube. In Figure 6.4, the vibrations are presented only in the vertical axis because the magnitudes of vibrations of the seatpost in the longitudinal and lateral orientations are negligible. In Figure 6.5, the vibrations are presented in the vertical and longitudinal axis because the magnitudes of vibrations of the steering tube in the lateral orientations are negligible. It can be observed on the vibrations of the seatpost that the shapes of the PSDs in the vertical direction are similar for the two postures with variations in the magnitudes of some peaks. For all the sets, in most of the frequency regions in which a difference between the PSDs is noticeable, the magnitudes of ABhigh are higher than those of ABlow. It can be observed on the steering tube's vibrations that the differences of the PSDs between the postures vary for the different riders.

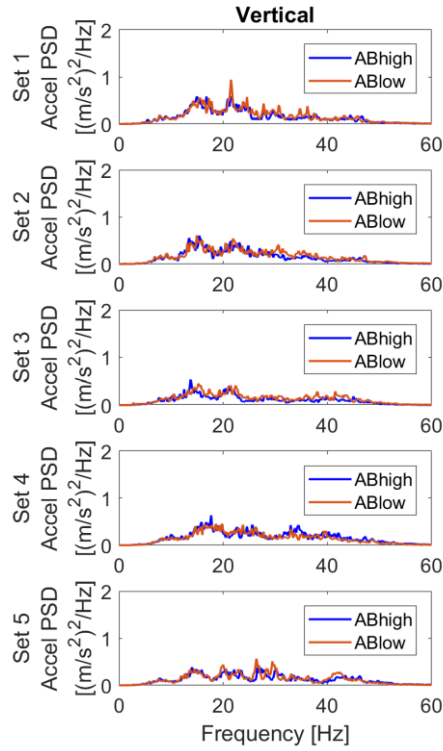


Figure 6.4. Effect of posture on the average acceleration power spectral densities in the seatpost.

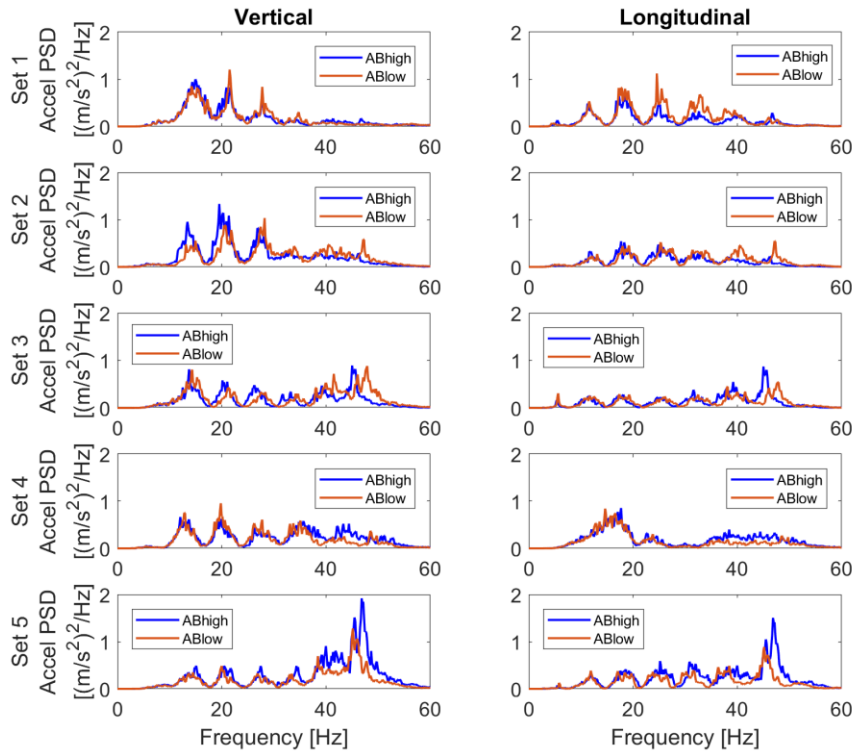


Figure 6.5. Effect of posture on the average acceleration power spectral densities in the steering tube.

6.4.2. Effect of posture on vibration total values

The results obtained for the weighted rms accelerations on the vertical, horizontal, and lateral axes (a_{wver} , a_{wlon} , and a_{wlata} , respectively), and the vibration total values (a_v) are presented in Table 6.2 for the seatpost and in Table 6.3 for the steering tube. It can be observed that the values computed for the steering tube are higher than the ones computed for the seatpost. It can also be observed that, in the seatpost, the vertical direction of vibration is more relevant than the longitudinal and lateral directions. For both postures, a_{wver} represents in average 80% of a_v , while a_{wlon} represents 12%, and a_{wlata} represents 8%. For the steering tube, a_{wlon} is almost as relevant as a_{wver} . In average, a_{wver} represents 47% of a_v , while a_{wlon} represents 37%, and a_{wlata} represents 16%.

Variable	Units	Posture	Set				
			1	2	3	4	5
a_{wver}	[m/s ²]	ABhigh	2.94	2.90	2.50	3.00	2.70
		ABlow	3.08	3.10	2.84	3.09	2.83
a_{wlon}	[m/s ²]	ABhigh	0.48	0.43	0.47	0.47	0.47
		ABlow	0.49	0.44	0.51	0.41	0.47
a_{wlata}	[m/s ²]	ABhigh	0.28	0.30	0.23	0.25	0.17
		ABlow	0.23	0.31	0.25	0.25	0.21
a_v	[m/s ²]	ABhigh	3.00	2.95	2.56	3.04	2.74
		ABlow	3.13	3.15	2.90	3.13	2.88

Table 6.2. Acceleration indices (vibration total values) obtained for the seatpost.

Variable	Units	Posture	Set				
			1	2	3	4	5
a_{wver}	[m/s ²]	ABhigh	3.26	3.60	3.15	3.58	4.06
		ABlow	3.04	3.52	3.39	3.25	3.33
a_{wlon}	[m/s ²]	ABhigh	2.68	2.60	2.72	3.24	3.62
		ABlow	3.10	2.84	2.61	2.90	2.99
a_{wlata}	[m/s ²]	ABhigh	0.89	1.27	0.79	0.89	1.06
		ABlow	0.82	1.33	0.92	0.91	1.00
a_v	[m/s ²]	ABhigh	4.32	4.62	4.24	4.91	5.54
		ABlow	4.42	4.71	4.37	4.45	4.59

Table 6.3. Acceleration indices (vibration total values) obtained for the steering tube.

The results of the vibration total values (a_v) are graphically presented in Figure 6.6 for the seatpost, and Figure 6.7 for the steering tube. The tendency in the results is also presented in Figures 6.8 and 6.9. The average and standard deviations are presented for both postures. A one-way ANOVA was performed using a significance level of 0.05 to verify the differences in the a_v between postures. From the results of the vibrations measured in the saddle, it can be observed that for all the sets, the acceleration index increased when changing from ABhigh to ABlow (between 3% and 12%). Nevertheless, only for sets 2 and 3, the difference was statistically significant. From the results of

the vibrations measured in the steering tube, it can be observed that a significant difference was found only for set 5, for which the acceleration index decreased 21% when changing from ABhigh to ABlow. From the results, it can be seen that the magnitude of the difference in the av of the seatpost and the steering tube between the postures changes for each set. The results indicate that for some cyclists, ABlow is less comfortable in the saddle and more comfortable in the steering tube than ABhigh.

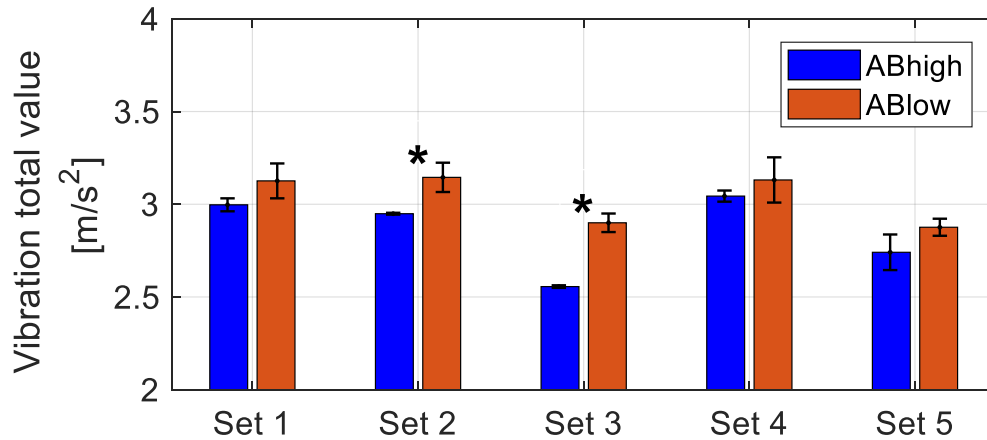


Figure 6.6. Vibration total values computed for the seatpost.

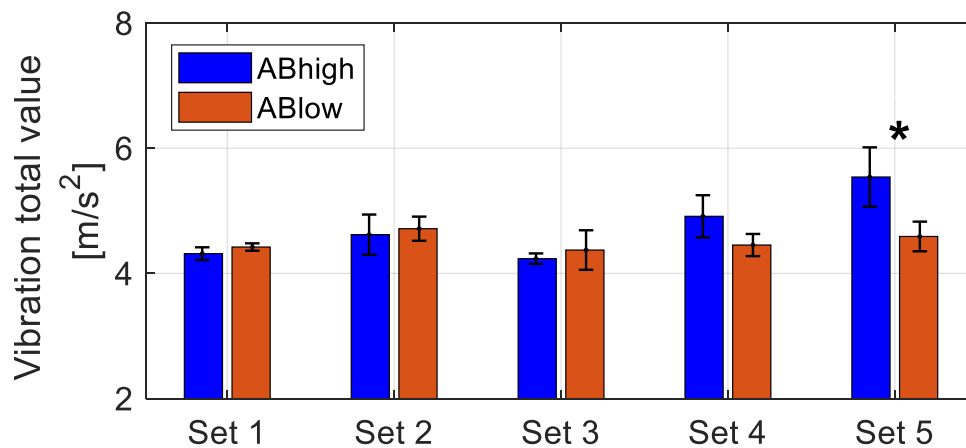


Figure 6.7. Vibration total values computed for the steering tube.

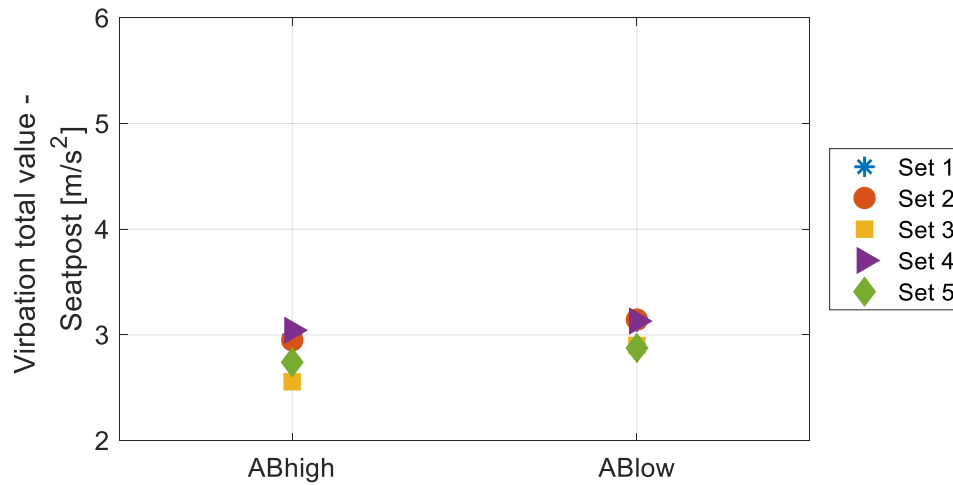


Figure 6.8. Tendency in vibration total values computed for the seatpost.

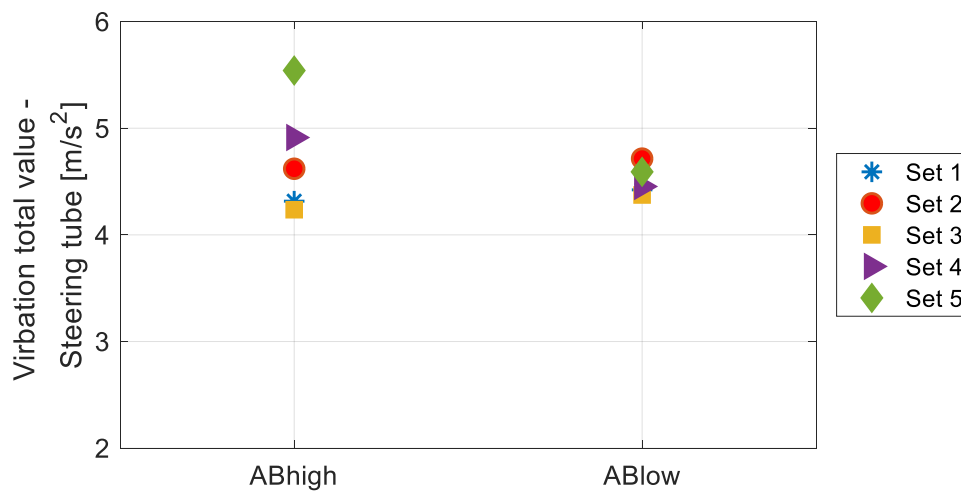


Figure 6.9. Tendency in vibration total values computed for the steering tube.

It should be noticed that the a_v reported are representative only of the tested conditions of this study. Variables as the bicycle speed and the testing route roughness influence the vibrations transmitted to the bicycle. Nevertheless, the values obtained agree with the ones reported by [33] in which the vibration indices in the stem are approximately 67% higher than the ones in the seatpost (the average difference in this study was computed as 61%). Additionally, the average magnitudes of the acceleration index in the seatpost and steering tube in this study were 2.9 m/s² and 4.6 m/s², respectively, while in [33], the values reported for an aerodynamic posture are close to 3.25 m/s² and 5.5 m/s², respectively.

For the analysis of vibration transmitted to the human body, not only the magnitudes of acceleration are important, but also the time of exposure is relevant. For this reason, the ISO 2631 has curves of health guidance caution zones for whole-body vibration, and the ISO 5349 mentions a threshold for an increased probability of presenting the hand-arm vibration syndrome. Thresholds of exposure

increasing health risks can be defined from the information of the standards considering the equivalency between vibration exposures as in Eq. (6.3) [108]. In this expression, a_{w1} and a_{w2} are the weighted accelerations of two exposures, and T_1 and T_2 are the corresponding exposure durations.

$$a_{w1}\sqrt{T_1} = a_{w2}\sqrt{T_2} \quad (6.3)$$

From this expression, it is possible to estimate an acceptable acceleration threshold a_a for a given exposure time t_e as in Eq. (6.4).

$$a_a = A_{ref} \sqrt{\frac{T_{ref}}{t_e}} \quad (6.4)$$

To define the acceleration-time threshold curve for the seatpost, the A_{ref} was identified in the curve for health guidance caution zones of the ISO 2631 for a T_{ref} of 4 hours. The resulting expression is presented in Eq. (6.5). To define the threshold curve for the stem, the 8-hours energy-equivalent vibration total value presented in the ISO 5349 was used. For this reference exposure time, the standard suggests a hand-transmitted acceleration threshold of 2m/s^2 . The resulting expression is presented in Eq. (6.6).

$$a_{a,seatpost} = 1.2\sqrt{4/t_e} \quad (6.5)$$

$$a_{a,stem} = 2\sqrt{8/t_e} \quad (6.6)$$

The acceleration-time threshold curve for the seatpost and the stem are presented in Figure 6.10. The ranges of the accelerations obtained in this study in the seatpost and the stem are included in the figure. It can be observed that the exposure duration to enter the zone of health caution for the registered a_v values varies between 30 minutes and 2 hours. These time ranges are commonly exceeded in cycling during training and competition. Also, it can be observed that even though the magnitudes of vibration in the steering tube are higher than in the seatpost, the potential adverse effect on the health of the rider is higher for vibrations transmitted through the saddle-buttocks interface.

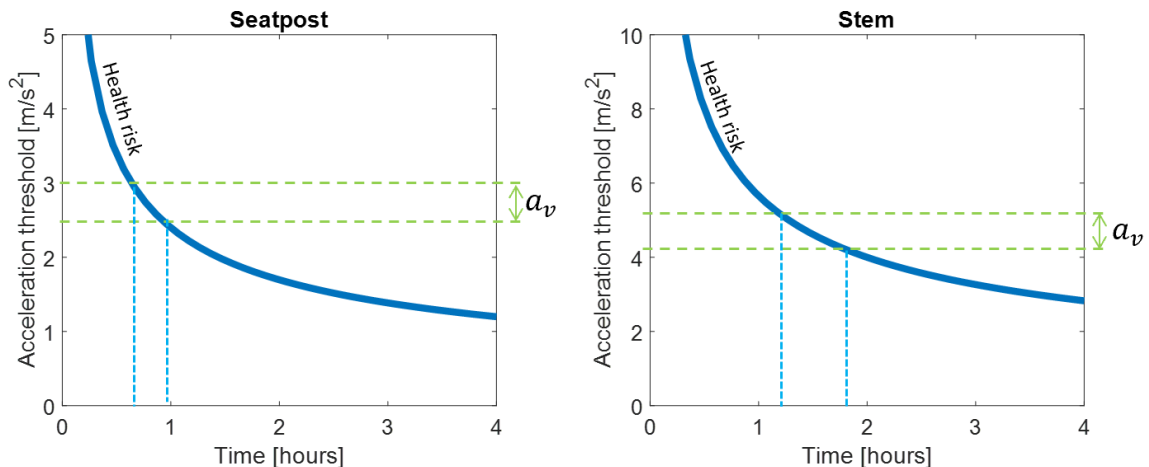


Figure 6.10. Acceleration-time threshold for increased health risks.

The analysis of the relation between time of exposure and vibration amplitudes registered highlights the relevance of reducing the levels of vibration transmitted to cyclists. It is worth highlighting that the testing route used in this study is smooth, and the tested speed is relatively low for road cycling, implying that in actual cycling conditions, the vibration values can be higher than the ones reported here. Nevertheless, it should be considered that the actual vibrations in the contact points with the rider are lower as the saddle and elbow pads paddings mitigate the vibrations transmitted.

6.5. CONCLUSION

A methodology for the measurement of vibrations in the seatpost and the steering tube was successfully implemented. Vibration indices were computed in the seatpost and the steering tube from the rms of the accelerations measured in three orthogonal directions. For all the riders who participated in the study, at least one of the acceleration indices (seatpost or steering tube) presented a statistically significant difference; this shows that the methodology has enough sensibility to measure differences in vibration transmission due to the variation in aerobars' height.

For the bicycle-cyclist sets studied through the implementation of the methodology, it was obtained that the effect of the aerobars' height on the acceleration index varies for each bicycle-cyclist set. For the riders that presented variations, reducing the height of the aerobars led to higher accelerations in the seatpost and lower accelerations in the steering tube. The results indicate that for some cyclists reducing the height of the aerobars' pads improves the vibrations in the elbows and worsens the vibrations in the buttocks. It was also obtained that the accelerations in the steering tube are higher than in the seatpost.

The relation between the vibration amplitudes registered in the seatpost and the stem and the usual times of exposure while cycling represents a scenario of possible health risk considering the caution zones for health and suggested maximum acceleration values presented in international standards for the study of human vibration (ISO 2631 and ISO 5349).

CHAPTER 7. Effect of posture on cyclist's performance and interaction with the bicycle.

Case of study: height of aerobars

Related publications:

[122] A. Polanco, L. Muñoz, A. Doria, and D. Suárez, "Selection of posture for time-trial cycling events," *Appl. Sci.*, vol. 10, (18), 2020.

7.1. ABSTRACT

The aerobars postures are of interest for riders competing in cycling and triathlon events in which the aerodynamics are relevant, and the collision risk is reduced. The aerobars postures are characterized by their aerodynamic advantages, but they are also associated with an increased difficulty to sustain the posture for long periods. There are some studies about postures while riding in aerobars. Nevertheless, further studies are needed. For this reason, a methodology for the study of the influence that variations in the body posture while riding in aerobars have on the performance of cyclists and their interaction with the bicycle is presented. The methodology aims at minimizing the race time subject to vibration and pressure exposure thresholds.

Five bicycle-cyclist sets were included in the study. The power delivery capacity, drag area, vibration transmission, and pressure in contact areas were previously measured for two postures. The postures were defined by the aerobars' height fit limits of each bicycle, and the characterization of the mentioned variables was performed in such postures. The information was used to select and optimize the aerobars height for each bicycle-cyclist set considering a 20-km race and various road inclinations and wind speeds (inclination range from -5 to 5%, and wind speed range from -2 to 5 m/s).

The race time was computed for each set for different race conditions. It was obtained that the results vary for each bicycle-cyclist set. Regarding race time, it is obtained that it increases for higher inclination and headwind conditions. Congruently, regarding the constraints, smaller acceptable thresholds are obtained for larger race times, leading to unfeasible race conditions. For all the sets, it was obtained that the vibration in the saddle was the variable that limited the feasible race conditions. The results showed that for a race condition of flat terrain, the posture with the lowest aerobars height was only advantageous for two riders riding at headwind speeds higher than 10.5 km/h. For a race condition with zero wind speed, it was found that the road inclination for which the change of posture was advantageous varied between -3.6% and 1.0%. For a race condition with zero-wind speed and zero-inclination, the race time improvements of the different bicycle-cyclist sets varied for a 20-km distance, between 14 and 97 seconds (corresponding to variations of 0.6% and 5.6%, respectively), with an average of 60.2 seconds were found when changing the posture.

A methodology for selecting and optimizing aerobars' height of bicycle-cyclist sets was successfully implemented to minimize race time considering pressure and vibration exposure constraints. It is concluded that posture optimization should be performed for each bicycle-cyclist set. The relation between the variation of the performance and the variation of the interaction variables when changing the posture is relevant for posture optimization. The suggested posture depends on the race conditions as road inclination, wind speed, and distance, among others.

7.2. INTRODUCTION

The riders use aerobars postures during cycling to take advantage of the aerodynamic drag reduction with respect to traditional postures [37]. Nevertheless, riding in aerobars leads to stricter constraints in the posture as, for example, higher trunk flexion and neck extension, which leads to

variations in the power delivery capacity [6], [7], [38]-[42], and can increase the discomfort. Given that the race time is affected by the aerodynamic drag and the power delivery capacity, it is necessary to evaluate if a posture modification is advantageous by verifying how much these variables fluctuate when changing the posture. For example, if a modification in posture improves the aerodynamic drag, but the rider's power delivery capacity has a substantial reduction, it is possible that the posture variation is not advantageous. In addition, even if the posture modification is advantageous regarding an improvement in the race time, but the posture increases the discomfort or has a higher potential to lead to overuse injuries, the posture may not be used. The potential to cause discomfort and eventually overuse injuries can be objectively quantified by measuring the pressure in contact areas between the bicycle and the rider and the vibrations transmitted to the rider.

It is possible to find some suggestions for the definition of posture when riding in aerobars. Nevertheless, studies on the effect of postural parameters in aerobars postures are scarce. For example, suggestions about the repositioning of the saddle [45], the hip flexion angles [44], and the location of the elbow pads [13], [44] have been given. Studies about the effect of the head and torso inclinations and the position of the elbows, saddle, and handlebar on performance have been reported [11], [13], [38], [43]. The effect of the variation in aerobars postures on the vibration transmission to the rider or the pressure in contact areas has not been found to date. For this reason, the rider's exact position when using aerobars is currently usually defined to reduce the aerodynamic drag as much as possible, estimating that the rider can hold the posture for the entire race duration.

This chapter presents a methodology for studying the influence that variations in the body posture while riding in aerobars have on cyclists' performance and their interaction with the bicycle. One postural parameter is varied in this study: the height of the aerobars. The performance is assessed in terms of total race time computed for specific race conditions (*i.e.*, race length, wind speed, and road grade). The total race time is computed using the bicycle-cyclist set's drag area coefficient and the rider's power delivery capacity. The interaction is assessed in terms of vibration transmission and pressure in contact areas. The methodology is based on an optimization problem to minimize race time subjected to restrictions imposed by interaction variables when changing the posture. The objective is to implement a methodology for selecting aerobars' height considering simultaneously aerodynamic drag, power delivery capacity, pressure in contact areas, and vibration transmission for different race conditions (*i.e.*, defined by the race distance, average road grade, and average wind speed). The methodology is implemented with a group of bicycle-cyclist sets riding on their own bicycles.

7.3. METHODS

This section describes the optimization problem, the scenarios, conditions, and bicycle-cyclist sets studied, and the variables used for its solution.

7.3.1. Optimization problem

The optimization problem was defined as: Finding the value of the aerobars' height that minimizes the total race time for a given race condition subjected to thresholds of vibration on the seatpost and steering tube, and thresholds on the pressure in the buttocks-saddle and elbows-pads contact areas.

For this optimization problem, the design variable is the height of the aerobars (h). The objective function is the total race time t_r , which is computed using the drag area ($C_D A$) and power delivery capacity (\bar{P}) performance indices. The race condition refers to the race distance (X_r), wind speed (v_w), and road grade (θ) for which the problem is solved. The constraints are related to limit values for the vibration transmission and pressure in contact points. On the one hand, the global average pressure on the saddle (\bar{p}_S) and the aerobars' elbow pads (\bar{p}_{AB}) cannot exceed the pressure thresholds on the saddle (p_{thS}) and elbow pads (p_{thAB}). On the other hand, the vibration total values measured close to the saddle (a_{vS}) and the aerobars (a_{vAB}) cannot exceed the respective vibration thresholds on the saddle (V_{thS}) and the aerobars (V_{thAB}). The values of V_{thS} , V_{thAB} , \bar{p}_{thS} , and \bar{p}_{thAB} are time-dependent.

The standard form of the optimization problem is presented in Eq. (7.1):

$$\begin{aligned} & \text{minimize} \quad t_r(h) \\ & \text{subject to:} \quad h \in \mathcal{H}, \quad g_k(h) \leq 0, \quad k = 1, 2, 3, 4 \end{aligned} \quad (7.1)$$

where \mathcal{H} is the set of aerobars' heights under study, and the restrictions g_k are:

$$g_1(h) = \bar{p}_S(h) - p_{thS}(t_r(h)) \quad (7.2)$$

$$g_2(h) = \bar{p}_{AB}(h) - p_{thAB}(t_r(h)) \quad (7.3)$$

$$g_3(h) = a_{vS}(h) - V_{thS}(t_r(h)) \quad (7.4)$$

$$g_4(h) = a_{vAB}(h) - V_{thAB}(t_r(h)) \quad (7.5)$$

Two scenarios were considered to solve the optimization problem. Scenario 1: two discrete options for the aerobars' height are considered (see Eq. (7.6)). Scenario 2: continuous options of aerobars' heights in an interval are considered (see Eq. (7.7)). The values of h_1 and h_2 are defined by the lower and upper limits of the aerobars' height according to the bicycle fit window (named ABlow and ABhigh, respectively).

$$\mathcal{H} = \{h_1, h_2\} \quad (7.6)$$

$$\mathcal{H} = [h_1, h_2] \quad (7.7)$$

For both scenarios, multiple race conditions were studied varying v_w between a tailwind of 2 m/s and a headwind of 5m/s, and θ between -5% and 5%. A constant X_r of 20 km was defined for all the race conditions.

7.3.2. Definition of the objective function: race time

The total race time (t_r) of a given race condition was computed from the bicycle speed (v_b) and the race distance (X_r) as in Eq. (7.8).

$$t_r = \frac{X_r}{v_b} \quad (7.8)$$

The v_b was computed from the equation of the longitudinal dynamics of the bicycle-cyclist set presented in Eq. (3.9) under the assumption of a constant bicycle speed leading to Eq. (7.9).

$$\frac{1}{2} \rho C_D A (v_b + v_w)^2 + mg \cos(\theta) f_r = \eta \left(\frac{\bar{P}}{v_b} \right) - mg \sin(\theta) - c_1 - c_2 v_b \quad (7.9)$$

In Eq. (7.9) ρ is the air density, m is the bicycle-cyclist set mass, g is the gravitational acceleration, f_r is the rolling resistance coefficient, η is the power transmission efficiency, and c_1 and c_2 are parameters of the equivalent bearing resistance. The v_w and θ values were defined for each race condition from the ranges previously described (-2 to 5 m/s and -5% to 5%, respectively). The ρ , g , η , c_1 , and c_2 were defined as constants, as presented in Table 7.1. The m was measured for each bicycle-cyclist set. In addition, for h_1 and h_2 the $C_D A$ and f_r were measured according to the protocol presented in Chapter 3, and the \bar{P} was obtained with the protocol presented in Chapter 4 for the Functional threshold power measurement.

Parameter	Units	Value
Air density (ρ)	[kg/m ³]	0.9
Gravitational acceleration (g)	[m/s ²]	9.8
Power transmission efficiency (η)	[%]	97
Equivalent bearing resistance parameter 1 (c_1)	[N]	0.091
Equivalent bearing resistance parameter 2 (c_2)	[N.s/m]	0.0087

Table 7.1. Constants used in the longitudinal dynamics model.

For Scenario 1 (two postures ABlow and ABhigh), for each posture, each bicycle-cyclist set, and each combination of v_w and θ of the race conditions considered, a t_r was computed. Then, based only on the performance information, the posture with the minimum value in the objective function was chosen for each rider and race condition.

For Scenario 2 (continuous options of aerobars' heights between ABhigh and ABlow), the t_r was also computed for the intermediate postures. For each rider and combination of v_w and θ the aerobars' height corresponding to the lowest t_r was registered. Considering that the variables of the bicycle-cyclist sets were measured for the extreme postures (ABhigh and ABlow) and not for the intermediate postures, the estimation of t_r for these postures was performed using a linear interpolation of $C_D A$ and \bar{P} between the tested postures.

7.3.3. Definition of the constraints: thresholds for pressure and vibration

The constraints associated with the variables of the interaction between the bicycle and the rider were defined in terms of pressure and vibration thresholds. The thresholds are associated with the race time because the potential adverse effects of vibration and pressure depend on the exposure time. High levels of vibration and pressure can be supported with no harm for short periods, while even relatively low magnitudes of these variables can have adverse effects if sustained for long periods.

For the pressure, the thresholds were defined using the pressure-time threshold curve for the apparition of saddle sores in humans described in Eq. (7.10), where p_{thS} and p_{thAB} are in kPa for a given exposure time t_e in hours. The threshold curve is presented with further detail in Figure 5.15. This curve was approximated for this study using the model reported in [96], which was fitted by the authors to the data of [99]. It is assumed that the thresholds for the pressure in the saddle and the elbow pads are the same, as there is no specific information for different contact points.

$$p_{thS} = p_{thAB} = [471.9 * (t_e^{-4/3}) + 11.5] * 0.13 \quad (7.10)$$

The pressure index compared with the pressure thresholds is the global average pressure in the saddle and aerobars (\bar{p}_S and \bar{p}_{AB}), which is computed as an average over pedaling cycles of the average pressure registered for the contact area in different time steps. This index was used because the average is one of the indices of the cumulative behavior over time, representing the effect on human tissue. In addition, as the peak pressure position varies over time, the use of the average pressure on the contact area is more suitable. Further information about pressure indices and thresholds can be found in Chapter 5.

For the vibration, the thresholds were defined using the information reported in the ISO 2631-1 [108] for the vibration measured close to the buttocks, and the ISO 5349 [109] for the vibration measured close to the elbows. The pressure-time threshold for the seatpost and the aerobars are represented by Eq. (7.11) and Eq. (7.12), respectively. In these equations, the vibration thresholds V_{thS} and V_{thAB} are in m/s^2 for a given exposure time t_e in hours. The threshold curves are presented with further detail in Figure 6.10. The curve for the saddle was defined from curves of health guidance caution zones for whole-body vibration presented in the ISO 2631. The curve for the aerobars was defined from a threshold for an increased probability of presenting the hand-arm vibration syndrome presented in the ISO 5349.

$$V_{thS} = \frac{2.4}{\sqrt{t_e}} \quad (7.11)$$

$$V_{thAB} = \frac{5.6}{\sqrt{t_e}} \quad (7.12)$$

The vibration index compared with the vibration thresholds is the vibration total value computed for the saddle and the aerobars (a_{vS} and a_{vAB}). This index is computed as presented in Eq. (6.2), including the root mean square of the accelerations in three orthogonal directions. Further information about vibration indices and thresholds can be found in Chapter 6.

For Scenario 1 (two postures ABlow and ABhigh), from the data registered for each bicycle-cyclist set on each posture and using the t_r computed for each combination of v_w and θ , the pressure and vibration thresholds were estimated. For each race condition, it was verified if the value measured for the variable during the tests exceeded or not the threshold value of the same condition. If one of the variables (*i.e.*, a_{vS} , a_{vAB} , \bar{p}_S , or \bar{p}_{AB}) exceeded its corresponding threshold, the condition was considered as not feasible. For the feasible race conditions, the percentage of the variables with respect to the corresponding thresholds was computed as described by Eq. (7.13) to Eq. (7.16).

$$p_{pS} = \frac{\bar{p}_S}{p_{thS}} * 100 \quad (7.13)$$

$$p_{pAB} = \frac{\bar{p}_{AB}}{p_{thAB}} * 100 \quad (7.14)$$

$$V_{pS} = \frac{a_{vS}}{V_{thS}} * 100 \quad (7.15)$$

$$V_{pAB} = \frac{a_{vAB}}{V_{thAB}} * 100 \quad (7.16)$$

For Scenario 2 (continuous options of aerobars' heights between ABhigh and ABlow), the thresholds were computed for the aerobars' height with the corresponding t_r obtained from the interpolated $C_D A$ and \bar{P} . The variables \bar{p}_S , \bar{p}_{AB} , a_{vS} , and a_{vAB} were also obtained as a linear combination of the measured postures for the intermediate postures. The same process described for Scenario 1 was followed to include the constraints in the problem solution.

7.3.4. Considerations for the optimization

The assumptions and considerations performed for the solution of the optimization problem are described in this section.

The computation of the total race time is performed assuming that the cyclists compete in an ideal scenario with constant road grade, constant wind speed, and constant air density. It is also considered that the riders are pedaling with a constant power output leading to constant bicycle speeds. For the pressure and vibration indices, it is assumed that the indices also remain constant over the race. For this to hold true, the road should have a constant roughness without abrupt disruptions not to affect the vibration levels. It should be noticed that the protocols used for the measurement of vibrations and pressure indices consider the measurement in flat terrain. As the road grade changes, the rider's weight distribution on the contact points varies, and it is being assumed that the same values of the indices hold for different road inclinations. These assumptions were performed to simplify the information of the racing stages to get an idea of the results that would be obtained and to have the possibility of comparing the results between race conditions and riders. Nevertheless, the methodology could be implemented in future researches for racing scenarios with varying conditions for the definition of racing strategies in different segments of the route.

Due to the capability of the anemometer developed to measure the wind speed relative to the bicycle, it is assumed that there is no crosswind during the drag area estimation and race time

computation. For the tests performed to estimate the drag area, it was verified with an additional anemometer that the crosswind speeds on the testing site are negligible. For the estimation of the race time, this is an additional consideration of the problem solution to take into account.

Regarding the pressure and vibration thresholds, it should be noted that, for the vibrations, the thresholds were originally defined considering the measurement of accelerations in the interfaces between the person and the vibration source, and in this case, the vibrations are measured on the bicycle before the interface. The vibrations on the interfaces are probably lower than those registered in this study because the saddle and elbow pads mitigate the vibrations. It is worth observing that the ISO 5349 addresses hand-transmitted vibration, and in this study, the vibration is transmitted through the elbows; nevertheless, the ISO information is the closest available to the representation of the phenomena in this contact point.

The pressure thresholds were obtained for constant loads, and in the case of cycling, the oscillating motion of the hip and legs created an oscillation of the pressure field, which allows blood to flow, reducing the negative effect on the tissue. Nevertheless, there are no specific thresholds defining loads that can be harmful to the human body while cycling.

As only the extreme postures (*i.e.*, ABhigh and ABlow) were characterized, it is assumed for the solution of Scenario 2 that the variables can be linearly interpolated between the tested postures. This assumption was performed considering that the posture variations are relatively small and that measuring intermediate postures increases the experimental cost regarding economic resources, and more importantly, the time. The time required to perform the tests is relevant because the implementation of the tests to characterize different postures can interrupt the normal training calendar of the riders, or the tests can be extended for several weeks modifying the tested conditions (e.g., training or detraining, change in the rider's mass).

7.3.5. Bicycle-cyclist sets studied

Five recreational-level cyclists voluntarily participated in the tests after signing an informed consent form (mass: 73.8 ± 11.8 kg, height: 1.75 ± 0.06 m, age: 35 ± 7 years). The riders used their own bicycles and standard cycling clothes. All the riders had extensive previous experience riding in aerobars. The tests were performed in two aerobars postures with different heights. For road bicycles, clip-on aerobars were used. Depending on each bicycle's characteristics, the height was varied using spacers on the headtube stem or the aerobars support. Different types of riders and bicycles were included in the study to explore the results obtained for riders and bicycles with specific characteristics. Also, the inclusion of a group of cyclists with varied characteristics allows exploring possible scenarios that can be found during the posture selection process. Table 7.2 presents a summary of the information of each bicycle-cyclist set (further detail can be found in Tables 2.1, 2.2, and 2.3 in Chapter 2).

	Variable	Units	Set				
			1	2	3	4	5
Rider	Mass	[kg]	59	72	92	73	73
	Height	[m]	1.67	1.72	1.76	1.78	1.83
	Age	[years]	38	26	42	39	30
	Gender	[-]	Female	Male	Male	Male	Male
Bicycle	Type	[-]	Aero	Time trial	Aero	Endurance	Time trial
	Mass	[kg]	11.1	10.2	11	11.5	9.9
	Aerobars' height	[mm]	55	55	55	55	40
	Saddle	[-]	Lady, Selle Italia, Italy	Adamo PS 1.1, ISM, USA	300, Oval concepts, USA	Galápagos, GW, Colombia	Stealth, PRO, The Netherlands
	Aerobars	[-]	Parabolica uno, Deda elementi, Italy	Revo, 3T, Italy	Parabolica uno, Deda elementi, Italy	Parabolica uno, Deda elementi, Italy	Trimax, Vision, USA

Table 7.2. Bicycle-cyclist sets included in the posture optimization process.

The values of the performance and interaction variables obtained for the different bicycle-cyclist sets are presented in Table 7.3. It can be observed that for all the sets changing from ABhigh to ABlow led to an improvement in the drag area and a deterioration in the average power delivery capacity, pressure on the saddle, and vibrations on the saddle. Regarding the pressure and vibration on the aerobars' elbow pads, the effect varied over the group of cyclists.

Variable	Units	Posture	Set				
			1	2	3	4	5
Drag area ($C_D A$)	[m ²]	ABhigh	0.28	0.26	0.27	0.33	0.29
		ABlow	0.25	0.23	0.23	0.31	0.26
Rolling resistance coefficient (f_r)	[-]	[-]	0.005	0.005	0.007	0.007	0.004
Average power delivery capacity (\bar{P})	[W]	ABhigh	161	228	180	179	223
		ABlow	140	217	168	169	193
Global average pressure on the saddle (\bar{p}_S)	[kPa]	ABhigh	13.9	39.0	52.2	15.8	26.1
		ABlow	14.7	48.6	58.5	20.9	28.1
Global average pressure on the aerobars (\bar{p}_{AB})	[kPa]	ABhigh	19.5	29.8	28.9	25.1	31.8
		ABlow	22.0	25.9	31.5	23.4	35.8
Vibration total values on the saddle (a_{vS})	[m/s ²]	ABhigh	3.00	2.95	2.56	3.04	2.74
		ABlow	3.13	3.15	2.90	3.13	2.88
Vibration total values on the aerobars (a_{vAB})	[m/s ²]	ABhigh	4.32	4.62	4.24	4.91	5.54
		ABlow	4.42	4.71	4.37	4.45	4.59

Table 7.3. Variables of performance and interaction of each bicycle-cyclist set.

7.4. RESULTS AND DISCUSSION

The results and discussion are presented for the selection of posture between two options with different aerobars' height and for the optimization of posture identifying the best feasible aerobars' height solution.

7.4.1. Scenario 1: selection of posture between two options

Figures 7.1 to 7.5 present the detailed results obtained for the selection of posture between ABhigh and ABlow for the bicycle-cyclist sets measured for different race conditions. Each figure presents a set of 10 subplots representing the data of ABhigh on the left column and the data of ABlow on the right column. Each subplot presents the results for the range of v_w and θ considered. The first row presents the results associated only with performance displaying the estimated total race times in seconds. The other rows present the results associated with the constraints displaying the percentage of the variables with respect to the corresponding thresholds for the pressure and vibrations in the saddle and aerobars. Only the feasible conditions are presented, meaning that if a variable exceeds its corresponding exposure threshold for a given condition, it is not plotted.

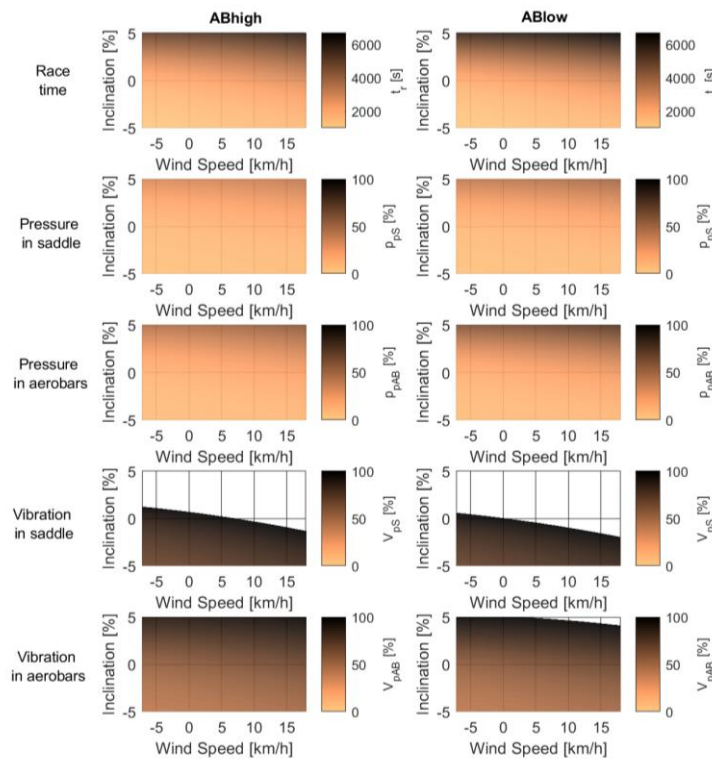


Figure 7.1. Detailed results obtained for the posture selection of the bicycle-cyclist set 1.

Effect of posture on performance and interaction

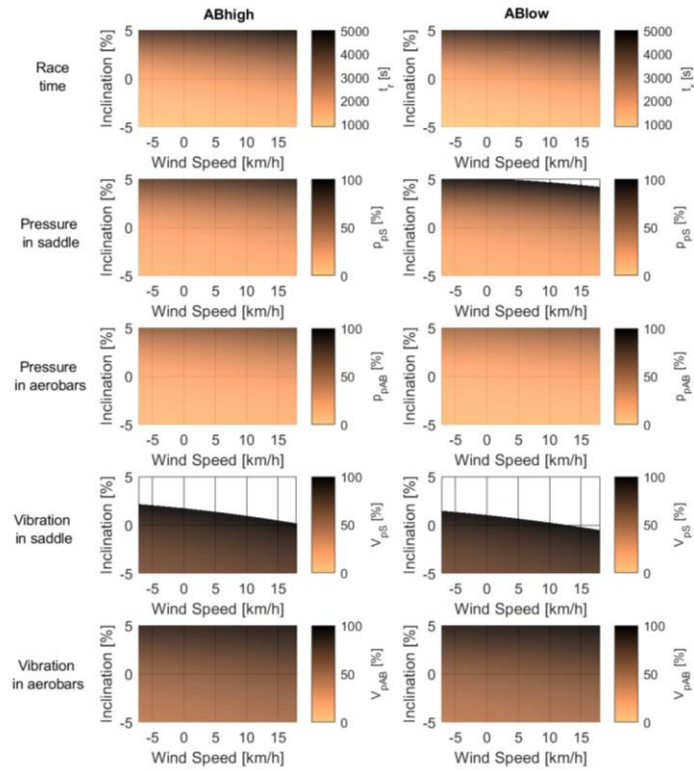


Figure 7.2. Detailed results obtained for the posture selection of the bicycle-cyclist set 2.

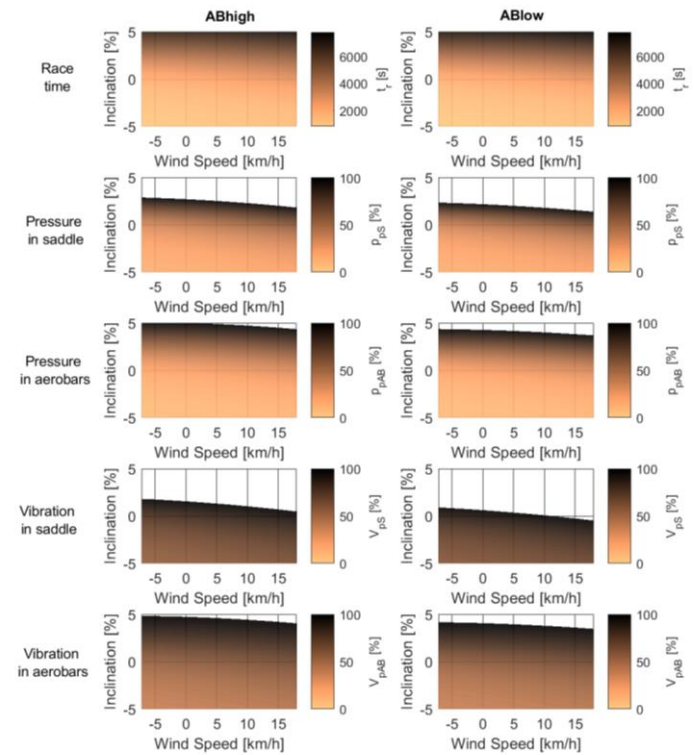


Figure 7.3. Detailed results obtained for the posture selection of the bicycle-cyclist set 3.

Effect of posture on performance and interaction

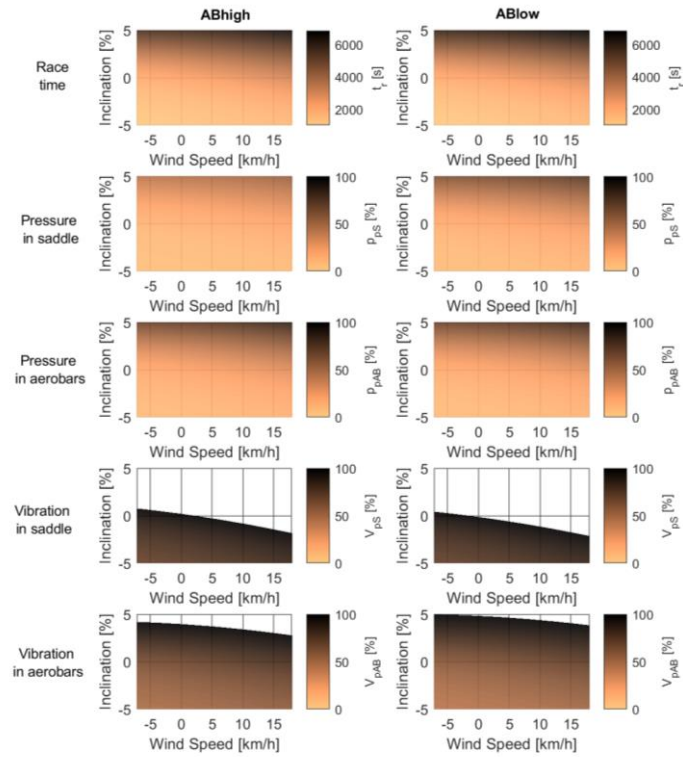


Figure 7.4. Detailed results obtained for the posture selection of the bicycle-cyclist set 4.

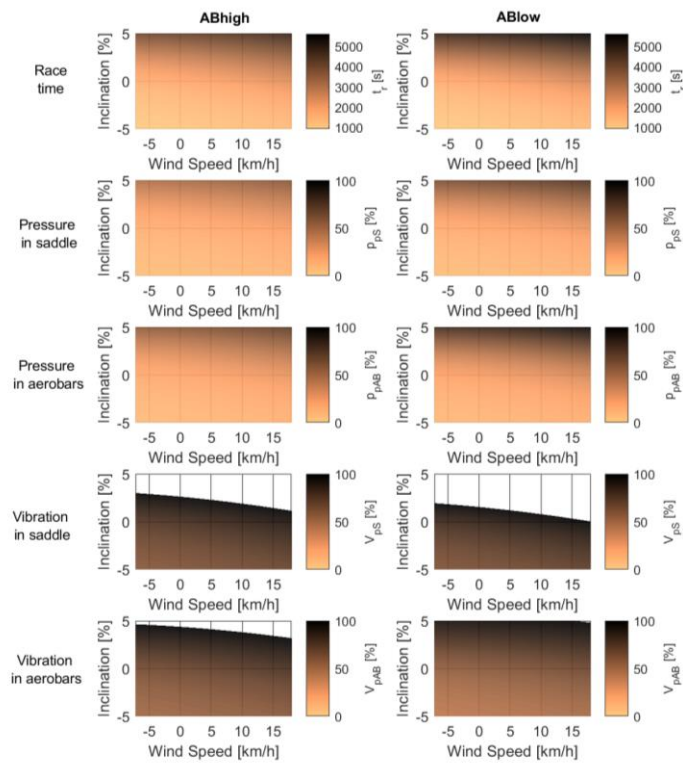


Figure 7.5. Detailed results obtained for the posture selection of the bicycle-cyclist set 5.

As expected, the results predict higher race times for the conditions with higher inclination and headwind. Congruently, as the race time increases, the time of exposure to vibration and pressure increases, leading to smaller acceptable thresholds. For this reason, the unfeasible conditions are obtained at higher inclinations and headwinds. It can also be observed that for all the interaction-related variables, there are unfeasible race conditions; nevertheless, the vibrations in the saddle represent the strictest constraint with more unfeasible race conditions. This means that the posture selection is being modified due to this variable. For all the bicycle-cyclist sets, the vibration on the saddle was found to represent the strictest constraint.

Figures 7.6 to 7.10 present the selected posture for the studied race conditions of the bicycle-cyclist sets measured. The posture is selected considering that it leads to the best time while satisfying all the constraints. If the posture with the best time does not satisfy one of the constraints, then the other posture is selected. If the other posture does not satisfy one of the constraints as well, then the race condition is considered as unfeasible, and it is not plotted. The plot presents the posture selected for each race condition using light color when the selected posture is ABlow and dark color when it is ABhigh. In addition, a dotted line is included in the plot representing the threshold that would be obtained between the zones of posture selection if only the race time was considered (*i.e.*, without including interaction constraints).

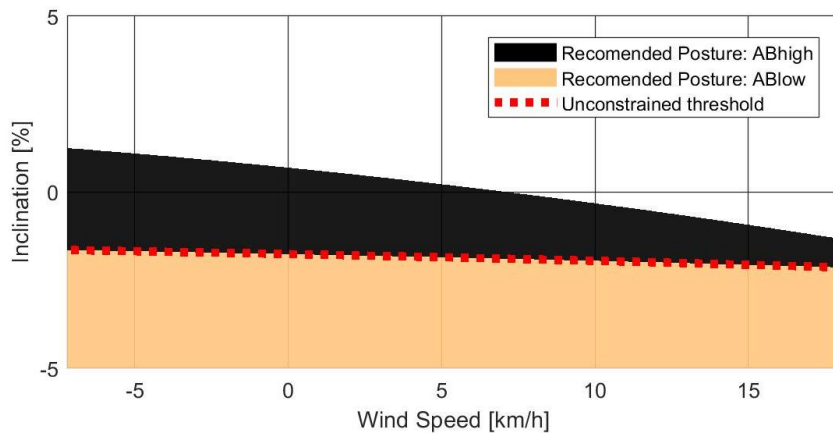


Figure 7.6. Posture selection for bicycle-cyclist set 1.

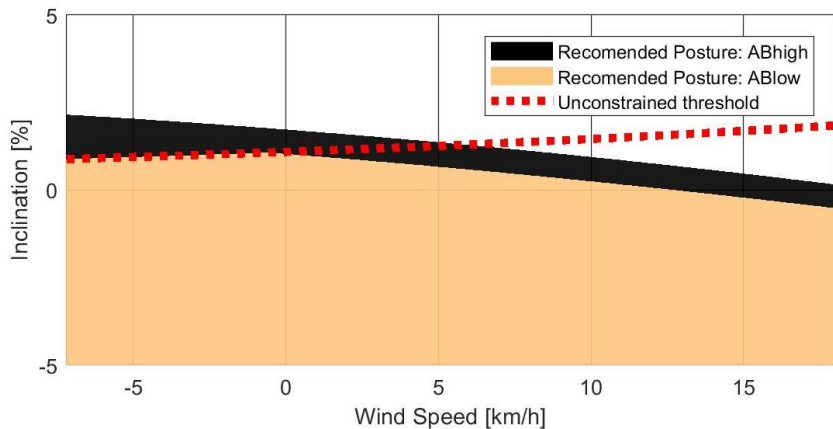


Figure 7.7. Posture selection for bicycle-cyclist set 2.

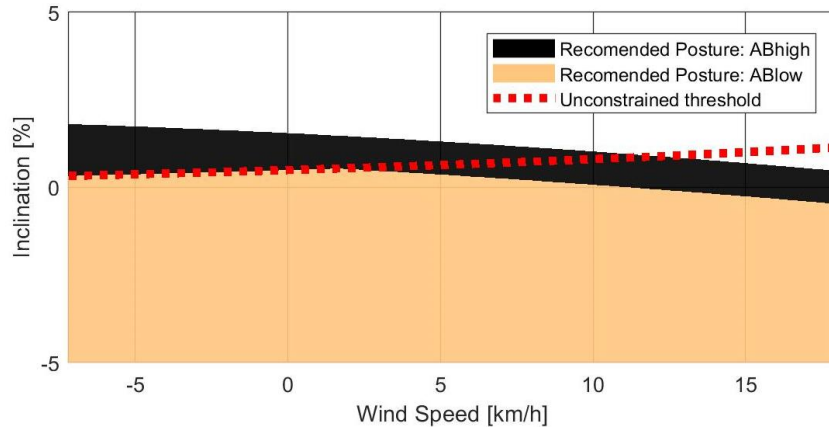


Figure 7.8. Posture selection for bicycle-cyclist set 3.

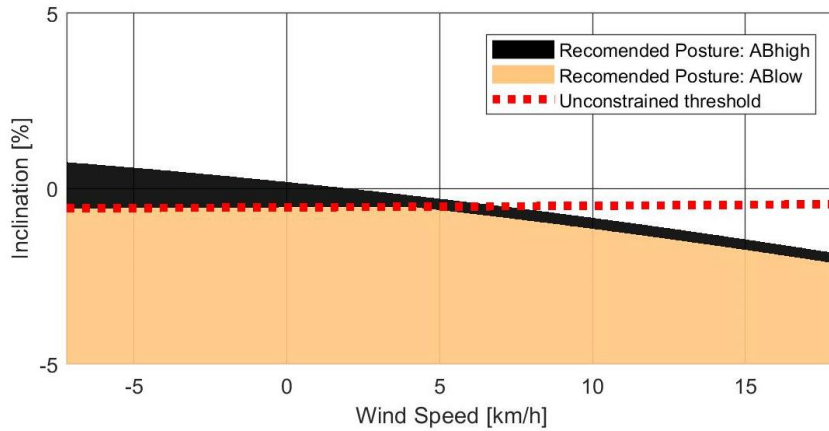


Figure 7.9. Posture selection for bicycle-cyclist set 4.

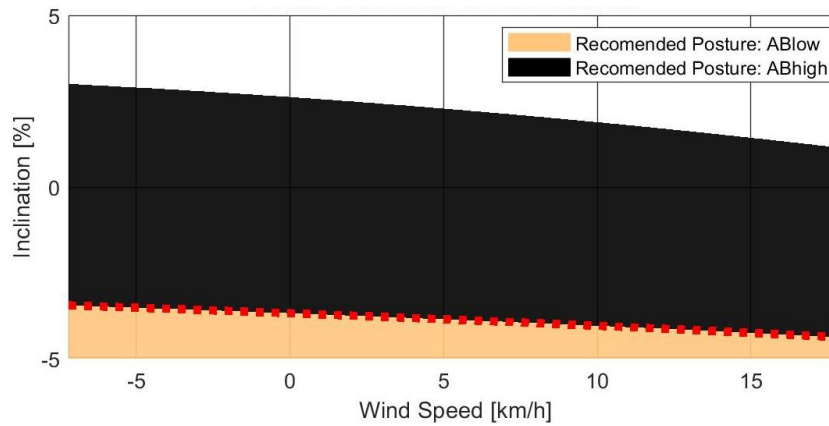


Figure 7.10. Posture selection for bicycle-cyclist set 5.

It can be observed that the posture selection results for a race condition have a substantial variation over the bicycle-cyclist sets. This indicates that the posture selection process should be performed for each bicycle-cyclist set. As the process depends on several bicycle-cyclist set parameters, generalizing the results can lead to inaccurate results. This finding complements the results of Fintelman et al. [38], who noted that the optimal time-trial posture is defined considering

characteristics of the rider (i.e., frontal area, physiology) and race conditions (i.e., cycling speed, course inclination, and duration). With this study's results, the characterizations of comfort and wind speed are added to the variables defining optimal time-trial posture.

It can also be observed in Figures 7.6 to 7.10 when comparing the posture threshold line due to race time (dotted line) with the zones of posture selection (light and dark color areas), that for some cyclists, the line corresponds with the change between the postures (i.e., sets 1, and 5), while for others, the line does not match (i.e., sets 2, 3, and 4). A difference between the line and the shades' interface implies that, for some race conditions, the selection of posture is modified by the constraints (i.e., vibrations or pressure thresholds). A match between the line and the shades' interface implies that the posture selection can be performed based on performance only (i.e., race time).

It was found that for several race conditions, the less aerodynamic posture, ABhigh in this study, can be more advantageous than the aerodynamically efficient posture ABlow. For example, it can be observed when considering a race condition in flat terrain (i.e., zero road grade) that for sets 1, 4, and 5, ABhigh is the recommended posture for all the displayed wind speeds. Moreover, for sets 2 and 3, ABlow posture is recommended for all the displayed race conditions when the selection is performed based only on performance (i.e., below the dotted line). Nevertheless, when the interaction constraints are considered, there is a range of wind speeds for which ABhigh is recommended instead of ABlow. The race conditions for which ABhigh is recommended are found at higher headwinds. This can be seen in Figures 7.7 and 7.8 for a 0% inclination as the change from light to dark color when increasing headwind speed. The change is found at 13 km/h for set 2 and 10.5 km/h for set 3. This result can be counterintuitive because the aerodynamic drag gains relevance at higher wind speeds, indicating that the more aerodynamically efficient posture ABlow should be selected. Nevertheless, at higher headwinds, the race times also increase, leading to stricter pressure and vibration exposure thresholds, turning ABlow into an unfeasible posture for some race conditions.

Another example is a race condition with no wind speed. In this case, it can be observed that for each set, there are specific road inclinations in which the recommended posture changes from ABlow to ABhigh. It can be observed that the road inclination of change for each set is the same if the selection is performed based on performance only or considering the interaction constraints. In this case, the posture selection depends entirely on the variation of drag area and power delivery capacity of each cyclist when changing the posture. The road inclination of change between recommended postures varied over the sets between -3.6% and 1%, meaning that for some of them, even on descending roads, ABhigh is more advantageous than ABlow (see sets 1, 4, and 5). This occurs because their power delivery capacity was significantly reduced when adopting the more aerodynamic posture, so unless the aerodynamic advantage compensated the power delivery reduction, ABlow would not be recommended. These results highlight that a more aggressive aerodynamic posture does not necessarily lead to race time improvements, and on the contrary, it can have adverse effects on the comfort of the riders.

Figure 7.11 presents a comparison of the posture threshold lines due to race time (red line in Figures 7.6 to 7.10) for the different bicycle-cyclist sets. It can be observed that the lines have two types of general behaviors. Sets 2 and 3 have a trend and sets 1, 4, and 5 have another trend. It was identified that the behavior is related to the relation between the variation of drag area and the variation of power delivery capacity when changing the posture. The riders of sets 2 and 4 had a relatively low drop of power delivery capacity with respect to the gains of aerodynamic drag reduction when changing from ABhigh to ABlow. This means that the aerodynamic advantage is relevant for more race conditions, leading to the possibility of riding in ABlow at lower speeds. On the contrary, for the riders of sets 1 and 4 and the power delivery capacity drop is higher than the gains due to the aerodynamic drag reduction when changing from ABhigh to ABlow, for this reason, for these sets, the use of ABlow is recommended only at high speeds at which the aerodynamic drag is relevant because of the bicycle speed (the aerodynamic drag has a quadratic increment with speed). For cases as the ones of riders 1 and 5, the use of more aerodynamically aggressive postures (as ABlow) requires performing specific training to improve power delivery capacity in those postures before using the posture for competition.

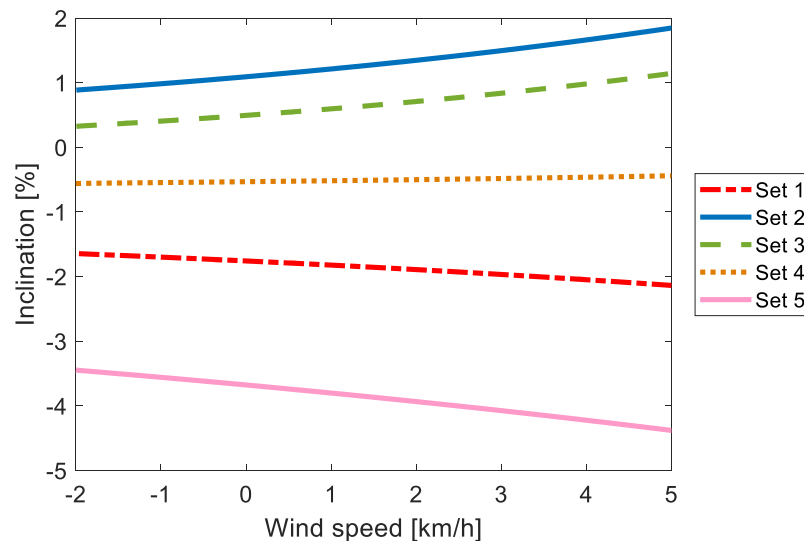


Figure 7.11. Comparison of the change of posture threshold due to performance for the different bicycle-cyclist sets.

Table 7.4 presents the race time and the thresholds for vibration and pressure in saddle and aerobars for the zero-wind speed and zero-grade race condition. The table also presents the selected posture for each bicycle-cyclist set on the same race condition. It can be observed that if only race times are considered, the sets 1, 2, and 3 would select the posture ABlow; nevertheless, for set 1, ABlow is unfeasible as it does not satisfy the constraint for vibration on the saddle. Similarly, for set 4, the posture ABlow does not satisfy the constraint of vibration on the saddle, but for this set, the time associated with ABhigh is better than the one of ABlow. For the race conditions contemplated, the time gains due to the posture selection vary between 14 and 97 seconds with an average of 47.2 s. The percentages of pressure and vibration also reflect that the stricter constraints are related to the vibration thresholds as the percentages of the variables are higher than those registered for pressure.

Variable	Units	Posture	Set				
			1	2	3	4	5
t_r	[s]	ABhigh	2032	1751	2095	2162	1745
		ABlow	2098	1724	2063	2176	1842
p_{pS}	[%]	ABhigh	10	23	40	13	16
		ABlow	11	29	44	17	18
p_{pAB}	[%]	ABhigh	14	18	23	20	19
		ABlow	17	15	25	19	23
V_{pS}	[%]	ABhigh	94	86	82	98	80
		ABlow	unfeasible	91	92	unfeasible	86
V_{pAB}	[%]	ABhigh	57	57	57	67	68
		ABlow	60	58	58	61	58
Posture selected	[-]	[-]	ABhigh	ABlow	ABlow	ABhigh	ABhigh

Table 7.4. Race time and pressure and vibration thresholds computed for the tested postures on a zero-wind and zero-grade race condition.

7.4.2. Scenario 2: optimization of posture

Figures 7.12 to 7.16 present the results obtained for the optimization of aerobars’ height to minimize race time for the bicycle-cyclist sets measured for different race conditions. The optimal aerobars’ height as the percentage of the aerobars’ height fit window (100% is ABhigh, and 0% is ABlow) is presented in each figure.

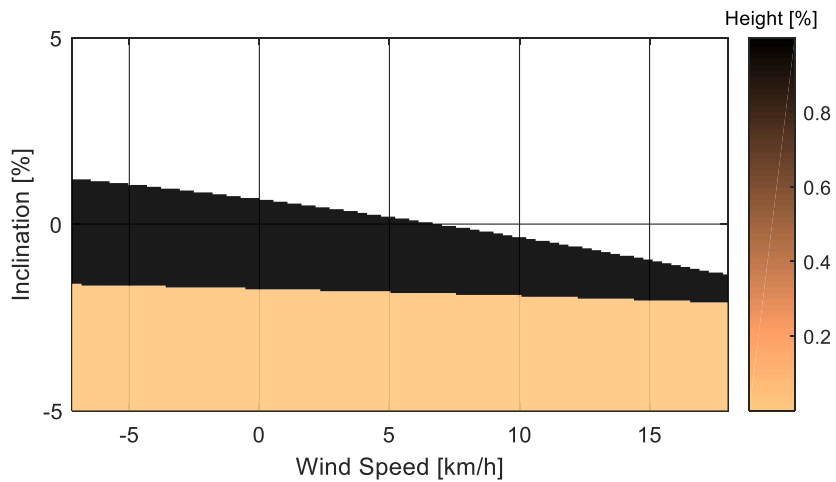


Figure 7.12. General results for the optimization of aerobars height. Bicycle-cyclist set 1.

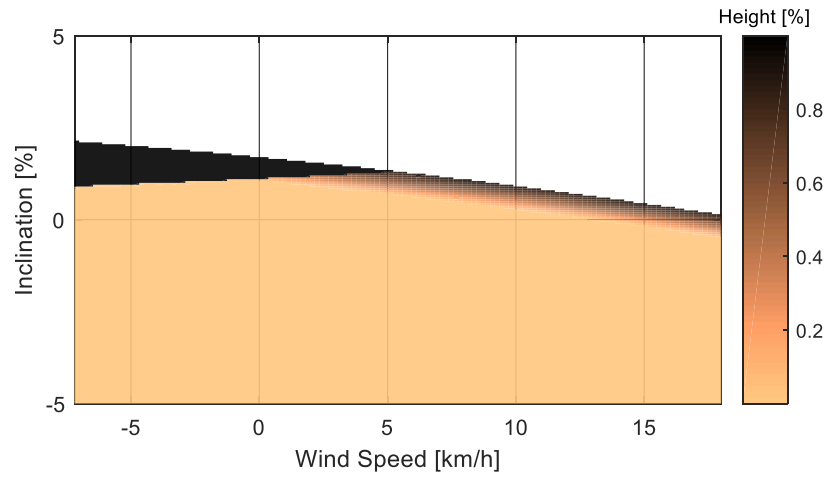


Figure 7.13. General results for the optimization of aerobars height. Bicycle-cyclist set 2.

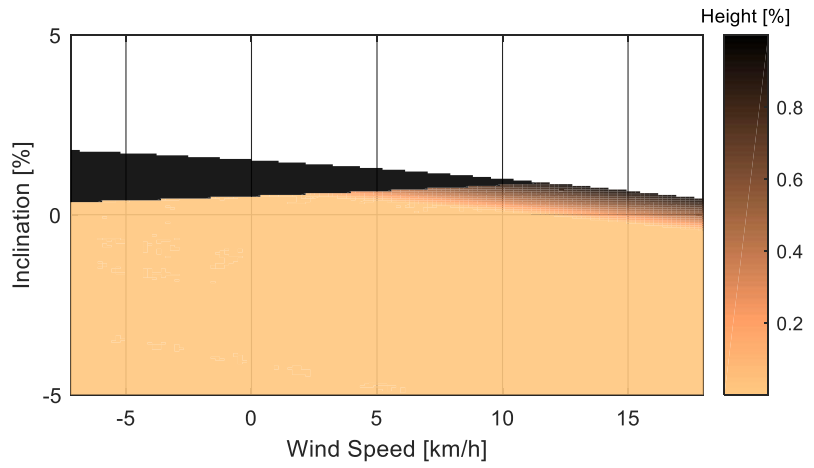


Figure 7.14. General results for the optimization of aerobars height. Bicycle-cyclist set 3.

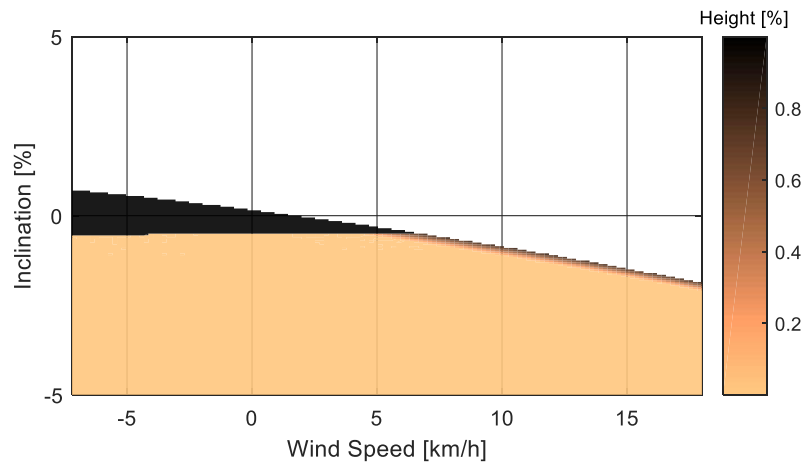


Figure 7.15. General results for the optimization of aerobars height. Bicycle-cyclist set 4.

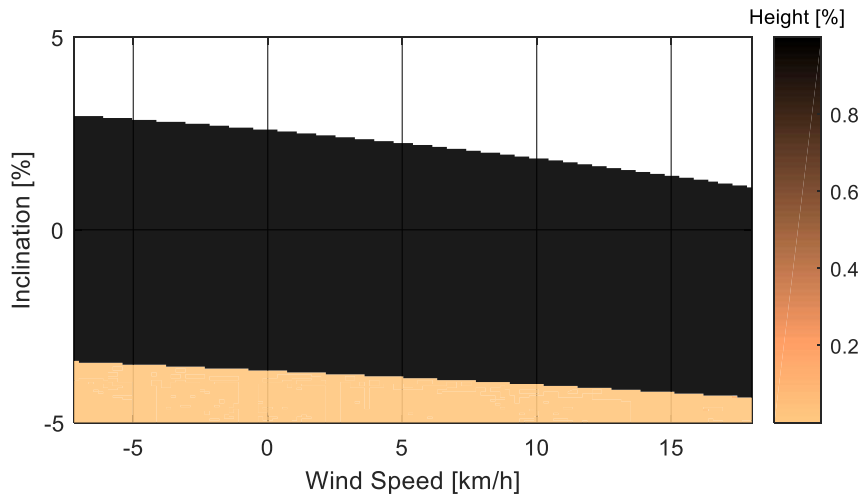


Figure 7.16. General results for the optimization of aerobars height. Bicycle-cyclist set 5.

It can be observed that for sets 1 and 5, the optimal solutions always lie in the boundary postures (*i.e.*, ABhigh or ABlow), while for sets 2, 3, and 4, for some race conditions, the optimal height lies in the intermediate postures. It can be observed that the intermediate heights are identified as optimal for the race conditions in which the selection of posture was restricted by the constraints (*i.e.*, when the unconstrained threshold does not match the ABhigh-ABlow interface as in figures 7.7 to 7.9). This occurs because the race time as a function of aerobars height is monotonous in the range of analysis. For this reason, if only performance is considered, the posture selected is one of the boundary postures (ABhigh or ABlow). When the constraints limit the solution, they force the selection of an intermediate height even if it is not related to the best race time. It is worth highlighting that the final selection of the aerobars' height depends on each bicycle's fit window as the postures can be fixed in certain positions and not in the exact height proposed by the optimization solution.

7.5. CONCLUSION

A methodology for the selection and optimization of aerobars' height of bicycle-cyclist sets was successfully implemented. The methodology considers simultaneously aerodynamic drag, power delivery capacity, pressure in contact areas, and vibration transmission characteristics of each bicycle-cyclist set. The optimization is performed to minimize the race time estimated using the set's drag area and power delivery capacity. The solution is constrained by thresholds associated with the exposure to pressure in contact areas and vibration transmission to the rider to reduce potential adverse effects on the riders.

It is concluded that posture optimization should be performed for each bicycle-cyclist set. This, because the effect of posture on the performance and interaction variables measured is particular for each bicycle-cyclist set. The power delivery capacities are different for each rider, and the drag area, pressure in contact points, and vibration transmission are particular for each bicycle-cyclist set. In addition, it is concluded that the relation between the variation of the performance and the

variation of the interaction variables, when changing the posture, is relevant for posture optimization. It is also concluded that the appropriate postures depend on the race conditions as road inclination, wind speed, and distance, among others.

CHAPTER 8. Concluding remarks

The aim of this research project was to select appropriate postures for cyclists considering the effect of posture on performance and interaction with the bicycle simultaneously. Performance and interaction variables are considered because they represent cyclists' main objectives: improving performance while avoiding adverse effects like discomfort or overuse injuries. In this study, an appropriate posture refers to a body configuration that leads to the best overall performance while satisfying constraints imposed by acceptable limits of exposure to pressure and vibration transmitted to the rider. The performance is assessed in terms of race time estimated from the characteristics of the bicycle-cyclist set, including the aerodynamic drag and the power delivery capacity of the rider, and the characteristics of the race. The limits of exposure are defined from time-dependent thresholds associated with an increased potential of generating adverse effects on the human body.

The effects of posture on the aerodynamic drag, the power delivery capacity, the pressure in contact areas, and the vibration transmission to the rider have been acknowledged separately in different studies. Nevertheless, the available information cannot be used for posture selection because the information is not comparable over different studies as the participating bicycle-cyclist sets, and the tested postures are varied. In addition, the behavior of the mentioned variables, when changing the posture, has a strong dependence on the characteristics of the bicycle-cyclist set for which the posture is going to be defined. For these reasons, the proposed methodology to select appropriate postures includes protocols to characterize the aerodynamic drag, power delivery capacity, pressure in contact areas, and vibration transmission of bicycle-cyclist sets in different postures.

8.1. EFFECT OF POSTURE IN PERFORMANCE

8.1.1. *Aerodynamic drag*

An outdoor method to estimate the drag area of bicycle-cyclist sets was proposed (Chapter 3). The method included the measurement of wind speed relative to the bicycle to reduce the error associated with the assumption of zero-wind conditions in an open testing route. For the measured bicycle-cyclist sets, the method was able to quantify differences in the drag area when riding in postures with different aerobars' height (differences in the height of 40 mm and 55 mm). The results of the tested sets presented a trend corresponding to an improvement of the drag area when reducing the aerobars' height. The results also show that the magnitude of the difference in the drag area due to the posture variation strongly depends on the bicycle-cyclist set.

The method proposed for estimating the drag area has the advantage of including onboard anemometry and information on the road grade. Nevertheless, due to the onboard anemometer's limitations, it is assumed that there is no crosswind; for this reason, the testing site should be selected verifying that there is no strong crosswind.

8.1.2. *Power delivery capacity*

A protocol was selected to estimate cyclists' power delivery capacity in terms of the Functional threshold power (FTP) (Chapter 4). For the participating cyclists, it was possible to quantify the

difference in the average power output due to the variation of the aerobars' height (differences in the height of 40 mm and 55 mm). The results of the tested cyclists presented a trend corresponding to a reduction of power delivery capacity when reducing the aerobars' height. The results also show that the magnitude of the difference in power output due to the posture variation strongly depends on the rider.

The advantage of the protocol used is that it allows registering the cyclist fitness status through a direct measure of the power delivered, which is useful for estimating the total race time. Another advantage is that the protocol is performed with relatively simple instrumentation, which, thanks to the development of technological cycling equipment (as smart trainers and power-meters), is more affordable, and hence, more common as indoor training equipment.

A drawback associated with the protocol is that the FTP was used to represent the average power output that the cyclists can deliver for 20 minutes or more, and the measurement was performed in a 20-minutes window. However, the FTP test is performed after the warm-up and a series of cycling drills, which fatigues the cyclists approaching the power delivered in the test to the power that the cyclist could deliver for an hour in normal riding conditions (*i.e.*, without the previous drills).

8.1.3. Aerodynamic drag and power delivery capacity trade-off

From the results of the performance variables, a trade-off was observed between the improvement of the aerodynamic drag and the power delivery capacity. It was obtained that when reducing the aerobars' height, the drag area improves (*i.e.*, reduces), and the power output worsens (*i.e.*, reduces). Considering that the importance of the aerodynamic drag depends on the speed, the selection of an advantageous posture regarding performance depends on the bicycle speed and road inclination. At higher speeds, the aerodynamic advantages become more relevant than the power output drop, which is relevant for roads with zero or descending inclinations and high wind speeds. At lower speeds, as in roads with ascending inclinations, the difference in the power delivery capacity becomes the main criteria for selecting advantageous postures.

8.2. EFFECT OF POSTURE IN INTERACTION

8.2.1. Pressure in contact areas

A method for characterizing the pressure fields in the contact areas between the rider and the bicycle was implemented (Chapter 5). As aerobars postures were tested, the method considered the measurement of pressure in the buttocks-saddle and the elbow-aerobars' pads interfaces. The longitudinal position of the center of pressure, the average, and the peak pressure were computed for the contact areas. For the measured bicycle-cyclist sets, the method was able to quantify differences in the longitudinal position of the center of pressure, the global average pressure, and the maximum of the average pressure over time when riding in postures with different aerobars' heights (differences in the height of 40 mm and 55 mm). The results of the tested sets presented a trend for the buttocks-saddle indices corresponding to a translation of the center of pressure to the anterior zone and an increment of the average pressure, indicating worst interaction conditions

when reducing the aerobars' height. For the other indices, there was not a trend when changing the posture, and the results varied among the cyclists. The results highlight the importance of studying the pressure in contact areas for each set as the characteristics of the rider, saddle, and elbow pads, and how the rider positions the body in the contact areas are specific for each set.

A characteristic of the pressure fields' characterization that should be taken into account is that it is influenced by riding variables, the power output and cadence, and road characteristics as the inclination and roughness. For this study, the pressure fields were characterized, assuming that the rider pedals at a constant power output equivalent to the FTP, with a constant cadence, and on a leveled and smooth road.

8.2.2. Vibration transmitted to the rider

A method for estimating the vibration transmitted to the rider due to the road unevenness was implemented (Chapter 6). The method considered the measurement of vibrations on the seatpost and the steering tube as an approximation of the vibrations transmitted to the buttocks and elbows. A vibration index computed as the rms of the weighted accelerations in three orthogonal directions was used. The weighting function used for computing the index considered the human sensitivity to vibrations according to the International Standards ISO 2631 for the seatpost vibrations and the ISO 5349 for the steering tube. The effect of posture on vibration varied for the different measured bicycle-cyclist sets. For some sets, the difference of vibrations in the seatpost was relevant, while for other sets, the difference of vibrations in the steering tube was relevant. The method was able to quantify the difference in the vibration of at least one point of interest (*i.e.*, seatpost or steering tube) when riding in postures with different aerobars' height (differences in the height of 40 mm and 55 mm). The results of the sets presented a trend corresponding to an improvement of the vibration in the steering tube and a worsening of the vibrations in the seatpost when reducing the aerobars' height. The results highlight the importance of studying the vibration transmission for each set as the results are varied.

It should be taken into account that a limitation of the method for the characterization of vibration transmission used is that the vibrations are measured in the bicycle instead of the interfaces between the bicycle and the riders due to the size of the instrumentation used. For this reason, the vibrations reported are an approximation, and the actual vibrations transmitted to the rider are lower as the saddle and elbow pads paddings mitigate them. Another consideration is that the vibrations are influenced by the bicycle speed, road roughness, and inclination, meaning that the values reported are representative of the tested conditions (*i.e.*, leveled, smooth asphalt, and constant 25 km/h speed).

8.3. SELECTION OF POSTURE

A methodology for the selection and optimization of the aerobars' height of bicycle-cyclist sets was successfully implemented. The methodology aims at minimizing the race time while meeting constraints associated with the exposure to pressure in contact areas and vibration transmission to the rider. The methodology was implemented to identify advantageous postures for a 20-km time

trial race with different wind conditions and road grades. It is concluded that the posture selection should be performed for each bicycle-cyclist set considering its performance and interaction features, and considering the overall race conditions as road inclination, wind speed, and distance, among others.

The results highlighted the importance of considering the effect of posture on various variables when selecting the posture. This, considering that conflicting directions of improvement were found for some variables when changing the posture, meaning that when one variable is improved, at least one of the other variables is worsened. This can have negative implications on performance, increasing the race time, or the characteristics of interaction with the bicycle, negatively affecting the overall cycling experience. For example, for a race condition of no wind and no grade, from the five tested sets, it is predicted that the most aerodynamically efficient posture (*i.e.*, low aerobars' height) is advantageous only for two sets. For one of the other tested sets, the race time associated with the most aerodynamically efficient posture was advantageous; nevertheless, the posture was not feasible because the constraint of vibration on the saddle was not satisfied, leading to select the other posture (*i.e.*, high aerobars' height). For the two remaining sets, the loss in power delivery capacity when reducing the aerobars' height was more significant than the gain due to the aerodynamic improvement, leading to a global reduction of performance (*i.e.*, higher race times) leading to the selection of the posture with high aerobars.

Besides the drawbacks, limitations, and assumptions associated with the protocols to characterize aerodynamic drag, power delivery capacity, pressure in contact areas, and vibration transmission, the following considerations were performed for the selection of posture. First, ideal scenarios with constant road grade, wind speed, air density, and road roughness, in which the rider pedals at constant power output and cadence, were assumed. Nevertheless, the methodology could be implemented in future researches for racing scenarios with varying conditions for the definition of racing strategies in different segments of the route. Second, the vibration thresholds were approximated from thresholds for whole-body vibrations and hand-transmitted vibrations; nevertheless, in this study, the vibrations are transmitted through the saddle while the rider adopts a posture different from the ones contemplated in the standards, and through the elbows instead of the hands. However, the information used is the closest available to the representation of the phenomena for the case studied. Third, the pressure thresholds used were adapted from pressure-time curves reported in the literature, which were obtained considering exposure to constant loads; nevertheless, during cycling, there is an oscillating motion of the body, which creates variations in the magnitudes of the pressures on the contact areas, potentially modifying the pressure-time relations. Nonetheless, to the author's best knowledge, there are no specific thresholds reported in the literature defining loads that can be harmful to the human body while cycling. Fourth, for each set, the aerobars' height was varied to the maximum according to the bicycle fit window, and the sets were characterized in the extreme postures. To study the optimal height of the aerobars, it was assumed that the characteristics of the intermediate postures could be linearly interpolated from the data of the extreme postures. This assumption was performed to reduce the testing time to avoid affecting the volunteers' training calendar and avoid possible training or detraining effects during the measurements.

8.4. PRACTICAL IMPLICATIONS

The results obtained from the methodology's implementation indicate that the methodology can be used as a tool for the selection and optimization of the aerobars' height of bicycle-cyclist sets, including objective measurements of performance and interaction variables. A methodology that simultaneously considered aerodynamics, power delivery capacity, pressure, and vibration was not previously available. The results highlight the importance of performing the characterization of the variables for each bicycle-cyclist set on postures close to the postures of interest as the results have a strong dependence on the characteristics of the rider, bicycle, postures, and race conditions. This means that the posture selection process should be customized considering the interest of the rider.

The successful implementation of the proposed methodology to select the height of aerobars opens the possibility of implementing the methodology for other postural parameters (*e.g.*, handlebar inclination), including potential crossed interactions of various postural parameters (*e.g.*, simultaneous variation of height and longitudinal position of aerobars' elbow pads).

The results obtained through the methodology's implementation allow the riders to select an appropriate posture for a given race condition and contain information about possible routes of improvement. For example, if when changing the posture to a more aerodynamically efficient posture, the power delivery capacity of the rider drops significantly, leading the aerodynamic posture to be disadvantageous in terms of performance, the rider can focus on training in aerodynamic postures to improve its capacity to deliver power. On the other hand, if the vibrations or pressure registered exceed the corresponding thresholds, bicycle components and special cycling equipment could be modified to improve the interaction characteristics.

8.5. FUTURE RESEARCH

The results obtained in this study for performance and interaction could be further refined by including other relevant variables. For example, requirements associated with bicycle stability [123] and pacing strategies [124], [125] could be explored.

The methodology to select postures could be coupled with the development of race strategies. For this, the race conditions should be defined and divided into segments, and the rider could be characterized in a range of possible postures that can be adopted during the race (without modifying the bicycle) to estimate the best posture for each segment.

In this study, it was necessary to use approximations of threshold curves for acceptable exposures to vibration and pressure. This, because there is not enough information available regarding the potential damage of these interaction variables on the human body. Nevertheless, according to this study's results, due to the long duration of cycling-related activities, the exposure to vibration and pressure while cycling leads to scenarios of possible discomfort health risk. For this reason, further studies on this subject are necessary.

Considering that, besides performance, comfort is an important objective for cyclists, a comparison between subjective comfort ratings and objective interaction variables (in this case, vibration and

pressure) should be performed, seeking for possible correlations that could be related to the exposure thresholds.

To be able to characterize the sets in more conditions (*e.g.*, intermediate postures, road inclinations), it would be useful to improve the methods reducing the time required to perform the tests. In this way, it would be possible to collect more data on the bicycle-cyclist set without affecting the cyclists' training calendar or taking the risk of a change of fitness level during the tests.

References

- [1] H. Allen and S. S. Cheung, "Optimizing bike fit," in *Cutting-Edge Cycling*, 1st ed., H. Allen and S. S. Cheung, Eds. Champaign, IL, USA: Human Kinetics, 2012, pp. 149-169.
- [2] M. Egaña, S. Smith and S. Green, "Revisiting the effect of posture on high-intensity constant-load cycling performance in men and women," *Eur. J. Appl. Physiol.*, vol. 99, (5), pp. 495-501, 2007. DOI: <https://doi.org/10.1007/s00421-006-0365-8>.
- [3] M. Egaña *et al.*, "Effect of posture on high-intensity constant-load cycling performance in men and women," *Eur. J. Appl. Physiol.*, vol. 96, (1), pp. 1-9, 2006. DOI: <https://doi.org/10.1007/s00421-005-0057-9>.
- [4] U. Emanuele and J. Denoth, "Influence of road incline and body position on power-cadence relationship in endurance cycling," *Eur. J. Appl. Physiol.*, vol. 112, (7), pp. 2433-2441, 2012. DOI: <https://doi.org/10.1007/s00421-011-2213-8>.
- [5] E. Welbergen and L. P. Clijsen, "The influence of body position on maximal performance in cycling," *Eur. J. Appl. Physiol. Occup. Physiol.*, vol. 61, (1-2), pp. 138-142, 1990. DOI: <https://doi.org/10.1007/BF00236708>.
- [6] M. C. Ashe *et al.*, "Body position affects performance in untrained cyclists," *Br. J. Sports Med.*, vol. 37, (5), pp. 441-444, 2003. DOI: <http://dx.doi.org/10.1136/bjism.37.5.441>.
- [7] P. Gnehm *et al.*, "Influence of different racing positions on metabolic cost in elite cyclists," *Med. Sci. Sports Exerc.*, vol. 29, (6), pp. 818-823, 1997. DOI: <https://doi.org/10.1097/00005768-199706000-00013>.
- [8] F. Grappe *et al.*, "Effect of cycling position on ventilatory and metabolic variables," *Int. J. Sports Med.*, vol. 19, (05), pp. 336-341, 1998. DOI: <https://doi.org/10.1055/s-2007-971927>.
- [9] C. Scrugham, "Field Testing the Upright Versus the Aero Cycling Position." M.S. Thesis, University of Nevada, Las Vegas, NV, USA, 2013.
- [10] M. Origenes, S. Blank and R. Schoene, "Exercise ventilatory response to upright and aero-posture cycling," *Med. Sci. Sports Exerc.*, vol. 25, (5), pp. 608-612, 1993.
- [11] N. Barry *et al.*, "Aerodynamic performance and riding posture in road cycling and triathlon," *Proc. Inst. Mech. Eng. P J Sports Eng. Tech.*, vol. 229, (1), pp. 28-38, 2015. DOI: <https://doi.org/10.1177/1754337114549876>.

- [12] L. Oggiano *et al.*, "Aerodynamic optimization and energy saving of cycling postures for international elite level cyclists," *Eng. of Sport* 7, pp. 597-604, 2008. DOI: https://doi.org/10.1007/978-2-287-09411-8_70.
- [13] V. Chabroux, C. Barelle and D. Favier, "Aerodynamics of cyclist posture, bicycle and helmet characteristics in time trial stage," *J. Appl. Biomech.*, vol. 28, (3), pp. 317-323, 2012. DOI: <https://doi.org/10.1123/jab.28.3.317>.
- [14] H. Chowdhury and F. Alam, "Bicycle aerodynamics: an experimental evaluation methodology," *Sports Eng.*, vol. 15, (2), pp. 73-80, 2012. DOI: <https://doi.org/10.1007/s12283-012-0090-y>.
- [15] A. E. Jeukendrup and J. Martin, "Improving cycling performance," *Sports Med.*, vol. 31, (7), pp. 559-569, 2001. DOI: <https://doi.org/10.2165/00007256-200131070-00009>.
- [16] T. Defraeye *et al.*, "Aerodynamic study of different cyclist positions: CFD analysis and full-scale wind-tunnel tests," *J. Biomech.*, vol. 43, (7), pp. 1262-1268, 2010. DOI: <https://doi.org/10.1016/j.jbiomech.2010.01.025>.
- [17] N. J. Dettori and D. C. Norvell, "Non-traumatic bicycle injuries," *Sports Med.*, vol. 36, (1), pp. 7-18, 2006. DOI: <https://doi.org/10.2165/00007256-200636010-00002>.
- [18] C. Wilber *et al.*, "An epidemiological analysis of overuse injuries among recreational cyclists," *Int. J. Sports Med.*, vol. 16, (03), pp. 201-206, 1995. DOI: <https://doi.org/10.1055/s-2007-972992>.
- [19] H. Christiaans and A. Bremner, "Comfort on bicycles and the validity of a commercial bicycle fitting system," *Appl. Ergon.*, vol. 29, (3), pp. 201-211, 1998. DOI: [http://dx.doi.org/10.1016/S0003-6870\(97\)00052-5](http://dx.doi.org/10.1016/S0003-6870(97)00052-5).
- [20] L. Laios and J. Giannatsis, "Ergonomic evaluation and redesign of children bicycles based on anthropometric data," *Appl. Ergon.*, vol. 41, (3), pp. 428-435, 5, 2010. DOI: <http://dx.doi.org/10.1016/j.apergo.2009.09.006>.
- [21] M. Chiu, H. Wu and N. Tsai, "The relationship between handlebar and saddle heights on cycling comfort," in *Human Interface and the Management of Information.*, S. Yamamoto, Ed. Berlin, Germany: Springer, 2013, pp. 12-19.
- [22] Y. Chen and Y. Liu, "Optimal protruding node length of bicycle seats determined using cycling postures and subjective ratings," *Appl. Ergon.*, vol. 45, (4), pp. 1181-1186, 7, 2014. DOI: <https://doi.org/10.1016/j.apergo.2014.02.006>.
- [23] A. P. Polanco, D. R. Suárez and L. E. Muñoz, "Effect of body posture on comfort during cycling," in *Proc. ASME International Design Engineering Technical Conf.* Cleveland, OH, USA, 2017, pp. V003T01A012-V003T01A012. DOI: <https://doi.org/10.1115/DETC2017-68124>.
- [24] E. Bressel and J. Cronin, "Bicycle seat interface pressure: Reliability, validity, and influence of hand position and workload," *J. Biomech.*, vol. 38, (6), pp. 1325-1331, 2005. DOI: <https://doi.org/10.1016/j.jbiomech.2004.06.006>.

- [25] J. J. Potter *et al.*, "Gender differences in bicycle saddle pressure distribution during seated cycling," *Med. Sci. Sports Exerc.*, vol. 40, (6), pp. 1126-1134, 2008. DOI: <https://doi.org/10.1249/MSS.0b013e3181666eea>.
- [26] K. de Vey Mestdagh, "Personal perspective: in search of an optimum cycling posture," *Appl. Ergon.*, vol. 29, (5), pp. 325-334, 10, 1998. DOI: [https://doi.org/10.1016/S0003-6870\(97\)00080-X](https://doi.org/10.1016/S0003-6870(97)00080-X).
- [27] R. Verma *et al.*, "Effect of seat positions on discomfort, muscle activation, pressure distribution and pedal force during cycling," *J. Electromyogr. Kines.*, vol. 27, pp. 78-86, 2016. DOI: <https://doi.org/10.1016/j.jelekin.2016.02.003>.
- [28] B. D. Lowe, S. M. Schrader and M. J. Breitenstein, "Effect of bicycle saddle designs on the pressure to the perineum of the bicyclist," *Med. Sci. Sports Exerc.*, vol. 36, (6), pp. 1055-1062, 2004. DOI: <https://doi.org/10.1249/01.mss.0000128248.40501.73>.
- [29] F. P. Carpes *et al.*, "Bicycle saddle pressure: effects of trunk position and saddle design on healthy subjects," *Urol. Int.*, vol. 82, (1), pp. 8-11, 2009. DOI: <https://doi.org/10.1159/000176017>.
- [30] J. M. Gemery *et al.*, "Digital three-dimensional modelling of the male pelvis and bicycle seats: Impact of rider position and seat design on potential penile hypoxia and erectile dysfunction," *BJU Int.*, vol. 99, (1), pp. 135-140, 2007. DOI: <https://doi.org/10.1111/j.1464-410X.2007.06542.x>.
- [31] J. Slane *et al.*, "The influence of glove and hand position on pressure over the ulnar nerve during cycling," *Clin. Biomech.*, vol. 26, (6), pp. 642-648, 2011. DOI: <https://doi.org/10.1016/j.clinbiomech.2011.03.003>.
- [32] D. J. Sanderson, E. M. Hennig and A. H. Black, "The influence of cadence and power output on force application and in-shoe pressure distribution during cycling by competitive and recreational cyclists," *J. Sports Sci.*, vol. 18, (3), pp. 173-181, 2000. DOI: <https://doi.org/10.1080/026404100365072>.
- [33] J. Lépine, Y. Champoux and J. Drouet, "Road bike comfort: on the measurement of vibrations induced to cyclist," *Sports Eng.*, vol. 17, (2), pp. 113-122, 2014. DOI: <https://doi.org/10.1007/s12283-013-0145-8>.
- [34] Union Cycliste Internationale, "Clarification guide of the UCI technical regulation," 2019. Available: https://www.uci.org/docs/default-source/equipment/clarificationguideoftheucitechnicalregulation-2018-05-02-eng_english.pdf.
- [35] R. R. Bini, P. A. Hume and J. Croft, "Cyclists and triathletes have different body positions on the bicycle," *Eur. J. Sport Sci.*, vol. 14, (sup1), pp. S109-S115, 2014. DOI: <https://doi.org/10.1080/17461391.2011.654269>.
- [36] D. J. Cipriani, J. D. Swartz and C. M. Hodgson, "Triathlon and the multisport athlete," *J. Orthop. Sport Phys.*, vol. 27, (1), pp. 42-50, 1998. DOI: <https://doi.org/10.2519/jospt.1998.27.1.42>.

- [37] E. Burke and A. Pruitt, "Body positioning for cycling," in *High-Tech Cycling*, 2nd ed., E. Burke, Ed. Champaign, IL, USA: Human Kinetics, 2003, pp. 69-92.
- [38] D. Fintelman *et al.*, "The effect of time trial cycling position on physiological and aerodynamic variables," *J. Sports Sci.*, vol. 33, (16), pp. 1730-1737, 2015. DOI: <https://doi.org/10.1080/02640414.2015.1009936>.
- [39] L. R. Hubenig, A. B. Game and M. D. Kennedy, "Effect of different bicycle body positions on power output in aerobically trained females," *Res. Sports Med.*, vol. 19, (4), pp. 245-258, 2011. DOI: <https://doi.org/10.1080/15438627.2011.608039>.
- [40] R. L. Jensen, "Power output, muscle activity, and frontal area of a cyclist in different cycling positions," in *XXV International Symp. on Biomechanics in Sports*, Ouro Preto, Brazil, 2007, pp. 172-175. Available: <https://ojs.ub.uni-konstanz.de/cpa/article/view/428>.
- [41] J. M. Charlton *et al.*, "Respiratory Mechanical and Cardiorespiratory Consequences of Cycling with Aerobars," *Med. Sci. Sports Exerc.*, vol. 49, (12), pp. 2578-2584, 2017. DOI: <https://doi.org/10.1249/mss.0000000000001393>.
- [42] P. Burt, "Specialist areas of cycling," in *Bike Fit: Optimise Your Bike Position for High Performance and Injury Avoidance*, 1st ed., P. Burt, Ed. Bloomsbury, 2014, pp. 121-145.
- [43] L. Underwood and M. Jermy, "Optimal handlebar position for track cyclists," *Sports Eng.*, vol. 16, (2), pp. 81-90, 2013. DOI: <https://doi.org/10.1007/s12283-013-0111-5>.
- [44] M. S. Briggs and T. Obermire, "Clinical considerations of bike fitting for the triathlete," in *Endurance Sports Medicine*, T. Miller, Ed. Springer, 2016, pp. 215-227.
- [45] M. R. Silberman *et al.*, "Road bicycle fit," *Clin. J. Sport Med.*, vol. 15, (4), pp. 271-276, 2005. DOI: <https://doi.org/10.1097/01.jsm.0000171255.70156.da>.
- [46] L. Garvican-Lewis *et al.*, "Impact of altitude on power output during cycling stage racing," *Plos One*, vol. 10, (12), pp. e0143028, 2015. DOI: <https://doi.org/10.1371/journal.pone.0143028>.
- [47] A. Polanco *et al.*, "Influence of wind speed and road grade for the estimation of drag area in cycling," *Sports Biomech.*, 2020 (Submitted).
- [48] A. Polanco *et al.*, "Methodology for the estimation of the aerodynamic drag parameters of cyclists," in *Proc. ASME International Design Engineering Technical Conf.* Anaheim, CA, USA, 2019, pp. V003T01A028. DOI: <https://doi.org/10.1115/DETC2019-98067>.
- [49] S. Porras *et al.*, "Experimental study of the aerodynamic drag on light vehicles," in *IV AMDM Congr.* Manizales, Colombia, 2018, pp. 516-517. Available: <https://congresos.autonoma.edu.co/sites/default/files/documentos/memorias-amdm2018-2.pdf>.
- [50] P. Debraux *et al.*, "Aerodynamic drag in cycling: methods of assessment," *Sport Biomech.*, vol. 10, (3), pp. 197-218, 2011. DOI: <https://doi.org/10.1080/14763141.2011.592209>.

- [51] A. C. Lim *et al.*, "Measuring changes in aerodynamic/rolling resistances by cycle-mounted power meters." *Med. Sci. Sports Exerc.*, vol. 43, (5), pp. 853-860, 2011. DOI: <https://doi.org/10.1249/mss.0b013e3181fcb140>.
- [52] F. Grappe *et al.*, "Aerodynamic drag in field cycling with special reference to the Obree's position," *Ergonomics*, vol. 40, (12), pp. 1299-1311, 1997. DOI: <https://doi.org/10.1080/001401397187388>.
- [53] J. Garcia-Lopez *et al.*, "Reference values and improvement of aerodynamic drag in professional cyclists," *J. Sports Sci.*, vol. 26, (3), pp. 277-286, 2008. DOI: <https://doi.org/10.1080/02640410701501697>.
- [54] C. Capelli *et al.*, "Energy cost and efficiency of riding aerodynamic bicycles," *Eur. J. Appl. Physiol. Occup. Physiol.*, vol. 67, (2), pp. 144-149, 1993. DOI: <https://doi.org/10.1007/BF00376658>.
- [55] B. Blocken *et al.*, "CFD simulations of the aerodynamic drag of two drafting cyclists," *Comput. Fluids*, vol. 71, pp. 435-445, 2013. DOI: <https://doi.org/10.1016/j.compfluid.2012.11.012>.
- [56] R. Candau *et al.*, "Simplified deceleration method for assessment of resistive forces in cycling," *Med. Sci. Sports Exerc.*, vol. 31, pp. 1441-1447, 1999. DOI: <https://doi.org/10.1097/00005768-199910000-00013>.
- [57] S. Tengattini and A. Bigazzi, "Validation of an outdoor coast-down test to measure bicycle resistance parameters," *J. Transp. Eng.*, vol. 144, (7), pp. 04018031, 2018. DOI: <https://doi.org/10.1061/JTEPBS.0000152>.
- [58] W. Hucho, "Aerodynamic drag of passenger cars," in *Aerodynamics of Road Vehicles*, 1st ed., W. Hucho, Ed. Society of Automotive Engineers, 1998, pp. 106-213.
- [59] J. C. Martin *et al.*, "Modeling sprint cycling using field-derived parameters and forward integration," *Med. Sci. Sports Exerc.*, vol. 38, (3), pp. 592-597, 2006. DOI: <https://doi.org/10.1249/01.mss.0000193560.34022.04>.
- [60] A. Picard *et al.*, "Revised formula for the density of moist air (CIPM-2007)," *Metrologia*, vol. 45, (2), pp. 149, 2008. DOI: <https://doi.org/10.1088/0026-1394/45/2/004>.
- [61] C. Kyle, "Selecting cycling equipment," in *High Tech Cycling*, 2nd ed., E. Burke, Ed. Champaign, IL, USA: Human Kinetics, 2003, pp. 1-48.
- [62] JCGM, "Evaluation of measurement data - Supplement 1 to the "Guide to the expression of uncertainty in measurement" - Propagation of distributions using a Monte Carlo method. JCGM 101:2008." 2008. Available: https://www.bipm.org/utils/common/documents/jcgm/JCGM_101_2008_E.pdf.
- [63] A. Polanco *et al.*, "Effect of the use of a noncircular chainring on the power delivered by recreational cyclist," in *Proc. ASME International Design Engineering Technical Conf.* Quebec City, Quebec, Canada, 2018, pp. V003T01A023. DOI: <https://doi.org/10.1115/DETC2018-86368>.

- [64] O. Acevedo *et al.*, "Influence of the chainring geometry on the critical power of recreational cyclists," in *Proc. ASME International Design Engineering Technical Conf.* Virtual conference, 2020.
- [65] F. Mattioni *et al.*, "Critical power testing or self-selected cycling: Which one is the best predictor of maximal metabolic steady-state?" *J. Sci. Med. Sport*, vol. 20, (8), pp. 795-799, 2017. DOI: <https://doi.org/10.1016/j.jsams.2016.11.023>.
- [66] T. P. Gavin *et al.*, "Comparison of a field-based test to estimate functional threshold power and power output at lactate threshold," *J. Strength Cond. Res.*, vol. 26, (2), pp. 416-421, 2012. DOI: <https://doi.org/10.1519/JSC.0b013e318220b4eb10.1088/0026-1394/45/2/004>.
- [67] B. Karsten *et al.*, "Time Trials Versus Time-to-Exhaustion Tests: Effects on Critical Power, W' , and Oxygen-Uptake Kinetics," *Int. J. Sport Physiol.*, vol. 13, (2), pp. 183-188, 2017. DOI: <https://doi.org/10.1123/ijsp.2016-0761>.
- [68] P. T. Morgan *et al.*, "Road cycle TT performance: Relationship to the power-duration model and association with FTP," *J. Sports Sci.*, vol. 37, (8), pp. 902-910, 2019. DOI: <https://doi.org/10.1080/02640414.2018.1535772>.
- [69] H. Bergstrom *et al.*, "Responses during exhaustive exercise at critical power determined from the 3-min all-out test," *J. Sports Sci.*, vol. 31, (5), pp. 537-545, 2013. DOI: <https://doi.org/10.1080/02640414.2012.738925>.
- [70] J. Denham *et al.*, "Cycling power outputs predict Functional Threshold Power and maximum oxygen uptake," *J. Strength Cond. Res.*, 2017. DOI: <https://doi.org/10.1519/jsc.0000000000002253>.
- [71] M. Kordi *et al.*, "Influence of upright versus time trial cycling position on determination of critical power and W' in trained cyclists," *Eur. J. Sport Sci.*, vol. 19, (2), pp. 192-198, 2019. DOI: <https://doi.org/10.1080/17461391.2018.1495768>.
- [72] B. Karsten *et al.*, "Comparison of inter-trial recovery times for the determination of critical power and W' in cycling," *J. Sports Sci.*, vol. 35, (14), pp. 1420-1425, 2017. DOI: <https://doi.org/10.1080/02640414.2016.1215500>.
- [73] F. Mattioni *et al.*, "Critical power: How different protocols and models affect its determination," *J. Sci. Med. Sport*, vol. 7, (21), pp. 742-747, 2017. DOI: <https://doi.org/10.1016/j.jsams.2017.11.015>.
- [74] D. Bishop and D. G. Jenkins, "The influence of recovery duration between periods of exercise on the critical power function," *Eur. J. Appl. Physiol. Occup. Physiol.*, vol. 72, (1), pp. 115-120, 1995. DOI: <https://doi.org/10.1007/BF00964125>.
- [75] A. J. Bull *et al.*, "Effect of mathematical modeling on the estimation of critical power," *Med. Sci. Sport Exerc.*, vol. 32, (2), pp. 526, 2000. DOI: <https://doi.org/10.1097/00005768-200002000-00040>.
- [76] C. D. Paton and W. G. Hopkins, "Tests of cycling performance," *Sports Med.*, vol. 31, (7), pp. 489-496, 2001. DOI: <https://doi.org/10.2165/00007256-200131070-00004>.

- [77] W. G. Hopkins, E. J. Schabert and J. A. Hawley, "Reliability of power in physical performance tests," *Sports Med.*, vol. 31, (3), pp. 211-234, 2001. DOI: <https://doi.org/10.2165/00007256-200131030-00005>.
- [78] F. Mattioni *et al.*, "Can measures of critical power precisely estimate the maximal metabolic steady-state?" *Appl. Physiol. Nutr. Me.*, vol. 41, (11), pp. 1197-1203, 2016. DOI: <https://doi.org/10.1139/apnm-2016-0248>.
- [79] J. Dekerle *et al.*, "Maximal lactate steady state, respiratory compensation threshold and critical power," *Eur. J. Appl. Physiol.*, vol. 89, (3-4), pp. 281-288, 2003. DOI: <https://doi.org/10.1007/s00421-002-0786-y>.
- [80] J. Dekerle, A. Vanhatalo and M. Burnley, "Determination of critical power from a single test," *Sci. Sport*, vol. 23, (5), pp. 231-238, 2008. DOI: <https://doi.org/10.1016/j.scispo.2007.06.015>.
- [81] H. Vandewalle *et al.*, "Work-exhaustion time relationships and the critical power concept," *A Critical Review. J Sports Med Phys Fitness*, vol. 37, (2), pp. 89-102, 1997. Available: <https://pubmed.ncbi.nlm.nih.gov/9239986/>.
- [82] J. S. Pringle and A. M. Jones, "Maximal lactate steady state, critical power and EMG during cycling," *Eur. J. Appl. Physiol.*, vol. 88, (3), pp. 214-226, 2002. DOI: <https://doi.org/10.1007/s00421-002-0703-4>.
- [83] D. W. Hill, "The critical power concept," *Sports Med.*, vol. 16, (4), pp. 237-254, 1993. DOI: <https://doi.org/10.2165/00007256-199316040-00003>.
- [84] A. Vanhatalo, J. H. Doust and M. Burnley, "Determination of critical power using a 3-min all-out cycling test," *Med. Sci. Sports Exerc.*, vol. 39, (3), pp. 548-555, 2007. DOI: <https://doi.org/10.1249/mss.0b013e31802dd3e6>.
- [85] H. Allen and S. S. Cheung, "Tracking effort and performance," in *Cutting-Edge Cycling*, 1st ed., H. Allen and S. S. Cheung, Eds. Champaign, IL, USA: Human Kinetics, 2012, pp. 54-55.
- [86] E. Bressel, S. Bliss and J. Cronin, "A field-based approach for examining bicycle seat design effects on seat pressure and perceived stability," *Appl. Ergon.*, vol. 40, pp. 472-476, 2009. DOI: <https://doi.org/10.1016/j.apergo.2008.10.001>.
- [87] A. S. Larsen *et al.*, "The effect of saddle nose width and cutout on saddle pressure distribution and perceived discomfort in women during ergometer cycling," *Appl. Ergon.*, vol. 70, pp. 175-181, 2018. DOI: <https://doi.org/10.1016/j.apergo.2018.03.002>.
- [88] F. Sommer, I. Goldstein and J. B. Korda, "Bicycle riding and erectile dysfunction: a review," *J. Sex. Med.*, vol. 7, (7), pp. 2346-2358, 2010. DOI: <https://doi.org/10.1111/j.1743-6109.2009.01664.x>.
- [89] R. Rodano *et al.*, "Saddle pressure distribution in cycling: Comparison among saddles of different design and materials," in *XX International Symp. on Biomechanics in Sports*, Caceres, Spain, 2002, pp. 606-609. Available: <https://ojs.ub.uni-konstanz.de/cpa/article/view/806>.

- [90] F. P. Carpes *et al.*, "Effects of workload on seat pressure while cycling with two different saddles," *J. Sex. Med.*, vol. 6, (10), pp. 2728-2735, 2009. DOI: <https://doi.org/10.1111/j.1743-6109.2009.01394.x>.
- [91] I. R. Spears *et al.*, "The effect of saddle design on stresses in the perineum during cycling," *Med. Sci. Sports Exerc.*, vol. 35, (9), pp. 1620-1625, 2003. DOI: <https://doi.org/10.1249/01.mss.0000084559.35162.73>.
- [92] J. Dai, J. J. Yang and Z. Zhuang, "Sensitivity analysis of important parameters affecting contact pressure between a respirator and a headform," *Int. J. Ind. Ergonomics*, vol. 41, (3), pp. 268-279, 2011. DOI: <https://doi.org/10.1016/j.ergon.2011.01.007>.
- [93] S. Sprigle and S. Sonenblum, "Assessing evidence supporting redistribution of pressure for pressure ulcer prevention: a review." *J. Rehabil. Res. Dev.*, vol. 48, (3), 2011. DOI: <https://doi.org/10.1682/jrrd.2010.05.0102>.
- [94] C. Bar, "Evaluation of cushions using dynamic pressure measurement," *Prosthet. Orthot. Int.*, vol. 15, (3), pp. 232-240, 1991. DOI: <https://doi.org/10.3109/03093649109164293>.
- [95] E. Linder-Ganz *et al.*, "Pressure–time cell death threshold for albino rat skeletal muscles as related to pressure sore biomechanics," *J. Biomech.*, vol. 39, (14), pp. 2725-2732, 2006. DOI: <https://doi.org/10.1016/j.jbiomech.2005.08.010>.
- [96] A. H. Sacks, "Theoretical prediction of a time-at-pressure curve for avoiding pressure sores," *J. Rehabil. Res. Dev.*, vol. 26, (3), pp. 27-34, 1989. Available: <https://www.rehab.research.va.gov/jour/89/26/3/pdf/sacks.pdf>.
- [97] A. Gefen *et al.*, "Strain-time cell-death threshold for skeletal muscle in a tissue-engineered model system for deep tissue injury," *J. Biomech.*, vol. 41, (9), pp. 2003-2012, 2008. DOI: <https://doi.org/10.1016/j.jbiomech.2008.03.039>.
- [98] S. Hiemstra-van Mastriigt *et al.*, "Predicting passenger seat comfort and discomfort on the basis of human, context and seat characteristics: a literature review," *Ergonomics*, vol. 60, (7), pp. 889-911, 2017. DOI: <https://doi.org/10.1080/00140139.2016.1233356>.
- [99] J. Reswick and J. Rogers, "Experience at rancho los amigos hospital with devices and techniques to prevent pressure sores," in *Bed Sore Biomechanics*, R. M. Kenedi and J. M. Cowden, Eds. Palgrave, London: Strathclyde Bioengineering Seminars, 1976, pp. 301-310.
- [100] A. Doria *et al.*, "An experimental-numerical method for the prediction of on-road comfort of city bicycles," *Veh. Syst. Dyn.*, pp. 1-21, 2020. DOI: <https://doi.org/10.1080/00423114.2020.1759810>.
- [101] A. Polanco *et al.*, "Effect of rider posture on bicycle comfort," in *Proc. ASME International Design Engineering Technical Conf.* Anaheim, CA, USA, 2019, pp. V003T01A025. DOI: <https://doi.org/10.1115/DETC2019-97763>.

- [102] J. Drouet, C. Guastavino and N. Girard, "Perceptual thresholds for shock-type excitation of the front wheel of a road bicycle at the cyclist's hands," *Procedia Engineer.*, vol. 147, pp. 724-729, 2016. DOI: <https://doi.org/10.1016/j.proeng.2016.06.264>.
- [103] M. J. Griffin, *Handbook of Human Vibration*. London, UK: Academic Press, 1990.
- [104] J. Lépine, Y. Champoux and J. Drouet, "A Laboratory Excitation Technique to Test Road Bike Vibration Transmission," *Exp. Tech.*, vol. 40, pp. 227-234, 2013. DOI: <https://doi.org/10.1007/s40799-016-0026-8>.
- [105] Y. Champoux, S. Richard and J. Drouet, "Bicycle structural dynamics," *Sound Vib.*, vol. 41, (7), pp. 16-25, 2007. Available: <http://www.sandv.com/downloads/0707cham.pdf>.
- [106] N. Petrone and F. Giubilato, "Development of a test method for the comparative analysis of bicycle saddle vibration transmissibility," *Procedia Engineer.*, vol. 60, pp. 288-293, 2013. DOI: <https://doi.org/10.1016/j.proeng.2013.07.063>.
- [107] F. Giubilato and N. Petrone, "A method for evaluating the vibrational response of racing bicycles wheels under road roughness excitation," *Procedia Engineer.*, vol. 34, pp. 409-414, 2012. DOI: <https://doi.org/10.1016/j.proeng.2012.04.070>.
- [108] International Organization for Standardization, "ISO 2631-1 Mechanical vibration and shock - Evaluation of human exposure to whole-body vibration," 1997. Available: <https://www.iso.org/standard/7612.html>.
- [109] International Organization for Standardization, "ISO 5349-1 Mechanical vibration -- Measurement and evaluation of human exposure to hand-transmitted vibration," 2001. Available: <https://www.iso.org/standard/32355.html>.
- [110] J. Lépine, Y. Champoux and J. -. Drouet, "The relative contribution of road bicycle components on vibration induced to the cyclist," *Sports Eng.*, vol. 18, (2), pp. 79-91, 2015. DOI: <https://doi.org/10.1007/s12283-014-0168-9>.
- [111] J. Pelland-Leblanc *et al.*, "Using power as a metric to quantify vibration transmitted to the cyclist," *Procedia Engineer.*, vol. 72, pp. 392-397, 2014. DOI: <https://doi.org/10.1016/j.proeng.2014.06.067>.
- [112] A. Doria and E. Marconi, "A testing method for the prediction of comfort of city bicycles," in *Proc. ASME International Design Engineering Technical Conf.* Quebec City, Quebec, Canada, 2018, pp. V003T01A020. DOI: <https://doi.org/10.1115/DETC2018-85128>.
- [113] A. Doria, E. Marconi and P. Cialoni, "Modal analysis of a utility bicycle from the perspective of riding comfort," in *Proc. ASME International Design Engineering Technical Conf.* Anaheim, CA, USA, 2019, pp. V003T01A024. DOI: <https://doi.org/10.1115/DETC2019-97277>.
- [114] X. Chiementin *et al.*, "Hand-arm vibration in cycling," *J. Vib. Control*, vol. 19, (16), pp. 2551-2560, 2012. DOI: <https://doi.org/10.1177/1077546312461024>.

- [115] P. Macdermid, P. Fink and S. Stannard, "The Effects of Vibrations Experienced during Road vs. Off-road Cycling," *Int. J. Sports Med.*, vol. 36, (10), pp. 783-788, 2015. DOI: <https://doi.org/10.1055/s-0034-1398534>.
- [116] M. Olieman, R. Marin-Perianu and M. Marin-Perianu, "Measurement of dynamic comfort in cycling using wireless acceleration sensors," *Procedia Engineer.*, vol. 34, pp. 568-573, 2012. DOI: <https://doi.org/10.1016/j.proeng.2012.04.097>.
- [117] L. M. Roseiro *et al.*, "Hand-arm and whole-body vibrations induced in cross motorcycle and bicycle drivers," *Int. J. Ind. Ergonomics*, vol. 56, pp. 150-160, 2016. DOI: <https://doi.org/10.1016/j.ergon.2016.10.008>.
- [118] J. Vanwalleghem *et al.*, "Sensor design for outdoor racing bicycle field testing for human vibration comfort evaluation," *Meas. Sci. Technol.*, vol. 24, (9), pp. 095002, 2013. DOI: <https://doi.org/10.1088/0957-0233/24/9/095002>.
- [119] C. Hölzel, F. Höchtel and V. Senner, "Cycling comfort on different road surfaces," *Procedia Engineer.*, vol. 34, pp. 479-484, 2012. DOI: <https://doi.org/10.1016/j.proeng.2012.04.082>.
- [120] J. Lépine, Y. Champoux and J. Drouet, "Test protocol for in-situ bicycle wheel dynamic comfort comparison," *Procedia Engineer.*, vol. 147, pp. 568-572, 2016. DOI: <https://doi.org/10.1016/j.proeng.2016.06.241>.
- [121] P. W. Macdermid *et al.*, "Tyre volume and pressure effects on impact attenuation during mountain bike riding," *Shock Vib.*, vol. 2015, pp. 1-10, 2015. DOI: <https://doi.org/10.1155/2015/191075>.
- [122] A. Polanco *et al.*, "Selection of posture for Time-trial cycling events," *Appl. Sci.*, vol. 10, (18), 2020. DOI: <https://doi.org/10.3390/app10186546>.
- [123] S. Roa, A. Doria and L. Muñoz, "Optimization of the bicycle weave and wobble modes," in *Proc. ASME International Design Engineering Technical Conf.* Quebec City, Quebec, Canada, 2018, pp. V003T01A022. DOI: <https://doi.org/10.1115/DETC2018-86132>.
- [124] S. D. Roa and L. E. Muñoz, "Bicycle change strategy for uphill time-trial races," *P. I. Mech. Eng. P-J. Spo.*, vol. 231, (3), pp. 207-219, 2017. DOI: <https://doi.org/10.1177/1754337117724310>.
- [125] T. Dahmen, "Optimization of pacing strategies for cycling time trials using a smooth 6-parameter endurance model," in *Proc. Pre-Olympic Congr. on Sports Science and Computer Science in Sport (IACSS)*, Liverpool, United Kingdom, 2012, pp. 1-6. Available: <http://kops.uni-konstanz.de/handle/123456789/26676>.
- [126] R. R. Bini, P. A. Hume and A. E. Kilding, "Saddle height effects on pedal forces, joint mechanical work and kinematics of cyclists and triathletes," *Eur. J. Sport Sci.*, vol. 14, (1), pp. 44-52, 2014. DOI: <https://doi.org/10.1080/17461391.2012.725105>.

[127] W. Peveler *et al.*, "Effects of training in an aero position on metabolic economy," *J. Exerc. Physiol.*, vol. 8, (1), pp. 52-56, 2005. Available: https://www.asep.org/asep/asep/JEPonlineOCTOBER2004_Peveler.doc.

[128] J. Garcia-Lopez *et al.*, "The use of velodrome tests to evaluate aerodynamic drag in professional cyclists," *Int. J. Sports Med.*, vol. 35, (05), pp. 451-455, 2014. DOI: <https://doi.org/10.1055/s-0033-1355352>.

[129] J. C. Martin *et al.*, "Validation of a mathematical model for road cycling power," *J. Appl. Biomech.*, vol. 14, (3), pp. 276-291, 1998. DOI: <https://doi.org/10.1123/jab.14.3.276>.

Appendices

Appendix 2.1. Studies about cyclists riding in aerobars' postures

First author	Title	Number of subjects	Type of subject	Objective of study (input)	Output variable	Classification of output	Tools of study
Ashe [6]	Body position affects performance in untrained cyclists	10	Physically active, untrained, men,	Posture: upright, aero	VO2max, heart rate, maximum power output	Performance - Power delivery	Cycle ergometer: Incremental Steady-state at
Barry [11]	Aerodynamic performance and riding posture in road cycling and triathlon	1	-	Posture: 9 postures among traditional and	Drag area	Performance - Aerodynamics	Wind tunnel
Bini [126]	Cyclists and triathletes have different body positions on the bicycle	36	36 recreational cyclists	Type of rider Road cyclists (hoods posture) Triathletes	Trunk, pelvis, hip, knee, ankle angles	Posture	Trainer: MOCAP
Chabroux [13]	Aerodynamics of Cyclist Posture, Bicycle and Helmet Characteristics in Time Trial Stage	9	Professional, male cyclists	In aerobars: Hand position (x3), Elbow position (x2), Saddle position (x3), Helmet inclination (x3)	Drag force	Performance - Aerodynamics	Wind tunnel
Charlton [41]	Respiratory Mechanical and Cardiorespiratory Consequences of Cycling with Aerobars	11	Endurance-trained male cyclists	Posture: aerobars, drops, hoods.	Peak power output	Performance - Power delivery	Cycle ergometer: Incremental Constant-load

First author	Title	Number of subjects	Type of subject	Objective of study (input)	Output variable	Classification of output	Tools of study
Fintelman [38]	The effect of time trial cycling position on physiological and aerodynamic variables	19	Well-trained male cyclists	Torso angles (x5)	VO ₂ , CO ₂ expiration, Gross efficiency, peak power output, heart rate, cadence, frontal area	Performance - Power delivery and aerodynamics	Cycle ergometer: Incremental tests Frontal photo
Gemery [30]	Digital three-dimensional modelling of the male pelvis and bicycle seats: impact of rider position and seat design on potential penile hypoxia and erectile dysfunction	1	Adult male	Saddle design and posture	Vascular compression between bony pelvis and seat	Interaction - pressure	3D computational model of the pelvis
Gnehm [7]	Influence of different racing positions on metabolic cost in elite cyclists	14	Elite male bicycle racers	Posture: hoods, drops, aerobars	VO ₂ , heart rate at 70% VO ₂ max,	Performance - Power delivery	Wind braked trainer: Incremental Steady-state
Hubenig [39]	Effect of Different Bicycle Body Positions on Power Output in Aerobically Trained Females	18	Trained endurance female cyclists and triathletes	Aerodynamic upright	Power output in ventilatory thresholds 1 and 2	Performance - Power delivery	Cycle ergometer: 1 incremental 2 submaximal

First author	Title	Number of subjects	Type of subject	Objective of study (input)	Output variable	Classification of output	Tools of study
Jensen [40]	Power output, muscle activity, and frontal area of a cyclist in different cycling positions	9	Recreational or sub-elite cyclists	Posture: hoods, drops, aerobars	Power output EMG Frontal projected area	Performance - Power delivery and aerodynamics	Stationary trainer: Incremental Sprint
Peveler [127]	Effects of training in an aero position on metabolic economy	20	10 trained cyclists 10 trained triathletes	Postures used in training (cyclists in hoods vs. triathletes in aerobars)	VO2 max	Performance - Power delivery	Cycle ergometer: Spirometry Incremental test and 2 time trial tests
Underwood [43]	Optimal handlebar position for track cyclists	14	7 male, 7 female, track cyclists	Handlebar height and separation	Drag area	Performance - Aerodynamics	Wind tunnel

*Appendix 2.2. Informed consent form***INFORMED CONSENT FORM****EFFECT OF CYCLISTS' POSTURE ON PERFORMANCE AND INTERACTION WITH THE BICYCLE**

Dear participant:

You have been invited to participate in a research study. Before you decide to participate, it is important that you understand the reason behind the study and the activities in which you will participate. Please read the following information in detail. If anything is unclear or you want further information, please ask the researcher who is with you during the informed consent process. Once you have read this document and cleared any doubts, you will be asked to sign this form in acceptance to participate. Please note that participation in this study is absolutely voluntary, and you also have the freedom to withdraw your consent at any time and stop participating in the study without prejudice.

The research is focused on proposing postures for bicycle-cyclist sets considering the relationship between posture, performance, and interaction with the bicycle. Aerodynamic drag, power delivery capacity, vibrations, and pressure at contact points in different positions will be measured. This information is relevant as an input for cyclists to select their posture according to their interests considering the effect on performance and interaction with the bicycle.

Description of the tests:

The participation in the study consists of:

- Filling a form with information regarding your level of physical activity, your state of health, contact information in case of emergency, and information on your preferences to make use of the bicycle.
- Participating in 1 session for the definition of the postures to measure.
- Participating in 2 or 3 sessions for the photographic record of the defined postures.
- Participating in 2 or 3 sessions for the assessment of aerodynamic drag.
- Participating in 2 or 3 sessions for the assessment of power delivery capacity.
- Participating in 2 or 3 sessions for the assessment of pressure in contact points.
- Participating in 2 or 3 sessions for the assessment of vibration transmission.

Session for the definition of the postures to measure

The researcher will check your bike to record the current posture and verify the possibility of modifying its geometry (aerobars' height), and install the necessary instrumentation for the other tests. It will be decided whether the tests are performed on your bike or a test bike. In case the tests are carried out on a test bike, it will seek to imitate the configuration of your bike. The positions to be measured in the other test sessions will be defined.

Estimated duration: 30 minutes.

Session for the photographic record

This session takes place in a closed space with the bicycle in a cycle trainer. Using a green background, a photographic record of the cyclist-bicycle set will be made, taking photos from the front and side. During the photoshoot, you must wear your cycling clothes and equipment, including the helmet.

Estimated duration: 30 minutes.

Session for the assessment of aerodynamic drag

This session takes place in an open space on a bike path. A power sensor, speed sensor, GPS monitor, and an anemometer will be installed on the bicycle. You must travel 10 times on the route in the same direction at different speeds (between 18 and 27 km/h). Before starting the tests, you will recognize the segment to warm the muscles and become familiar with the bicycle, the road, and other test conditions. The weight of the cyclist-bicycle set will be recorded.

Estimated duration: 40 minutes of test and 20 minutes of displacement.

Session for the assessment of power delivery capacity

This session takes place in a closed space with the bicycle in a cycle trainer. You will pedal at different intensities for 1 hour following the investigator's instructions. This time includes the warm-up and cool-down. You will choose the intensity and cadence of the pedaling according to the description. The purpose is to measure your maximum power delivery capacity for intervals of 5 seconds, 1 minute, 5 minutes, and 20 minutes. You can hydrate as desired during the test. Your weight will be registered. Your heart rate will be monitored during the test.

Estimated duration: 1 hour 10 minutes.

Session for the assessment of pressure in contact points

This session takes place in a closed space with the bicycle in a cycle trainer. A flexible mat with pressure sensors will be fixed on the saddle and aerobars in different moments. Pressure will be recorded at these contact points for 1 minute while you pedal at a power close to your FTP (estimated by you from your historical records). Your weight will also be recorded.

Estimated duration: 30 min

Session for the assessment of vibration transmission

This session takes place in an open space on a bike path. Accelerometers will be installed on the saddle post and the stem of the bicycle. You must travel 3 times in one direction in the same direction at a constant speed (25 km/h). Before starting the tests, you will travel on the route to recognize the segment and warm the muscles while becoming familiar with the bicycle, the road, and other test conditions. The weight of the cyclist-bicycle set will be recorded.

Estimated duration: 10 minutes of test and 20 minutes of displacement.

Instrumentation

For the tests, the following instruments will be used:

- Accelerometers
- Anemometer
- Weighing machine
- Bicycle
- Digital camera
- Cyclo-trainer (for the sessions in closed space)
- GPS (for the sessions in open space)
- Display to present the data to the rider (for example, sports watch)
- Power, speed, cadence, and heart rate sensors
- Pressure measurement system (flexible mat and accessories)
- Thermometer/Hygrometer/Barometer: for the measurement of ambient conditions

Elements worn by the cyclist

For the testing sessions, you must assist with your cycling helmet, gloves, shirt, shorts, glasses, and shoes. If the tests are performed with your bike, you should bring it to the testing site. It is suggested to bring a bottle with hydration. Additionally, you must carry your identity document and health service card.

Risks

The risks of participating in the tests are those associated with the intense sports practice of cycling, so there is a possibility of dizziness or fainting from exhaustion. There is a risk of falling from the bicycle or colliding with other elements because the outdoor tests will be carried out on public roads. For these reasons, the tests will be carried out at low traffic times in the test route, and the use of protection elements is mandatory.

Clarifications

- During the development of the activities of this study, you will be permanently accompanied by a researcher. This person will be attentive to answer your questions and guide you during the development of the tests.
- The benefits of your participation will be to know your aerodynamic resistance, power delivery capacity, pressure in contact points, and vibration transmission for different positions, which will be informed at the end of the investigation.
- The information recorded during the sessions will be used for academic and research purposes and will be kept confidential. You will be given information about the results obtained from the study.
- In this study, there is no financial obligation between the parties. You will not receive any financial compensation for participating in the study. In the same way, you will not pay to participate in the study.

If you decide to participate in the investigation, please sign the informed consent. In case of any concerns, do not hesitate to contact us.

Informed consent

I have understood the explanations that have been given to me in a clear and simple language. The researcher has allowed me to express all my observations and has clarified all the doubts and questions I have raised regarding my participation in the study. I have been provided a copy of this document. By signing this document, I give my voluntary consent to participate in the study " Effect of cyclists' posture on performance and interaction with the bicycle " developed within the framework of the doctoral research of a student of the Pontificia Universidad Javeriana. I declare the Pontificia Universidad Javeriana and the personnel related to this investigation free of all responsibility for any fact or circumstance that occurs in the displacement or during the development of the activities related to the investigation in which I will participate.

PARTICIPANT

Signature:

Name:

Identity number:

Date (dd/mm/yyyy): ____/____/____

WITNESS

Signature:

Name:

Identity number:

Date (dd/mm/yyyy): ____/____/____

I authorize the use of my image in photographs and videos for academic purposes related to research. Note: the images will be presented in such a way that you are not identified.	YES	NO
--	-----	----

Alejandra Polanco

Student of the Ph.D. Engineering Program

Engineering Department – Pontificia Universidad Javeriana – Bogotá, Colombia

Carrera 7 # 40-62, Edificio 11 – José Gabriel Maldonado, piso 2.

Email: alejandra.polanco@javeriana.edu.co

Appendix 3.1. Values of drag area and rolling resistance coefficient reported in the literature obtained by different methods.

Author	Type of test	N	Rider body	Type of cyclist	Type of bicycle	Equipment	Postures	Drag area [m ²]	Rolling resistance coef. [-]
Barry et al. [11]	Wind tunnel	1	70 kg	National-level elite athlete	Road bicycle with aerobars	Road helmet, sleeveless triathlon racing skinsuit	Hoods Drops Aerobars	0.343 0.332 0.289	0.005 (assumed)
Blocken et al. [55]	Wind tunnel	1	72 kg 1.83m	Unclear	Standard racing bicycle with disk wheels	Aerodynamic helmet, tight-fitting racing suit with long sleeves	Tops Drops Aerobars	0.270 0.243 0.211	-
Defraeye et al. [16]	CFD	1	72 kg 1.83m	Unclear	Standard racing bicycle with disk wheels	Aerodynamic helmet, tight-fitting racing suit with long sleeves	Tops Drops Aerobars	0.212 0.172 0.134	-
García-López et al. [53]	Wind tunnel	5	71.6 kg 1.79m	Professional road cyclists	Time trial with aero handlebar	Aero helmet	Aerobars high Aerobars low and forward	0.341 0.293	-
García-López et al. [128]	Road tests (Velodrome)	12	68.3 kg 1.8m	Professional road cyclists	Time trial with rear lenticular wheel	Aero helmet and aero clothing (including shoe-covers)	Aerobars high Aerobars low	0.237 0.230	-
Grappe et al. [52]	Road tests (Velodrome)	1	67 kg 1.75m	National and regional competitor cyclists	Road bicycle	Unclear	Tops Drops Aerobars	0.299 0.276 0.262	0.003

RO: road bicycle, TT: time-trial bicycle, AB: aerobars posture

Author	Type of test	N	Rider body	Type of cyclist	Type of bicycle	Equipment	Postures	Drag area [m ²]	Rolling resistance coef. [-]
Lim et al. [51]	Road tests (Outdoor)	10	Unclear	Experienced road cyclists at professional or amateur level	Racing bicycle	Standard racing kit	Hoods Drops	0.3633 0.3238	0.0048 0.0047
Martin et al. [129]	Wind tunnel	6	71.9 kg 1.77m	Experienced cyclists	Road bicycle with rear disc wheel	Unclear	Aerobars	0.269	-
Martin et al. [59]	Road tests (Velodrome)	2	77.5kg 1.73m	World-class sprint cyclists	Road bicycle with rear disc wheel	Unclear	Aerobars	0.2	0.0043
Tengattini et al. [57]	Road tests (Indoor hallway and outdoor)	1	78 kg 1.83m	Unclear	Old road bicycle with commuter tires and rear panniers	Daily clothing, normal helmet	Tops	0.449 (indoor) 0.630 (outdoor)	0.0051 (indoor) 0.0064 (outdoor)

RO: road bicycle, TT: time-trial bicycle, AB: aerobars posture

Appendix 3.2. Summary of protocol and auto report for drag area estimation.

Equipment and instrumentation

- Anemometer and coupling to the handlebar
- Power sensor (pedal wrenches)
- Cadence sensor
- Speed sensor
- Monitor with GPS
- Monitor mount
- Weighing machine
- Manometer and pump for tires
- Thermometer / Barometer
- Tools: metric tape measure, Allen keys set, torque meter, level, tape, scissors
- Bicycle (aerobars)
- Cycling equipment: helmet, shoes, jersey, shorts, gloves, goggles
- Hydration bottle
- Rider's identity document

Preparation

- Check instruments' battery charge
- Check the general state of the bicycle and geometry (posture) for the test
- Installation of instrumentation
- Check and set tires' inflation pressure (8 bar)
- Measurement of rider's mass using cycling equipment
- Explain on the testing site:
 - Safety is the priority
 - Testing segment (beginning and end)
 - Testing speeds
 - Smooth pedaling for constant speed
 - Avoid drag from other bicycles in the front or behind the testing bicycle
 - Attention to the other cyclists on the route
- Familiarization with the route, the bicycle, and the instrumentation
- Connection of power, cadence, and speed sensors
- Calibration of the power sensor

Test

- The cyclist travels on the testing route several times at the defined speeds. The cyclist maintains a constant posture.
- The ambient conditions are registered during the tests.



**AERODYNAMIC DRAG
REPORT OF TESTS**

Rider: _____

Date and hour	Posture	Speed										Pressure	Temperature	Relative humidity	Mass with / without equipment	Observations	
		1	2	3	4	5	6	7	8	9	10						

Appendix 4.1. Studies on cyclist's fitness indices.

First author	Title	Number of subjects	Type of test	Output variables	Equipment	Minimum recovery time	Posture
Ashe [6]	Body position affects performance in untrained cyclists	10	Incremental peak power Incremental for anaerobic	LT VO2max	Cycle ergometer	24 h	Upright and Aerobars
Bergstrom [69]	Responses during exhaustive exercise at critical power determined from the 3-min all-out test	18	Constant work Incremental peak power Critical power	VO2max HR PC	Cycle ergometer	N/A	No description Seat height: leg almost fully extended on
Bishop [74]	The influence of recovery duration between periods of exercise on the critical power function	9	Critical power	PC	Cycle ergometer	3 h and 24 h	No description Seat height: leg almost fully extended on
Bull [75]	Effect of mathematical modeling on the estimation of critical power	9	Incremental peak power Critical power	PC	Cycle ergometer	24 h	No description
Denham [70]	Cycling power outputs predict functional threshold power and maximum oxygen uptake	40	Constant duration Incremental peak power	VO2max FTP	Cycle ergometer	3 days	No description
Egana [2]	Revisiting the effect of posture on high-intensity constant-load cycling performance in men and women	26	Incremental peak power	VO2max	Cycle ergometer	48 h	Upright and Supine
Gavin [66]	Comparison of a field-based test to estimate functional threshold power and power output at lactate threshold	7	Constant duration Incremental anaerobic	LT FTP	Cycle ergometer	N/A	No description

First author	Title	Number of subjects	Type of test	Output variables	Equipment	Minimum recovery time	Posture
Gnehm [7]	Influence of different racing positions on metabolic cost in elite cyclists	14	Incremental peak power	VO2max HR	Trainer	N/A	Upright and Drops
Karsten [67]	Time trial vs. time to exhaustion tests: effect on CP W' and oxygen uptake	12	Constant work Incremental peak power Critical power	VO2mx PC	Trainer	1 hour	No description
Karsten [72]	Comparison of inter-trial recovery times for the determination of critical power and W' in cycling	9	Incremental peak power Critical power	PC	Trainer	24 h, 3 h, and 30 min	No description
Kordi [71]	Influence of upright vs. TT cycling position on CP and W'	7	Constant work Incremental peak power	HR PC	Trainer	24 h	Hoods and Aerobars
Mattioni [73]	Critical power How different protocols and models affect its determination	13	Incremental peak power Critical power	PC	Cycle ergometer	24 h	No description
Mattioni [65]	Critical power testing or self-selected cycling: which one is the best predictor of maximal metabolic steady-state?	13	constant duration constant power incremental peak power	LT VO2max PC	Cycle ergometer	24 h	No description
Morgan [68]	Road cycle TT performance: relationship to the power-duration model and association with FTP	12	Constant work Constant duration Incremental peak power	VO2mx FTP	Trainer	24 h	No description
Welbergen [5]	The influence of body position on maximal performance in cycling	6	Incremental peak power	VO2max	Cycle ergometer	24 h	Upright, Bent forward, Recumbent

Appendix 4.2. Summary of protocol and auto report for power delivery capacity.

Equipment and instrumentation

- Smart cycle trainer with power measurement (or power sensor)
- Computer with software to control the cycle trainer
- Cadence sensor
- Heart rate sensor
- ANT+ stick
- Fan
- Weighing machine
- Manometer and pump for tires
- Thermometer / Barometer
- Tools: metric tape measure, Allen keys set, torque meter, level, tape, scissors
- Bicycle (aerobars)
- Cycling equipment: shoes, shorts, gloves
- Hydration bottle
- Rider's identity document

Preparation

- Check instruments' battery charge
- Check the general state of the bicycle and geometry (posture) for the test
- Installation of instrumentation
- Installation of the bicycle in the cycle trainer
- Check and set tires' inflation pressure (8 bar); if necessary, level front wheel
- Measurement of the rider's mass
- Explain test
- Connection of cadence and heart rate sensors
- Connection and calibration of cycle trainer
- Define with the rider preferred pedaling cadence

Critical power test

- Warm-up: 5 minutes at 50% FTP with 10-seconds sprints when completing minutes 2, 3, and 4. In the end, the rider rests on the bicycle for 3 minutes.
- Test: When the cadence is stabilized at the objective cadence, the trainer's resistance is increased to obtain the power output defined for the test. The rider pedals until exhaustion. Verbal encouragement is used during the tests. The cyclist maintains a constant posture. The rider can hydrate ad libitum.
- Cool-down: The rider pedals for 3 minutes without load.
- The ambient conditions are registered during the tests.

Functional Threshold Power test

- The rider pedals at the self-selected intensities following the curve developed by the commercial software TheSufferFest shown in Figure 4.1. This curve includes warm-up and cool-down.
- The ambient conditions are registered during the tests.



Rider:	Estimated FTP:
--------	----------------

Date and hour	Posture	Mass	Objective power	Pressure	Temperature	Observations



**POWER DELIVERY – FTP
REPORT OF TESTS**

Rider:	Estimated FTP:
--------	----------------

Date and hour	Posture	Mass	Trainer level	Pressure	Temperature	Observations

Appendix 5.1. Studies on the pressure in bicycle-cyclist interfaces

First author	N	Gender of sample	Interface under analysis	Input variable	Output index	Instrumentation	Registered indices' values	Testing conditions	Data length
Bressel [86]	30	Male/ Female	Saddle	Saddle design: standard, partial anterior	Mean handlebar pressure Mean saddle pressure	Pressure-sensing mat: 28x34 cm with 768 piezoresistive sensors	Total mean pressure: Male: 25.3-30.3 kPa Female: 17.6-18.9 kPa	Dynamic: pedaling on flat road 118 W, 80 rpm	3 pedal cycles
Bressel [24]	19	Male/ Female	Saddle	Posture: tops, drops	Mean saddle pressure Peak pressure	Pressure-sensing mat: 28x34 cm with 768 piezoresistive sensors	Mean pressure 17.5 kPa Peak pressure 125.6 kPa @ 118W Male: tops 19.3, drops 17.2 kPa Female: tops 15.3, drops 14.4 kPa @ 300W Male: tops 14.6 Female: tops 12.0	Dynamic: ergometer 118/300 W, 80 rpm	5 seconds
Carpes [29]	22	Male/ Female	Saddle	Posture: upright and forward trunk	Mean saddle pressure	Two instrumented insoles	Upright: 66-69 kPa Forward: 55-63 kPa	Static: Cycle simulator	5 seconds
Carpes [90]	22	Male/ Female	Saddle	Workload, saddle plain/holed	Mean saddle pressure (normalized)	Two instrumented insoles	Normalized mean pressure: 2.04 - 4.59 Pa/kg Normalized peak pressure: simulator	Dynamic: Cycle simulator	5 seconds
Larsen [87]	19	Female	Saddle	Nose geometries	Mean saddle pressure Center of Pressure	Pressure-sensing mat: 16x32 cm with 512 sensors	Static mean pressure: 0.27-0.30 kPa/kg Dynamic mean pressure: 0.31-0.32 kPa/kg	Static and dynamic: Ergometer 150 W, 80	55 seconds

First author	N	Gender of sample	Interface under analysis	Input variable	Output index	Instrumentation	Registered indices' values	Testing conditions	Data length
Lowe [28]	33	Male	Saddle (Pedal Handlebar)	Saddle design (x4)	Mean saddle pressure Peak saddle pressure Average perineal pressure Peak perineal pressure Mean foot and hand load	Pressure-sensing mat: 16x16 cm with 234 sensors Instrumented insoles: 1 for foot, 1 for handlebar	Mean saddle pressure: 20 kPa Peak saddle pressure: 70-100 kPa Average perineal pressure: 20-40 kPa Peak perineal pressure: 40-80 kPa	Dynamic: ergometer 150 W, 70 rpm	40 - 60 seconds
Potter [25]	22	Male/ Female	Saddle	Gender, power (100 and 200 W), and hand position (tops/drops)	Normalized force Peak pressure Center of pressure	Pressure-sensing mat: 90 piezo-capacitive sensors	Normalized peak pressure: 0.3-0.7 kPa/kg	Dynamic: 100/200 W, 90 rpm Stationary bicycle 100/200 W, 10 pedal cycles)	10 seconds (aprox. 10 pedal cycles)
Sanderson [32]	29	Male	Shoe	Cadence and power	Maximum resultant force	Pressure distribution unit with 12 piezoceramic transducers	Resultant force 100 - 450 N	Dynamic: Stationary trainer 100/200/300/400 W, 100 rpm	12 pedal cycles
Slane [31]	36	Male/ Female	Hands	Hand position (tops, drops, hoods) and glove type (without, unpadded,	Average peak pressure	Pressure-sensing mat: 229 piezocapacitive sensors	Peak pressures 134-165 kPa	Dynamic: Trainer Men: 159 W, 80 rpm Women: 116 W, 84 rpm	12 pedal cycles

First author	N	Gender of sample	Interface under analysis	Input variable	Output index	Instrumentation	Registered indices' values	Testing conditions	Data length
Spears [91]	1	Male	Saddle	Saddle width and inclination	Internal compressive stress	Finite element model and a pressure-sensitive film for validation	Maximum compressive stress: Anterior region: over 15 kPa Posterior region: over 140 kPa	Simulation and static validation	N/A

Appendix 5.2. Summary of protocol and auto report for pressure in contact areas.

Equipment and instrumentation

- Smart cycle trainer with power measurement (or power sensor)
- Computer with software to control the cycle trainer
- Pressure sensing mat hardware and software
- Cadence sensor
- Heart rate sensor
- ANT+ stick
- Fan
- Weighing machine
- Manometer and pump for tires
- Thermometer / Barometer
- Tools: metric tape measure, Allen keys set, torque meter, level, tape, scissors
- Bicycle (aerobars)
- Cycling equipment: shoes, shorts, gloves
- Hydration bottle
- Rider's identity document

Preparation

- Check instruments' battery charge
- Check the general state of the bicycle and geometry (posture) for the test
- Installation of the bicycle in the cycle trainer
- Installation of instrumentation
- Check and set tires' inflation pressure (8 bar), if necessary, level front wheel
- Measurement of the rider's mass
- Explain test
- Connection of cadence and heart rate sensors
- Connection and calibration of cycle trainer
- Define with the rider the preferred pedaling cadence

Test

For each measured contact area (saddle-buttocks and aerobars' pads-elbows):

- Warm-up: 10 minutes at 50% FTP
- Pressure sensing mat zero setting (unloaded)
- Sensing of contact area with constant pressure
- Test: When the cadence is stabilized at the objective cadence, the trainer's resistance is increased to obtain the power output defined for the test. The rider pedals for one minute while the pressure field is recorded.



**PRESSURE IN CONTACT AREAS
REPORT OF TESTS**

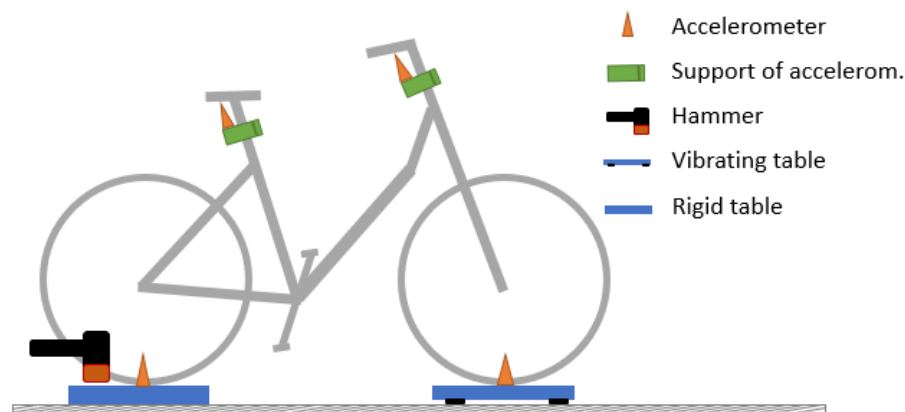
Rider:	Estimated FTP:
---------------	-----------------------

Date and hour	Posture / Contact area	Mass	Contact area registration	Pressure field registration	Observations

Appendix 6.1. Methodology for the measurement of vibrations through laboratory tests

Even though the laboratory tests have several advantages for the analysis of vibration transmission to cyclists, mainly regarding the possibility of controlling the testing conditions, this approach is not widely used. From the references found in the literature review for this Ph.D. project, most researches performed outdoor tests, and only one group of researchers reported results from whole-body and hand transmitted vibrations through laboratory tests. The reason can be associated with the equipment's high experimental costs or the difficulty to keep the bicycle vertical. For this reason, an experimental low-cost laboratory methodology was proposed with researchers of the Padova University, Universidad de Los Andes, and Universidad Javeriana for the prediction of on-road vibration transmission in bicycles [100], [112].

The methodology is based on the impulsive testing method. The frequency response functions between the acceleration of the studied points (i.e., steerer tube and seatpost) and the input on the wheels are obtained and processed to estimate the power spectral density of the accelerations transmitted to the rider. To perform this test, the bicycle is placed on two tables. One table is mounted on elastic mounts and is excited with a hammer for modal testing. Due to the hammer hit, this table vibrates and behaves as a simple shaker. The other table is mounted on rigid mounts to guarantee a leveled configuration. Accelerometers are located on the vibrating table (under the tire-table contact patch) to measure the input acceleration and on the studied points to measure the output acceleration. The following figure presents a scheme of the testing setup.



This methodology was implemented to measure the vibration transmission of two bicycle-rider sets. The results obtained with the laboratory tests were compared with measurements from road tests, and a general agreement was found. It was concluded that the method can replicate the most important features of road test results.

Appendix 6.2. Studies on vibration transmission in cycling

First author	Type of vibration	N	Output / index*	Instrumentation	Acceleration orientation	Type of test	Excitation source	Motion / Keep vertical
Chiementin [114]	Hand-arm	1	Accel rms	Triaxial accelerometers in Stem and wrist/elbow/clavicle	*X positive direction, Z collinear with gravity	Road	Paved road with paving stoned uniformly	Pedaling from 5 to 35 km/h
Drouet [102]	Hand-arm	10	Power absorbed	*Strain gauge instrumented brake hood *Uniaxial accelerometer under hands	Vertical	Laboratory	Treadmill with bump and rear wheel lifted, only front	Bungee cables wrapped on seat tube and fixed to a structure
Holzel [119]	Whole-body	1	Accel rms	*Accelerometer under seat	Vertical	Road	Four surfaces: asphalt, concrete slabs, cobblestones, Road	Initial speed of 10, 15 20 km/h, short track (15 m), not pedaling
Lepine [104]	Whole-body	1	Accel rms	*Triaxial accelerometer on rear wheel hub	Vertical	Road	Road	Towed by vehicle from the front fork (without wheel)
Lepine [33]	Whole-body	2	Accel rms force-filtered signal	*Strain gauge instrumented stem and seatpost *Uniaxial accelerometer	Vertical	Laboratory	*2 Hydraulic shakers *Treadmill	Bungee cables wrapped on seat tube and fixed to a structure (for both cases)

* rms a: acceleration root mean square, P abs: absorbed power, force: force filtered signal

First author	Type of vibration	N	Output / index*	Instrumentation	Acceleration orientation	Type of test	Excitation source	Motion / Keep vertical
Lepine [110]	Whole-body	1	Accel rms force-filtered signal	*Strain gauge instrumented stem, brake hood, and seatpost *Uniaxial accelerometer	Vertical	Laboratory	Hydraulic shakers	Bungee cables wrapped on seat tube and fixed to a structure
Lepine [120]	Whole-body	1	Power absorbed	Strain gauge instrumented brake hood and seatpost	Vertical	Road	Road	Pushed in the back by a person on a motorcycle
Maccdermid [115]	Whole-body	7	Accel rms	Triaxial accelerometers on leg, arm, seatpost, lumbar region, and forehead	Orthogonal: vertical, longitudinal and lateral	Road	Road	Pedaling
Maccdermid [121]	Whole-body	12	Accel rms	Triaxial accelerometers on leg, arm, seatpost, lumbar region, and forehead	Orthogonal: vertical, longitudinal and lateral	Road	Steps on descending stairs	Gravity
Olieman [116]	Whole-body	1	Accel rms	Inertial acceleration sensors on front and rear wheel, stem and seatpost.	Orthogonal: vertical, longitudinal and lateral	Road	Road	Pedaling

* rms a: acceleration root mean square, P abs: absorbed power, force: force filtered signal

First author	Type of vibration	N	Output / index*	Instrumentation	Acceleration orientation	Type of test	Excitation source	Motion / Keep vertical
Pelland [111]	Whole-body	1	Accel rms Power absorbed	Uniaxial accelerometers under brake hoods and triaxial accelerometer on seatpost.	Vertical	Road and Laboratory	Road Laboratory: Hydraulic shakers	Negative slope (not pedaling) Bungee cables wrapped on seat tube and fixed
Roseiro [117]	Whole-body and hand-arm	1	Accel rms	Triaxial accelerometers on seat pad and handlebar	Orthogonal: vertical, longitudinal and lateral	Road	Road	Pedaling
Vanwalleghe m [118]	Whole-body and hand-arm	1	Power absorbed	Six triaxial accelerometers on saddle and handlebar and Force gauges on	Vertical	Road	Road	Pedaling

* rms a: acceleration root mean square, P abs: absorbed power, force: force filtered signal

Appendix 6.3. Summary of protocol and auto report for vibration transmission measurement.

Equipment and instrumentation

- Two triaxial accelerometers with clamp mounts
- Cadence sensor
- Speed sensor
- Monitor with GPS
- Monitor mount
- Weighing machine
- Manometer and pump for tires
- Tools: metric tape measure, Allen keys set, torque meter, level, tape, scissors
- Bicycle (aerobars)
- Cycling equipment: helmet, shoes, jersey, shorts, gloves, goggles
- Hydration bottle
- Rider's identity document

Preparation

- Check instruments' battery charge
- Check the general state of the bicycle and geometry (posture) for the test
- Installation of instrumentation
- Check and set tires' inflation pressure (8 bar)
- Measurement of rider's mass using cycling equipment
- Explain on the testing site:
 - Safety is the priority
 - Testing segment (beginning and end)
 - Testing speeds
 - Constant speed and constant cadence (constant gear)
 - Attention to the other cyclists on the route
- Familiarization with the route, the bicycle, and the instrumentation
- Connection cadence and speed sensors

Test

- The cyclist travels on the testing route at the defined speed (25 km/h). The cyclist maintains a constant posture.

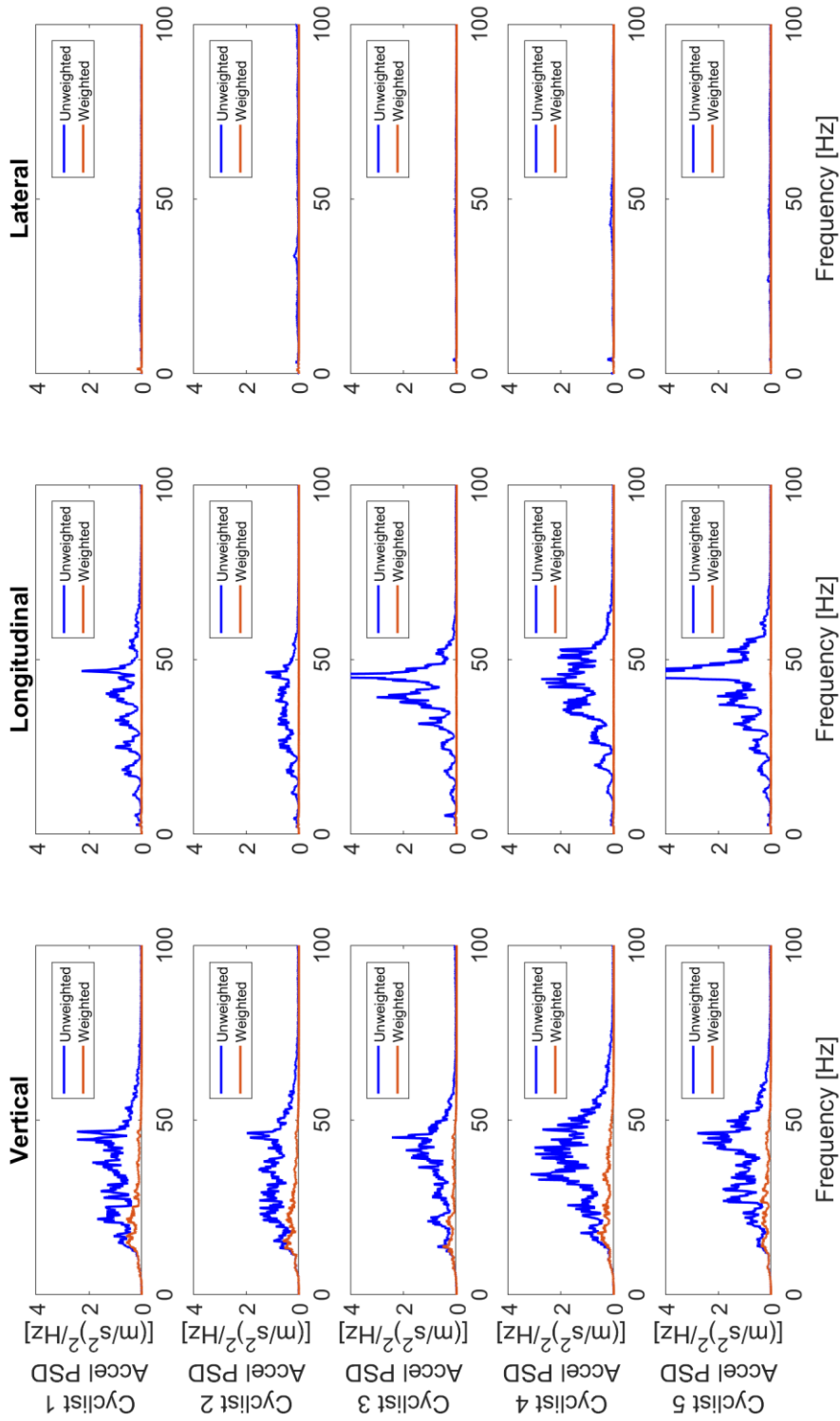


**VIBRATION TRANSMISSION
REPORT OF TESTS**

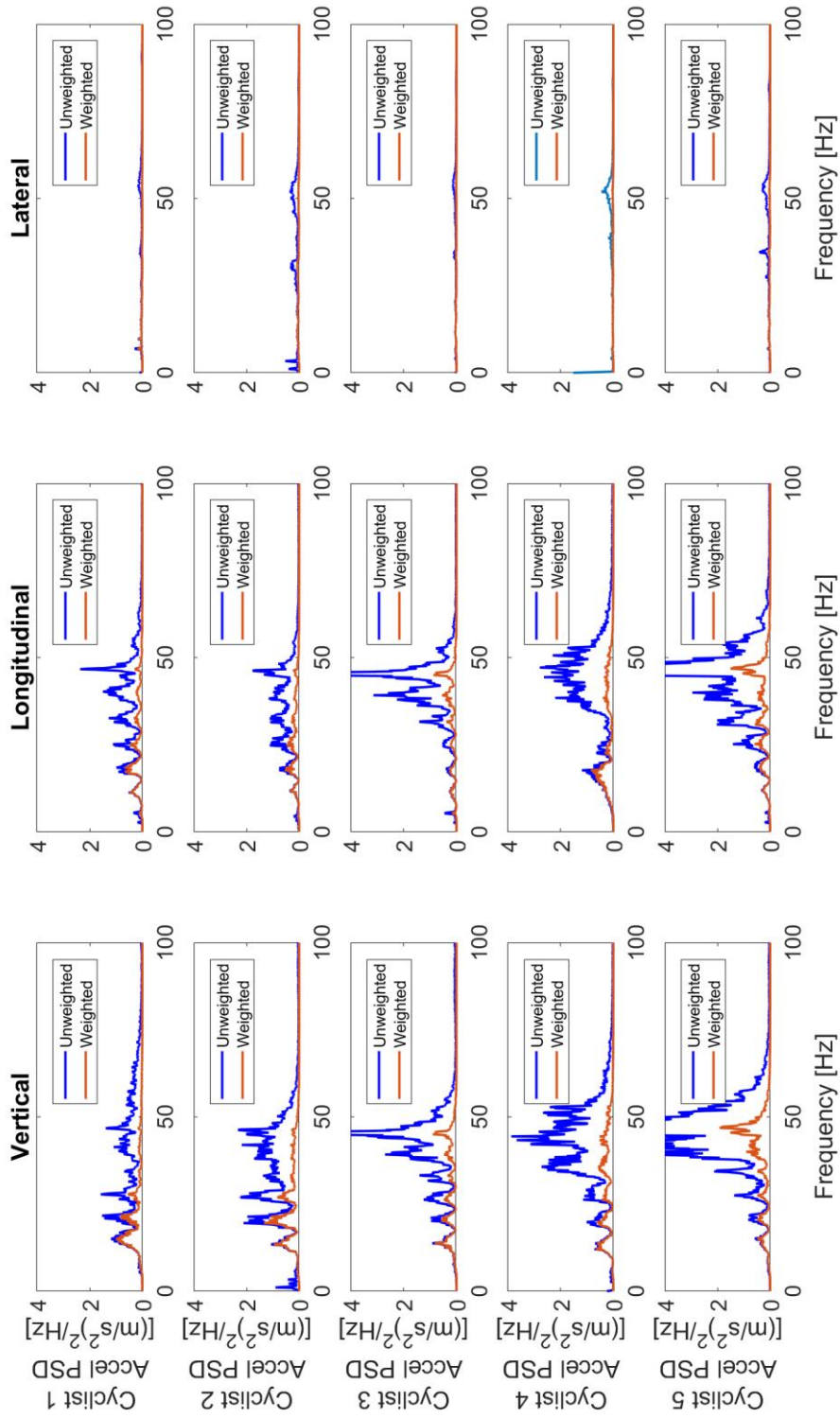
Rider:	Objective cadence:
--------	--------------------

Date and hour	Posture	Mass	Transmission setting	Vibration registration	Observations

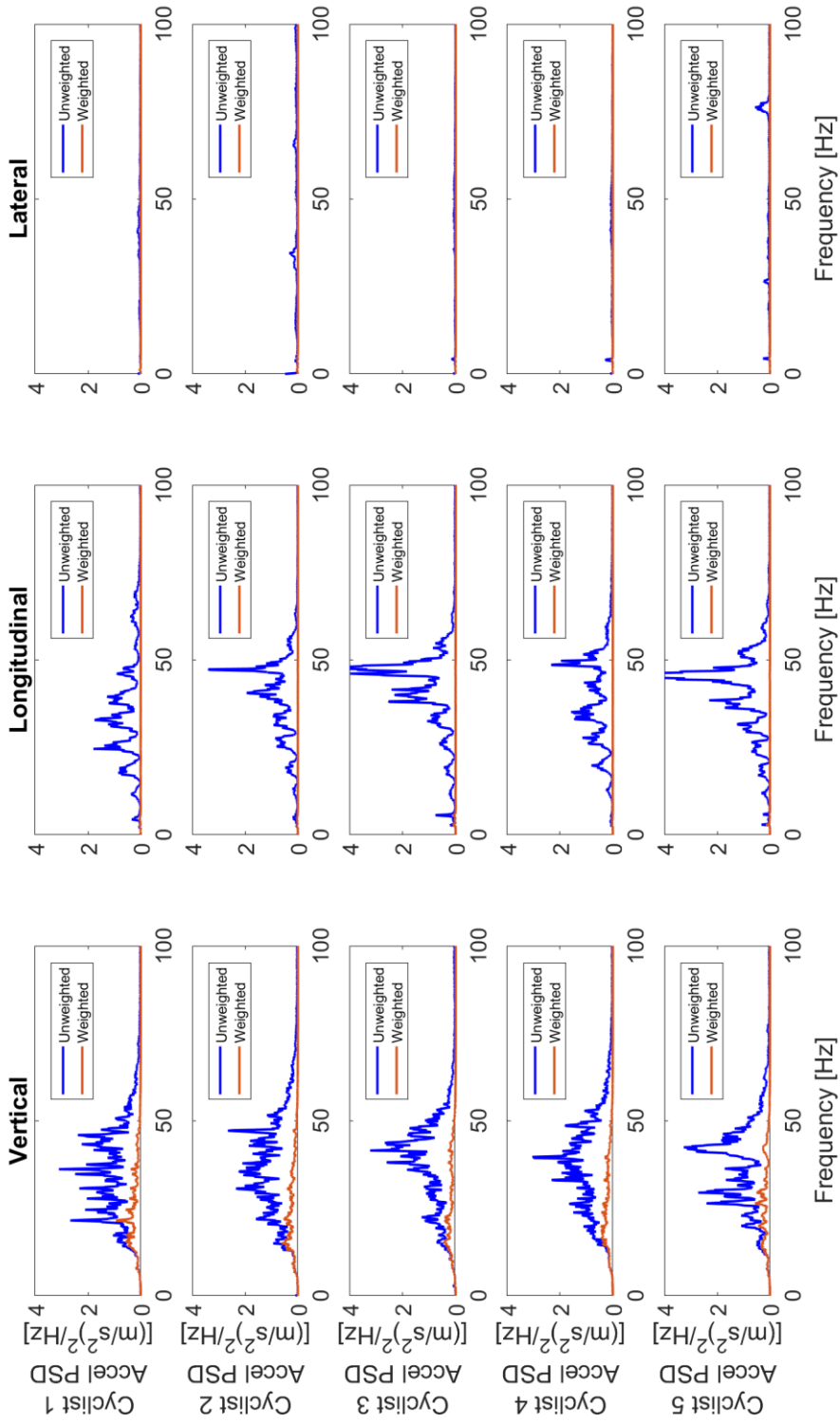
Appendix 6.4. Effect of human sensitivity on the average PSDs in seatpost. All cyclists riding in ABhigh posture.



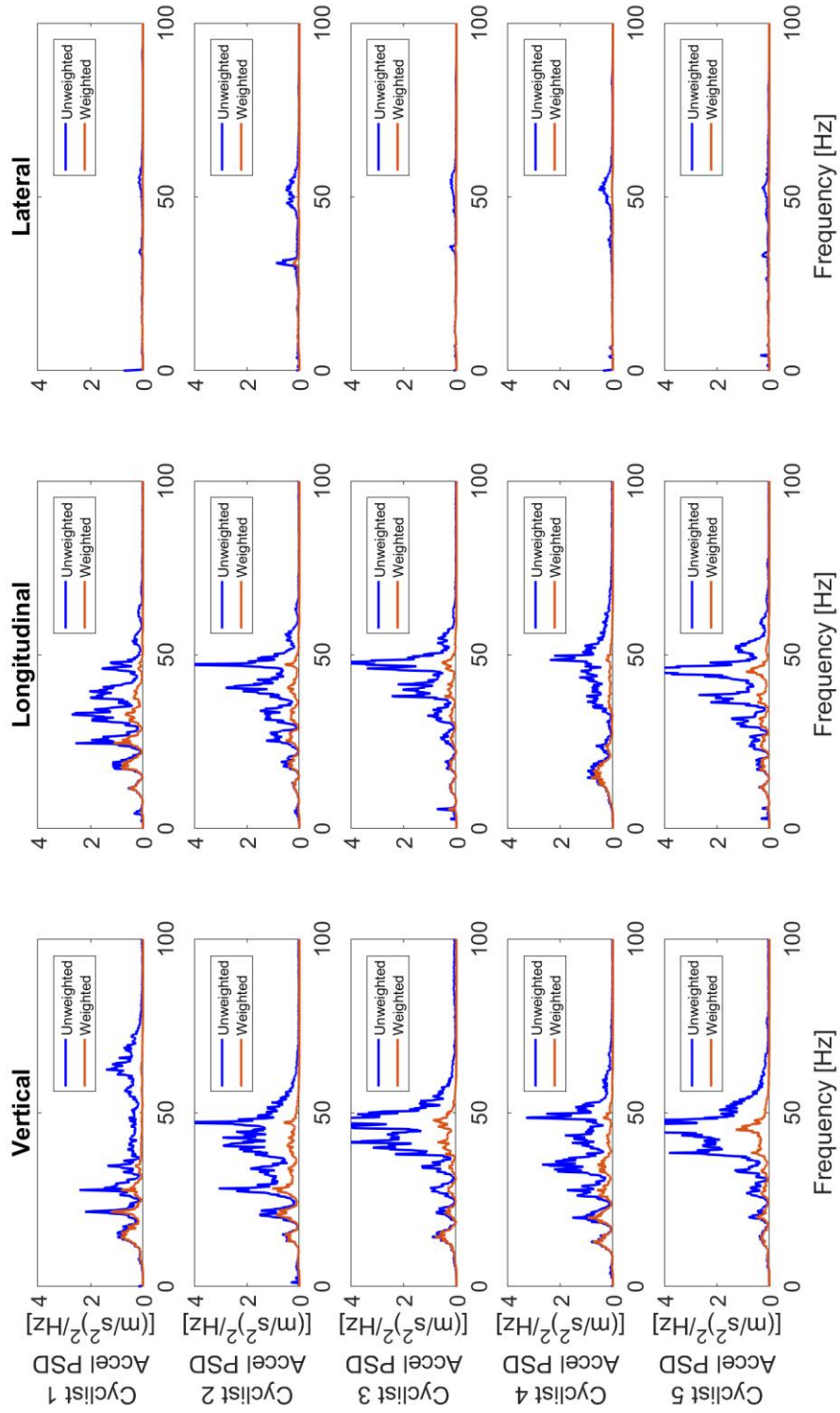
Appendix 6.5. Effect of human sensitivity on the average PSDs in steering tube. All cyclists riding in ABhigh posture.



Appendix 6.6. Effect of human sensitivity on the average PSDs in seatpost. All cyclists riding in ABlow posture.



Appendix 6.7. Effect of human sensitivity on the average PSDs in steering tube. All cyclists riding in ABlow posture.



Acknowledgments

The development of this research project was possible thanks to the support of a group of people and institutions who trusted me. I want to take the space to thank them:

To my advisor Prof. Daniel Suarez, for his unconditional trust and support.

To my co-advisor Prof. Alberto Doria, for giving me the opportunity of visiting the University of Padova to work with him and learn from him.

To my husband Luis, for everything. His support every day and on each step of the road was essential. I could not have realized this project without him. I hope we can keep growing together.

To my friend Sergio Roa, for being there from day one and being the best test subject.

To the volunteer cyclists for giving me the precious gift of their time to participate in the tests: Andres Ramirez, Camilo Aldana, Jhon Caro, Juan Camargo, Juan Pablo Casas, Julian Gomez, Julian Prieto, Luis Munoz, Mirtha Realpe, Natalia Castro, Paola Charris, Sergio Gomez, and Sergio Roa.

To the friends I made on the road: Carolina, Edoardo, Jhonathan, and Silene, for the great time we shared.

To Lissy and Juan in Fused Form, for helping me to build some ideas.

To the people in Centro Atico, the Electronic Engineering Department laboratory, and the laboratory of the Industrial Engineering Department of the Pontificia Universidad Javeriana, especially Samar Atta and German Yamhure, for helping me with their resources.

To the Administrative Department of Science, Technology and Innovation (Colciencias), and the Pontificia Universidad Javeriana for dedicating funds for my scholarship and project supplies.

Finally, to my family and friends who were attentive to the development of my project and shared the ups and downs of the process. They were essential.

Author's publications

Journal Articles

A. Polanco, L. Muñoz, A. Doria, and D. Suárez, "Selection of posture for time-trial cycling events," *Appl. Sci.*, vol. 10, (18), 2020.

A. Polanco, S. Roa, D. Suarez, O. Lopez and L. Munoz, "Influence of wind speed and road grade for the estimation of drag area in cycling," *Sport. Biomech.*, 2020 [under review: minor changes].

A. Doria, E. Marconi, L. Munoz, A. Polanco and D. Suarez, "An experimental-numerical method for the prediction of on-road comfort of city bicycles," *Vehicle Syst. Dyn.*, pp. 1-24, 2020.

Conference Articles

O. Acevedo, L. Muñoz, A. Polanco and D. Suárez, "Influence of the chainring geometry on the critical power of recreational cyclists," in *ASME 2020 International Design Engineering Technical Conference, IDETC 2020, Virtual Conference, August 17-19, 2020*

A. Polanco, E. Marconi, L. Munoz, D. Suarez and A. Doria, "Effect of rider posture on bicycle comfort," in *ASME 2019 International Design Engineering Technical Conference, IDETC 2019, Anaheim, USA, August 18-21, 2019*, pp. 1-8.

A. Polanco, J. Fuentes, S. Porras, D. Castiblanco, J. Uribe, D. Suarez and L. Munoz, "Methodology for the estimation of the aerodynamic drag parameters of cyclists," in *ASME 2019 International Design Engineering Technical Conference, IDETC 2019, Anaheim, USA, August 18-21, 2019*, pp. 1-8.

A. Polanco, C. Tarazona, D. Suárez and L. Muñoz, "Effect of the use of a noncircular chainring on the power delivered by recreational cyclists," in *ASME 2018 International Design Engineering Technical Conference, IDETC 2018, Quebec City, Canada, August 26-29, 2018*, pp. 1-6.

S. Porras, A. Polanco, S. Roa, D. Suarez, O. Lopez and L. Munoz, "Experimental study of the aerodynamic drag on light vehicles," in *IV Congreso Internacional sobre Tecnologías Avanzadas de Diseño, Mecatrónica y Manufactura, AMDM 2018, Manizales, Colombia, 7-9 November, 2018*, pp. 516-518.

A. Polanco, D. Suárez and L. Muñoz, "Effect of body posture on comfort during cycling," in *ASME 2017 International Design Engineering Technical Conference, IDETC 2017, Cleveland, USA, 6-9 August, 2017*, pp. 1-9.

Oral presentations

A. Polanco and D. Suarez, "Pressure in the saddle during road cycling," in *Make Health, Bogota, Colombia, 12-13 December, 2019*. Poster presentation.

E. Marconi, A. Polanco, and A. Doria, "An experimental-numerical method for the prediction of on-road comfort of city bicycles," in *Symposium on the Dynamics and Control of Single Track Vehicles, BMD 2019, Padua, Italy, 9-11 September, 2019*. Podium presentation.

A. Polanco, J. Fuentes, L. Munoz and D. Suarez, "Effect of posture on different indexes used to assess the aerodynamic drag forces acting on recreational road cyclists," in *24th Annual Congress of the European College of Sport Science, ECSS 2019, Prague, Czech Republic, 3-6 July, 2019*. Podium presentation.

A. Polanco and D. Suárez, "Use of motion capture for the analysis of comfort and performance in cycling," in *ASME 2017 International Design Engineering Technical Conference, IDETC 2017, Cleveland, USA, 6-9 August, 2017*. Podium presentation.

Curriculum Vitae

I was born in Bogota, Colombia, on April 30th, 1987. I got a Mechanical Engineer degree (2010) and a Master of Science in Mechanical Engineering degree (2011) from Universidad de Los Andes, Bogota, Colombia.

I worked as a research assistant at Universidad de Los Andes in 2010. Then, I worked as a projects' engineer in Wood group PSN Colombia between 2011 and 2012. I worked as projects' director in Fundacion Justicia Social from 2012 to 2015 and, simultaneously, as adjunct instructor in the Engineering School of the Pontificia Universidad Javeriana from 2013 to 2015, in Bogota, Colombia.

I began the Ph.D. program of the School of Engineering in the Pontificia Universidad Javeriana in 2016, under the supervision of Prof. Daniel Suarez, and became a Ph.D. candidate in 2018. In 2019 I spent one semester in the Industrial Engineering Department of the Università di Padova in Italy, under the supervision of Prof. Alberto Doria.

My research interests include bioengineering and sports engineering in topics as the measurement and simulation of systems' dynamic response and the analysis of human-machine interactions.